2020

SPATIAL MEMORY AND EXECUTIVE FUNCTIONING IN THE GOTO-KAKIZAKI RAT MODEL OF DIABETES

Lorielle Dietze
diet0770@mylaurier.ca

SPATIAL MEMORY AND EXECUTIVE FUNCTIONING IN THE GOTO-KAKIZAKI RAT MODEL OF DIABETES

by

Lorielle Mary Florence Dietze

Bachelor of Arts Honours Psychology, University of Waterloo, 2017

THESIS

Submitted to the Department of Psychology

in partial fulfilment of the requirements for

Master of Science in Behavioural Neuroscience

Wilfrid Laurier University

Abstract

Type 2 diabetes mellitus is a disease that adversely affects cognitive function in areas extending to memory and executive functioning. The Goto-Kakizaki (GK) rat provides a model of type 2 diabetes that can illustrate the mechanisms by which this disease works. The present study compared hyperglycaemic GK rats and age-matched Wistar rats in the Morris water maze to assess spatial memory, and in a perceptual attentional set-shifting task to assess putative prefrontal-dependent executive functioning. Results showed there was no difference in path length during training trials, however, GK and Wistar rats differed in the path length travelled in the target quadrant during the probe trial. Although search strategies became more precise for both strains over the spatial training days, GK rat search strategies were less precise than Wistar rats. A urinary glucose test performed on the first and last days of water maze testing revealed that urine glucose significantly decreased after the water maze for GK rats. Golgi-Cox staining was used to examine dendritic complexity and spine densities in the suprapyramidal layer of the dentate gyrus. There was significantly less dendritic arbour and branching complexity in the GK rat dentate gyrus, particularly in the middle molecular layer. Spine densities were significantly decreased for GK rats in each molecular layer in the suprapyramidal blade. Results suggest that spatial memory retrieval deficits may be linked to diabetes, a mechanism thought to be associated with the dentate gyrus.

In the attentional set-shifting task, Day 1 of the task involved training rats to dig for food rewards and discriminate between different odours, digging mediums, and textures. Day 2 of the task consisted of a series of 7 shifts including discriminations, an intradimensional shift, an extradimensional shift, and 3 reversals. GK rats required significantly more trials to reach criterion in the discriminations, but not the other shifts. Duration of the discrimination and

reversal 1 trials were also significantly greater for the GK rats. Urinary glucose tests validated hyperglycemia both before and after the task. Golgi-Cox staining was used to examine pyramidal neuron spine densities in the prelimbic cortex. Spine densities were significantly decreased for GK rats in layers II/III in the basilar and apical dendrites. Results suggest that GK rats have morphological changes in the prefrontal cortex despite having preserved executive function. The cognitive deficits observed in GK rats appear to be related to altered perception rather than executive functioning.

Keywords: Goto-Kakizaki rat; type 2 diabetes; dentate gyrus; prelimbic cortex

To Squeaker

AND

All the four-legged little heroes who helped make this research possible.

Acknowledgements

Foremost, I would like to thank my Mom and Dad for always being there for me, for the many pep talks throughout these two years, and telling me to follow my dreams. When the going got tough you were there for me, and I am forever grateful.

Thank you to my supervisors Dr. Paul Mallet and Dr. Diano Marrone - you are both an inspiration and neuroscientist role models. Thank you to Dr. Paul Mallet, my awesome co-supervisor, for your support and kindness, teaching me about neuroscience, having patience with my endless questions, and your enthusiasm for research. Even though you are incredibly busy as the Associate Dean of Science, you always managed to find time to meet with me. To Dr. Diano Marrone, my second awesome co-supervisor, thank you for answering my many questions, bouncing ideas around with me, and teaching me about behavioural neuroscience methods and the dentate gyrus. Coming from a cognitive neuroscience background, it was a pleasure to work with someone who can so eloquently explain concepts to someone from a different discipline.

Thank you to my committee members Dr. Noam Miller, and Dr. Elena Choleris, your suggestions and contributions during this process and to this document are greatly appreciated.

A HUGE thank you to my research assistants! To Lana Toameh and Cassie Vivian, thank you for sticking by me while being splashed with water maze rat water, and for figuring out the attentional set-shifting task with me. To Sam Peticca, thank you for the company in running the attentional set-shifting task, and for being my Golgi buddy in the endless hours of staining tissue. To Megan Shaver and Maya Selitser, thank you so much for the hours of video coding you put into this project. Last, but most definitely not least, thank you to George Saad. Not only are you a master at Sholl analysis, but your enthusiasm for learning is unparalleled. Honestly, this research would not have been possible without all of you.

Thank you to the staff of the Animal Care Facility, Kelley Putzu and Melissa Oldfield, for teaching me everything I know about handling animals, and taking care of the little heroes.

Lastly, thank you to my pet rat Squeaker, for tirelessly sitting up with me at night to discuss my thesis, and for providing inspiration and insight into the life of the rat.

Table of Contents

List of Tables

List of Figures

Chapter 1: General Introduction

Diabetes Mellitus

In the latest quinquennial report by the World Health Organization (WHO), diabetes mellitus was named as the sixth leading cause of death in the world (2016). There are two types of diabetes, type 1 diabetes mellitus (T1DM) and type 2 diabetes mellitus (T2DM), with the latter accounting for 90-95% of all diabetes cases (Centers for Disease Control and Prevention, 2017). While both are associated with hyperglycaemia, T1DM is characterized by little to no insulin secretion, while T2DM is non-insulin dependent. T1DM has an early onset, developing in childhood or adolescence, whereas T2DM has a slower onset generally developing in adulthood (Canadian Diabetes Association, 2019). Morbidity associated with all types of diabetes includes blindness, end stage renal disease, amputation, myocardial infarction, and stroke, where retinopathy, neuropathy, and nephropathy are all at a heightened risk with diabetes (Nathan, 1993). T2DM is even associated with an increased risk for coronary heart disease and stroke (Vinereanu, 2006). T1DM is a disease more associated with glucose control, whereas T2DM is a cerebrovascular disease (McCrimmon, Ryan, & Frier, 2012).

Uncontrolled T2DM has been associated with cognitive dysfunction, mostly with older adults (Ryan & Geckle, 2000). The cognitive dysfunction extends to verbal learning, memory, executive function, and psychomotor speed deficits (for reviews see Ryan & Geckle, 2000; Stewart & Liolitsa, 1999; Vincent & Hall, 2015). There are now a number of studies linking diabetes with the prevalence of dementia and Alzheimer's Disease (Biessels, Staekenborg, Brunner, Brayne, & Scheltens, 2006; Kopf & Frölich, 2009; Mayeda, Whitmer, & Yaffe, 2015), and also depression (De Groot, Anderson, Freedland, Clouse, & Lustman, 2001). Therefore, it is paramount that research into the effects and mechanisms of this disease are studied.

As the human lifespan is increasing, the study of T2DM is becoming more important. Although the cognitive deficits of T2DM, with relation to memory and executive function, have been thoroughly investigated in humans (Astur, Taylor, Mamelak, Philpott, & Sutherland, 2002; Biessels, Van der Heide, Kamal, Bleys, & Gispen, 2002; Ryan, 1997; Stewart & Liolitsa, 1999; Strachan, Deary, Ewing, & Frier, 1997; Vincent & Hall, 2015), there is a lack of literature characterizing cognitive deficits in an animal model of T2DM. It is important to be able to characterize deficits in an animal model of T2DM, because if the deficits align with human deficits, then this animal model can be used to test treatments as well as conduct invasive procedures that cannot be tested on humans to see if the effects of T2DM can be lessened.

Accelerated Aging Hypothesis

One hypothesis as to why we see impairments in cognition and in the body is the accelerated aging hypothesis which was first proposed by Kent (1976). The accelerated aging hypothesis proposes that diabetes is a form of accelerated aging, whereby it accelerates the aging process as well as the onset of other diseases that are co-morbid with diabetes. The accelerated aging hypothesis is supported by multiple studies. Myelin content has been shown to decrease earlier in aging diabetic rabbits compared to controls (Spritz, Singh, & Marinan, 1975). In humans, there is evidence of cognitive decline associated with diabetes relative to controls (Cukierman-Yaffe, 2014), as well as increased general brain atrophy (Araki et al., 1994). To study the impact of T2DM, animal models can be used to examine behaviour, and these models can elucidate the mechanisms by which this disease acts.

A Spontaneously Diabetic Rat Model

Throughout the study of T2DM, animal models have been used to understand the effects of diabetes and examine treatment approaches. There are various animal models of diabetes

employed in the literature. One popular model is the streptozotocin (STZ) diabetes-induced rat model, where diabetes is induced by injecting STZ into rats or mice (Junod et al., 1967; and characterized in Junod, Lambert, Stauffacher, & Renold, 1969), and where the number of pancreatic islet β-cells and immunoreactive insulin levels are selectively decreased producing effects that mimic T1DM (for a review see Furman, 2015; see also Junod et al., 1969). T1DM can be produced in mice models with multiple low doses of STZ or a single high dose of STZ, whereas in rats T1DM can be induced with a single dose (Furman, 2015). However, the downfall of the STZ model is that the majority of diabetes cases are T2DM in nature, which include very different effects and prognosis. A model of T2DM called the streptozotocin-nicotinamide rat model, can be also induced with STZ by using nicotinamide to partially protect against the effect of STZ. Here, the model is insulin-deficient but is not insulin-resistant (Masiello et al., 1998). Disadvantages of this model include but are not limited to hyperglycaemia only in the non-fasting state, toxic side effects of STZ on organs, and there is a possibility that remaining intact β-cells are damaged by STZ (Ghasemi, Khalifi, & Jedi, 2014).

Another model of T2DM that is a highly regarded model used in the study of T2DM is called the Goto-Kakizaki (GK) rat model, which is bred to be spontaneously hyperglycaemic and non-obese (Goto, Kakizaki, & Masaki, 1975). The GK rat was selectively bred from the Wistar strain using the outcome of glucose tolerance tests. Only rats with the highest blood glucose levels in the population were used for breeding (Goto et al., 1975) over many generations, serving to increase population blood glucose levels in these animals (Goto & Kakizaki, 1981). The onset of hyperglycaemia in GK rats typically occurs 3-4 weeks after birth (Movassat, Saulnier, & Portha, 1995); hyperglycaemia and glucose intolerance remains stable through 18 months of follow-up (Berthelier, Kergoat, & Portha, 1997). GK rats display impaired insulin

secretion consistent with an early stage of human T2DM (Kimura et al., 1982). Prior to the onset of hyperglycaemia, the total pancreatic insulin stores and β-cell mass are decreased in GK rats compared to a control (Movassat et al., 1995), presumably a result of polygenic inheritance (Östenson & Efendic, 2007). However, the presence of hyperglycaemia *in vivo* does not influence the severity of the loss of functioning islet tissue. It is suggested that the decreased total pancreatic insulin stores and β-cell mass, leading to eventual hyperglycaemia, appears to the full effect when GK genes are inherited from both parents (Serradas, Gangnerau, Giroix, Saulnier, & Portha, 1998).

The GK rat model of diabetes is widely used in the understanding of the effects of T2DM treatments. Although reviewing all studies using the GK rat model for treatment research is beyond the scope of this short review, some examples of studies limiting the effects of T2DM will be discussed here. One of the first treatment studies involving the GK rat model of T2DM used islet inactivating protein, derived from the Bordetella pertussis, which normalized glucose tolerance for over a month (Toyota et al., 1978). The injection of stevioside *in vivo* produced antihyperglycemic effects in the GK rat (Jeppesen, Gregersen, Alstrup, & Hermansen, 2002; Jeppesen et al., 2003). Glucagon-like peptide-1 or exendin-4 delayed onset and limited the severity of T2DM when given during the prediabetic period (Tourrel et al., 2002). In GK rats, an *in vivo* treatment of IL-1Ra reduced hyperglycaemia, improved insulin sensitivity, and reduced tissue inflammation (Ehses et al., 2009). More recently, a study involving the treatment of GK rats with caffeine, illustrated an improvement in spatial memory deficits, and reduction of neurochemical alterations to the hippocampus (Duarte et al., 2018). There are very few studies on the behavioural characterization of the GK rat relating to cognitive deficits, and these few

studies will be described later in this chapter, where one of the cognitive deficits seen in these few studies is impaired spatial memory.

Spatial Memory: Environmental Orientation

Spatial memory refers to a specific aspect of memory relating to the attention given to one's surroundings. This attention includes not only an observation of one's location, but also the ability to actively store and process this information. These mechanisms of attention and spatial memory are thought to overlap (Awh & Jonides, 2001). The contextual cueing effect allows us to use the global layout of our surroundings to remember a context and guide our attention to targets in a context (Chun & Jiang, 1998). It has been proposed that the hippocampus is partly used to form a cognitive map of one's surroundings (O'Keefe & Nadel, 1978). Both landmark information about an environment and layout are taken into account in the cognitive map to learn about the spatial environment (Kaplan, 1976; Newman et al., 2007).

Spatial Memory in Humans

A virtual version of an animal task called the Morris water maze (MWM), has been used in humans to test spatial memory. Using this task, a study revealed that patients with unilateral hippocampal removal to treat intractable epilepsy experienced deficits in spatial memory (Astur et al., 2002). Studies in humans with lesions have also provided evidence for the importance of the right medial temporal lobe (Smith & Milner, 1981, 1989) and parahippocampal cortex (Ploner, C. J., Gaymard, B. M., Rivaud-Péchoux, S., Baulac, M., Clémenceau, S., Samson, S., & Pierrot-Deseilligny, 2000) in spatial memory.

Individuals with T2DM have been shown to have mixed results in the literature of impaired and spared spatial memory (Stewart & Liolitsa, 1999). In older adults, cognitive dysfunction associated with T2DM increases with poor glycaemic control and time since

diabetes onset (Kloppenborg, van den Berg, Kappelle, & Biessels, 2008). Verbal learning and memory deficits in diabetes patients improve with glycaemic control (Gradman, Laws, Thompson, & Reaven, 1993). Visuospatial memory studies--which use visual presentation of spatial information, usually involving constructing or organizing objects--are for the most part not significantly impacted by T2DM (Awad, Gagnon, & Messier, 2004). A spatial task called the modified Location Learning Test, where participants had to remember the location of a grid containing objects for memory recall and delayed memory recall tests, showed that diabetic patients had impaired performance as compared to controls (Kessels, Nys, Brands, van den Berg, & Van Zandvoort, 2006). Studies of spatial memory including measures based on spatial environments are rare. One recent study used a block designed spatial n-back task to test spatial working memory in T2DM patients in an fMRI. Accuracy and reaction time for T2DM patients was significantly impaired. In addition, activation of the bilateral hippocampus/parahippocampal gyrus, among other cognition-related areas, was lower for T2DM patients relative to controls (Huang et al., 2016). Much of the literature on spatial memory impairments come from animal models of T2DM in a widely known spatial task – the MWM.

Spatial Memory in Rats

A commonly used behavioural task to examine spatial memory in rats is the standard MWM. A circular pool is filled with water made opaque using non-toxic paint or dye in a contrasting colour of the rat, the animal's movements are recorded from above. An escape platform is hidden just below the water surface (Morris, 1984). Rats use distal cues placed around the room for understanding their location within the maze. Rats are trained to find the escape platform to test spatial learning acquisition, and this platform is removed during a probe trial to test spatial memory (Morris, 1981). In prior studies, STZ diabetes-induced rats have been

found to have deficits in water maze learning during training, and these deficits are accompanied by changes in hippocampal long-term potentiation (Biessels et al., 1996, 1998). Using the original MWM paradigm, GK rats show spatial learning impairments (i.e., higher escape latencies across training days) relative to Wistar rats. In the probe trial, GK rats spend an equal amount of time swimming in each quadrant versus the Wistar controls, which spend more time in the target quadrant (Li et al., 2013). A study of similar design comparing GK rats and Wistar controls in the water maze found comparable spatial learning and memory deficits (Xiang et al., 2015).

Dentate Gyrus

As previously mentioned, the hippocampus is associated with spatial memory (O'Keefe & Nadel, 1978). Hippocampal lesions in rats suggest that spatial memory and recognition memory are dependent on the hippocampus, but spatial memory in particular is dependent on hippocampal volume (Broadbent, Squire, & Clark, 2004). The dentate gyrus (DG) is part of the hippocampus, along with areas CA1, CA2, and CA3. It is suggested that the DG underlies acquisition of new spatial memories (Goodrich-Hunsaker, Hunsaker, & Kesner, 2008; Nakazawa, McHugh, Wilson, & Tonegawa, 2004; Scoville & Milner, 1957; Squire, Stark, & Clark, 2004). A type of cell prominently found in the DG is called a granule cell. Research has shown that the DG continues to produce granule cells in adulthood (Cameron & Mckay, 2001).

The DG can be divided along the transverse axis into two separate areas, the suprapyramidal (DG_{sp}) and infrapyramidal (DG_{ip}) blades. Granule cells from the DG_{sp} have greater dendritic length and dendritic spine density than cells from the DG_{ip} (Desmond & Levy, 1982; Green & Juraska, 1985; Seress & Pokorny, 1981). The arbour of granule cells can be divided into three sections from closest to farthest from the soma, the inner molecular layer

(IML), the middle molecular layer (MML), and the outer molecular layer (OML; Amaral, Scharfman, & Lavenex, 2007). The MML conveys more spatial information than the OML (Knierim, Neunuebel, & Deshmukh, 2014), where the MML has more dendritic arbour in rats than the OML (Gallitano, Satvat, Gil, & Marrone, 2016). In GK rats, the area CA1 in the hippocampus has been examined, and it is known that there are significantly fewer dendritic spines in GK rats than in Wistar rats (Li et al., 2013; Xiang et al., 2015). The DG in the hippocampus has not been examined in GK rats making this region a primary area of interest.

Executive Function: Our Cognitive Control

A behavioural characterization that has not been investigated using the GK rat model of diabetes is executive functioning. There are many definitions in the literature that describe executive functioning (Miyake et al., 2000; Stuss, 1992; Suchy, 2009); most are operationally hard to define and involve complex attributes, but one definition stands apart from the others. Executive functioning can be defined as set-shifting, updating working memory, and response inhibition (Miyake et al., 2000). In this model of executive functioning, tasks that are used for experiments in psychology can be classified under either one of these terms, two terms at the same time, or contain parts of all three terms simultaneously.

Set-shifting is the ability to switch from one task or thought to another quickly with minimal cost in terms of time or errors committed in completing the new task. Updating working memory is the process of actively retaining, manipulating, and revising information when necessary. Response inhibition is the ability to stop and withhold an automatic response when it is required (Miyake et al., 2000). The present study is focused on set-shifting as an integral part of executive function, as there is a gap in understanding the behavioural characterization of set-shifting in the GK rat model. In the literature, set-shifting is also referred to as cognitive

flexibility, however the aspects covered under cognitive flexibility are various. The term cognitive flexibility encompasses the selective use of knowledge to apply to a decision, multiple representations of concepts, use of abstract concepts to facilitate understanding, using knowledge in practice, schema flexibility, interconnectedness of concepts, and active participation in the thought process (Spiro, Coulson, Feltovich, & Anderson, 2013; Spiro et al., 1987).

Set-Shifting in Humans

In humans with T2DM, evidence for increased impairments in set-shifting can be found across the literature on set-shifting, as there are widespread deficits in set-shifting abilities in those with T2DM (Vincent & Hall, 2015). Increased set-shifting impairments were also seen as part of the Maastricht Aging Study, a longitudinal study conducted over 12 years of follow-up. A concept-shifting task in this study showed that adults with T2DM performed worse than controls, where the longer the participant was diagnosed with T2DM, the worse that participant's performance on the task (Spauwen, Köhler, Verhey, Stehouwer, & Van Boxtel, 2013). In a review of fMRI studies involving T2DM, executive functioning was detrimentally affected by the presence of T2DM, and activity in associated brain regions was correlated with this performance (Macpherson, Formica, Harris, & Daly, 2017).

A classic set-shifting task in humans is the Wisconsin Card Sorting Task (WCST), which involves having participants sort cards by either the number, the colour, or the shapes of the figures appearing on each card (Grant & Berg, 1948). The set-shift in this task comes about by switching the sorting pattern partway through the task. In elderly patients with T2DM, glycaemic control was related to performance on the WCST (Reaven, Thompson, Nahum, & Haskins, 1990). These deficits appear to be prominent in the elderly population even in those with insulin resistance, without the presence of either diabetes or dementia (Abbatecola et al., 2004). These

studies suggest that executive dysfunction may be linked to the regulation and production of insulin. However, poor diabetes control in older adults with T2DM, including glycaemic control as mentioned earlier, is also associated with executive dysfunction (Munshi et al., 2006). Executive dysfunction that is seen in humans with T2DM can also be examined using rodent models.

Set-Shifting in Rats

Set-shifting as well as reversal learning experiments in rats targeting the prefrontal cortex (PFC), have been tested in many different types of tasks (for a review see Bizon, Foster, Alexander, & Glisky, 2012). As mentioned earlier, the WCST has been used in humans to assess set-shifting. Dias et al. developed a way to test shifts in primates by using an intradimensional shift (IDS) whereby the subject solves a problem using the same perceptual dimension but with novel stimuli, and an extradimensional shift (EDS) where the subject solves a problem with a different perceptual dimension and novel stimuli (1996; based on Slamecka, 1968). In case of an EDS, a perceptual dimension could be colour, and the shift based on discrimination of different colours. In rats, a type of task incorporating these shifts is the digging set-shift task, also called the attentional set-shifting task. Here, rats were trained to dig for a food reward in pots, and to discriminate between different examples of a dimension. There are a series of shifts that occur as part of the larger task that are completed in the same sequence. Partway through the task, just as in the EDS used with primates, the initial training pattern associated with food rewards is reversed to a second dimension (Birrell & Brown, 2000; Bizon et al., 2012; Floresco, Block, & Tse, 2008). The original version of this task used three dimensions for discrimination between exemplars: texture, odour, and digging medium. Shaping and training occurs on the first day, followed by a series of seven shifts including three reversals along with the IDS and EDS on the

second day. Rats with lesions to the medial prefrontal cortex (mPFC) limited to the infralimbic and prelimbic cortices, experience impairments on only the EDS (Birrell & Brown, 2000).

Prelimbic Cortex

The mPFC is widely associated with decision-making, and executive function (Bissonette, Powell, & Roesch, 2013; Euston, Gruber, & McNaughton, 2012). The prelimbic cortex (PrL), is part of the ventral medial prefrontal cortex, an area known for its involvement in executive functioning (Kesner & Churchwell, 2011). The PrL is located on the medial wall of the rostral cortex just dorsal to the infralimbic (IL). The PrL structure is divided by six layers that are distinct from one another. A type of neuron called the pyramidal neuron is prominent in the layers II/III and V of the mPFC. Pyramidal neurons are identifiable by a pyramidal-shaped somata, with a single apical branch extending from the soma towards the pial surface of the cortex, and basilar dendrites in the opposite direction. Layer III pyramidal neurons are difficult to separate from layer II neurons (Perez-Cruz, Müller-Keuker, Heilbronner, Fuchs, & Flügge, 2007), therefore these layers were grouped together in this study.

The breadth of afferent projections to the PrL is extensive and include the hippocampus (CA1/subiculum) and other orbital and limbic associated areas (Hoover & Vertes, 2007). It should be noted that these afferent projections to the PrL from the CA1 of the hippocampus reach mainly the deep layer V neurons in the PrL, with less dense connections to the layer II/III, and there the PrL does not receive projections from the DG, CA2, CA3, or the distal part of the subiculum (Jay & Witter, 1991). Efferent projections from the PrL are less extensive, connecting to the ventromedial caudate-putamen, core of the nucleus accumbens, and IL among others (Heidbreder & Groenewegen, 2003; Kesner & Churchwell, 2011). The PrL receives and integrates information in order to make a comparison of events present and past to make a

decision (Hoover & Vertes, 2007). One way to examine the morphology of neurons like pyramidal neurons is to use the Golgi staining method.

History of Golgi Staining

The Golgi staining technique, named by its inventor Camillo Golgi (1873), is used to stain brain tissue. The method stains whole neurons black against a lighter background. It was through this technique that Ramón y Cajal was able to stain and visualize much of the nervous system (Ramón y Cajal, 1909), and demonstrate the existence of dendritic spines as structures on nerve cells (Ramón y Cajal, 1888). This method of staining was largely forgotten during the first part of the 20th century until the 1960s. Armed with an electron microscope, it was determined that the neurons were stained due to the Golgi precipitate impregnating the neurons, essentially filling and staining them (Blackstad, 1965; Stell, 1965). Golgi staining allows for the visualization of only a small percentage of neurons (1-3%), and analysis of neuronal morphology with axonal and dendritic arborization and spines (Zaqout & Kaindl, 2016). Although there are different methods of utilizing Golgi's method, the Golgi-Cox method is the most reliable (Buell, 1982; Zaqout & Kaindl, 2016). Cox made a modification to the Golgi method protocol whereby mercuric chloride, potassium dichromate, and potassium chromate were introduced to help fill and stain the neurons (Cox, 1891). Although there are many protocols derived from the Golgi-Cox method, the protocol described by Gibb and Kolb (1998), which was used in the present study, allows for good resolution of dendritic morphology and dendritic spines.

The Importance of Spine Density

Dendritic spines were originally a hot topic of debate in the late 19th and early 20th centuries. As mentioned previously, Ramon y Cajal supported the existence of dendritic spines seen in Golgi stained tissue (Ramón y Cajal, 1888). However, Golgi and other researchers at the

time disagreed with the argument that these spines were part of the neuron morphology, discounting them instead as a by-product of the stain itself (Yuste, 2015). Although dendritic spines were not accepted as real for many years, Cajal was able to show that spines are visible in the cerebral cortex of other mammalian species (Ramón y Cajal, 1891b), and even appear in Ehrlich methylene-blue stained tissue (Ramón y Cajal, 1896a, 1896b).

Dendritic spines are projections from the surface of dendrites, which resemble thorns or nubs. There are different shapes of spines, such as M-type resembling a mushroom, L-type resembling a lollipop, N-type which are nubby with poor definition between spine head and neck, and D-type or a dimple which has no defined spine head or neck (Malone et al., 2008). The difference in morphology of dendritic spines as either thin or mushroom determines the strength of the synapse (Kasai, Matsuzaki, Noguchi, Yasumatsu, & Nakahara, 2003) and plasticity. Smaller spines are thought to undergo long-term potentiation which can change their morphology, whereas larger spines are more stable (Matsuzaki, Honkura, Ellis-Davies, & Kasai, 2004). Neuropsychiatric disorders such as Alzheimer's disease and schizophrenia are associated with synapse and spine loss (Penzes, Cahill, Jones, Vanleeuwen, & Woolfrey, 2011). Studies that use a behavioural assessment exhibit a strong correlation between cognitive dysfunction, neuronal spines, and branching (Luine, Villegas, Martinez, & McEwen, 1994; Park, Campbell, & Diamond, 2001; see also Malone et al., 2008).

Golgi Staining and Diabetes

Golgi-Cox staining has been used in GK rats previously (Li et al., 2013; Xiang et al., 2015). Dendritic spine morphology in the GK rat brain has been analysed in CA1 of the hippocampus. Dendritic spines in CA1 pyramidal neurons were compared between GK rats and control Wistar rats, where it was found that there were significantly fewer dendritic spines in GK

rats than in Wistar rats (Li et al., 2013; Xiang et al., 2015). In the STZ rat, dendritic length of pyramidal cells is significantly decreased (Martínez-Tellez, Gómez-Villalobos, & Flores, 2005). It has been shown through the use of Golgi staining, that there is significant loss of spines in the basilar tree of layer II/III in the parietal neocortex, as well as branching atrophy in the hyperglycaemic STZ rat (Malone et al., 2008). Number of dendritic spines in layer III of the prefrontal cortex, and layer IV of the occipital cortex in the STZ rat have also been found to be decreased relative to controls (Martínez-Tellez et al., 2005).

Present Study

The present study aimed to further understand the cognitive effect of T2DM on spatial memory and executive functioning by using the GK rat as a model for T2DM. Two behavioural tasks were utilized: the Morris water maze and the attentional set-shifting task. The Morris water maze was used to create a behavioural characterization of spatial memory impairments in the GK rat model, compared to the Wistar rat, while the attentional set-shifting task was used to create a behavioural characterization of executive functioning in the GK rat model as compared to a normal rat. Neuronal morphology within the DG of the hippocampus and layer II/III of the PrL was examined in both strains using the Golgi-Cox method. This research was conducted for the purpose of understanding 1) a behavioural characterization of the GK rat model of T2DM, and 2) revealing decreased morphology, if any, in associated brain regions of the GK rat model of T2DM.

Chapter 2: General Methods

In this chapter, the shared methods for the two behavioural experiments and histology methods are described. In the next two chapters, only methods and apparatus unique to each experiment will be elaborated on.

Ethics Statement

All applicable international, national, and institutional guidelines for the care and use of animals were followed. Research was approved by the Wilfrid Laurier University Animal Care Committee and followed the guidelines of the Canadian Council on Animal Care.

Subjects

A total of 16 animals including 8 Wistar rats (Charles River, QB, Canada) and 8 Goto-Kakizaki rats, bred in house (Wilfrid Laurier University, Waterloo, ON, Canada), were used (16 male). GK rats from the Wilfrid Laurier University colony did not display hyperglycaemia until 10 months of age, so rats aged 10 months were used for the MWM. Rats were housed in a humidity (50%) and temperature controlled (22°C) room on a 12-hour reversed light cycle with lights on at 7 p.m. For the water maze, rats were given *ad libitum* access to rat-chow (Teklad 8640 Rodent Chow, Envigo) and water. All rats were housed separately in individual cages. For the attentional set-shifting task, the same animals were used and were 11-12 months of age (mean age = 11.5 months; 16 male) at the start of the study as pairs were staggered to start in the task, since the attentional set-shifting task is a two-day task. Rats were given *ad libitum* access to water, and were food restricted based on the weight of the animal. All animals were food restricted for at least three days prior to the start of the experiment. Animals were weighed each day at the same time and given 15-20 g of rat chow each day for the days they were in the

experiment. Once finished day 2 of the task, rats were given *ad libitum* access to food. All rats were housed separately in individual cages with aspen sani chips as bedding.

Timeline of Present Study

See Figure 1. for a timeline of the methods used in this study. The 4-day MWM was run first followed by the attentional set-shifting task which involved day 1 habituation, day 2 series of shifts, and urine glucose the day after testing was finished for each rat. Urine glucose was measured for all rats the day before the MWM, the day after the MWM, and the day before food restriction started in all rats. Urine glucose was measured again the day after each rat finished the attentional set-shifting task day 2 as mentioned earlier, when they were no longer food restricted. All rats were sacrificed on the same day, and brains were put into the Golgi solution immediately after being sacrificed. Golgi solutions were refreshed and changed to sucrose for all rats on each of the corresponding days. Brain tissue was sectioned and stained in intervals and left to dry for 4 months or until the Permount (Fischer Chemical, Ottawa, ON, Canada) was cured.

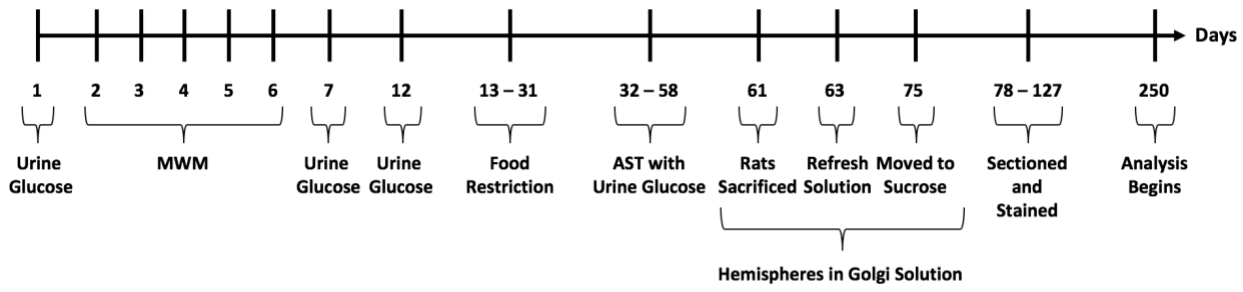

Figure 1. Timeline of the present study. Days 2 – 6 consisted of the 5-day MWM task, with the probe trial on Day 5, and visual trials on days 5 – 6. Urine Glucose was taken for a comparison before the attentional set-shifting task (AST) on Day 12. Rats were weighed and food restricted in the period between Days 13 – 31, and remained food restricted until completion of the series of shifts on day 2 of the attentional set-shifting task. From Day 32 – Day 58 rats were tested in

the attentional set-shifting task, where each rat had a habituation day, testing day, and urine glucose testing day. Rats were sacrificed on Day 61, where the hemispheres were placed in vials with Golgi-Cox solution immediately after being sacrificed. Golgi-Cox solutions were refreshed in all vials on Day 63 and were moved to vials containing a sucrose solution on Day 75. Sectioning waited until Day 78 when brain hemispheres sunk into the sucrose solution, where sectioning and staining mounted brain tissue occurred from Day 78 – Day 127. Stained brain tissue was light sensitive after staining and was kept in a dark place to fully cure until analysis of tissue began on Day 250.

Metabolic Measurements

Urinary glucose determinations were performed in all rats in the absence of fasting. Urinary glucose levels were measured by the Clarity Urocheck 2 GP reagent strip for urine (Diagnostic Test Group, Boca Raton, FL, USA). Glucose levels were determined by the colour change in the test strip from 5 mmol/L to a maximum of 110 mmol/L of glucose in urine. Urine glucose was tested one day before the start of the water maze, and again one day after the last day of the water maze for all rats. Individual rats were moved into empty plastic cages without bedding or environmental enrichment and given access to food and water. Samples of urine were tested by dipping the strip into urine in the cage. Urine glucose was tested on all rats in the absence of fasting before the start of the attentional set-shifting task, while on food restriction, and again one day after each individual rat completed day 2 of the attentional set-shifting task.

Golgi-Cox Staining

The materials and procedure used are as previously described (Gallitano et al., 2016; Gibb & Kolb, 1998). Animals were anesthetized under Isofluorane and decapitated with a guillotine, with brains extracted rapidly, rinsed in 0.9% saline and immersed in Golgi-Cox

solution for 14 days, and 30% sucrose for 3 days when brains could be sectioned. Brains were kept in sucrose solutions for a maximum of one month, then were sectioned on a microtome on the coronal plane at a thickness of 200 μm to ensure entire neurons and their arbour are within a section, and these sections were mounted on slides subbed with 2% gelatin. Tissue on the slides were covered with Parafilm to avoid moisture escaping and were blotted gently with Kimwipes (Kimberly-Clark Professional, Mississauga, ON, Canada). Slides were placed in a humid chamber in a darkroom. Coverslips were affixed to slides with Permount (Fischer Chemical, Ottawa, ON, Canada), and slides were left in a dark ventilated place for 4 months for the Permount to cure.

Fully impregnated cells were selected from each animal and imaged at 20x magnification in a z-stack using a bright-field microscope with attached XM10 camera using cellSens software (Olympus Corporation, Tokyo, Japan). Granule cells and pyramidal neurons were selected from brain regions associated with the behaviour investigated in this thesis. Cells were selected for imaging if they were identifiable based on morphology, clearly impregnated by the Golgi-Cox stain, and not obscured by other structures, where pyramidal neurons were selected if complete with all or most branches from both basilar and apical dendrites intact. Granule cells were selected from the septal third of the hippocampus (see Figure 2A; -2.28 mm to -3.24 mm from Bregma; Paxinos & Watson, 2007). Pyramidal neurons were selected from layer II/III of the prelimbic cortex (see Figure 3A; 5.16 mm to 2.52 mm from Bregma; Paxinos & Watson, 2007). Each of the histology analyses were conducted so the researcher was unaware of experimental groups, where a second researcher assigned random double letter combinations to each animal's slides and z-stacks.

Sholl Analysis

Dendritic arbour in the DG_{sp} and PrL layer II/III was measured using the Sholl technique (Sholl, 1953). This consisted of setting a region of interest (ROI) in the middle of the soma and centring concentric circles around it, 20 μm apart. For granule cells, the number of dendritic branches that intersected each concentric circle were counted to a maximal distance of 380 μm (see Figure 2B). For the pyramidal neurons, this consisted of two separate analyses, one for the basilar dendrites and the other for the apical dendrites. The number of dendritic processes, originating from the selected neuron, that passed through each concentric circle were counted separately for the basilar and apical dendrites, up to a maximal distance of 280 μm for basilar dendrites, and up to 380 μm for apical dendrites as no dendrites exceeded this length (see Figure 3B). Six fully impregnated cells were selected from the DG_{sp} and PrL layer II/III of each animal to measure dendritic arbour. ROI and concentric circles were placed on the z-stacked images using ImageJ (Schindelin et al., 2012), but due to the staining containing multiple neurons within each image the Sholl analysis was performed manually.

Branching Order

Centrifugal branching order was also calculated for all cells imaged. This involved numbering the branches originating from the soma to the terminals of each dendrite. Branches that originated from the soma were assigned the branch order of one, and subsequent branches from those dendrite bifurcations were assigned the branch order of two. In some cases, branches would trifurcate, and these branches would be given the same branching order. All successive branches from dendrite bifurcations were numbered sequentially to the dendrite terminal (Uylings et al., 1986; see Figure 2C). Branching order for PrL layer II/III neurons was performed separately for basilar and apical dendrites. For apical dendrites, a branch order of one was

assigned to the one apical dendrite originating from the soma, and subsequent branches from this bifurcation were counted as a branch order of two (see Figure 3C). For granule cells, branches were counted up to an order of 7, and for the pyramidal neurons the basilar dendrites were counted up to an order of 7 where apical dendrites were counted up to an order of 12.

Dendritic Spine Density

Dendritic spine density was obtained as previously described (Gallitano et al., 2016), at 100x under oil immersion. The length of the molecular layer in the DG_{sp} was divided into three equal sections corresponding with the IML, MML, and OML (see Figure 2B). A sample of six random 20-µm-long segments within each of the molecular layer zones in each cell imaged was used for dendritic spine density counts (see Figure 2A for an example). Dendritic spine densities were obtained for both the basilar and apical dendrites of layer II/III pyramidal neurons in the prelimbic cortex at 100x oil immersion. Spine density in the basilar dendrites was obtained by selecting random 20-µm-long segments within the breadth of the basilar dendrites of each animal, where six segments were counted per animal. The apical dendrites were divided into three equal sections corresponding to proximal, middle, and distal regions of the apical dendrites from soma to dendrite terminals respectively (see Figure 3B). The micrometre in the microscope eye piece was aligned with each dendritic segment, and all visible spines were counted manually within the segment (see Figure 3A for an example). In cases where a segment did not appear to be fully impregnated with Golgi-Cox solution, a different segment was chosen for counting spines.

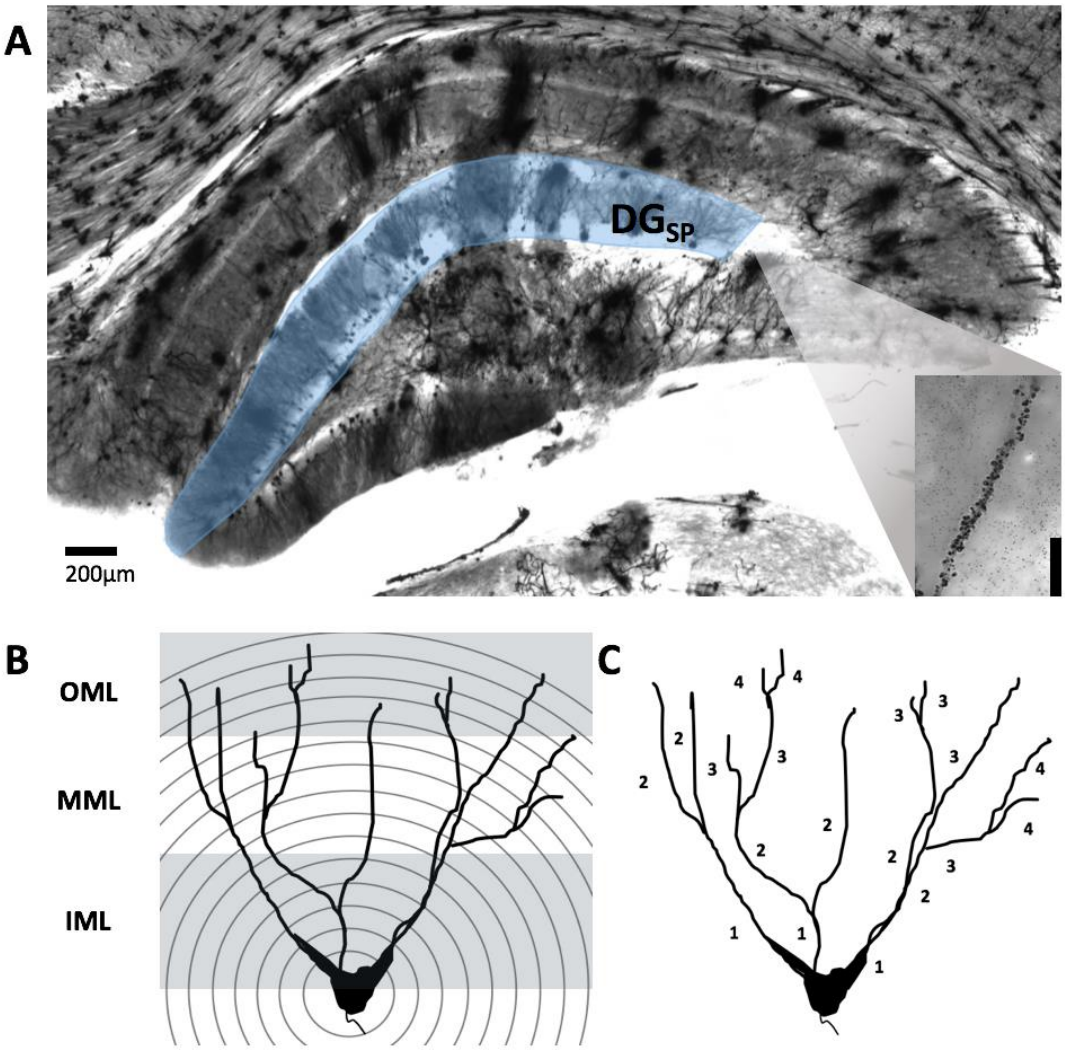

Figure 2. Overview of methods used in analysis of Golgi-Cox stained tissue. (A) Golgi-Cox stained tissue of a hippocampal slice, where granule cells were selected for analysis in the suprapyramidal blade of the dentate gyrus (blue overlay is the DG_{sp}; scale bar = 200 µm), random 20 µm-long-segments of dendrites were selected for spine density analysis in each of the molecular layers (example shown at lower right; scale bar = 20 µm). (B) Drawing of a granule cell with inner molecular layer (IML), middle molecular layer (MML), and outer molecular layer (OML) shown, demonstrating the Sholl analysis concentric circles. (C) Drawing of a granule cell with branching orders.

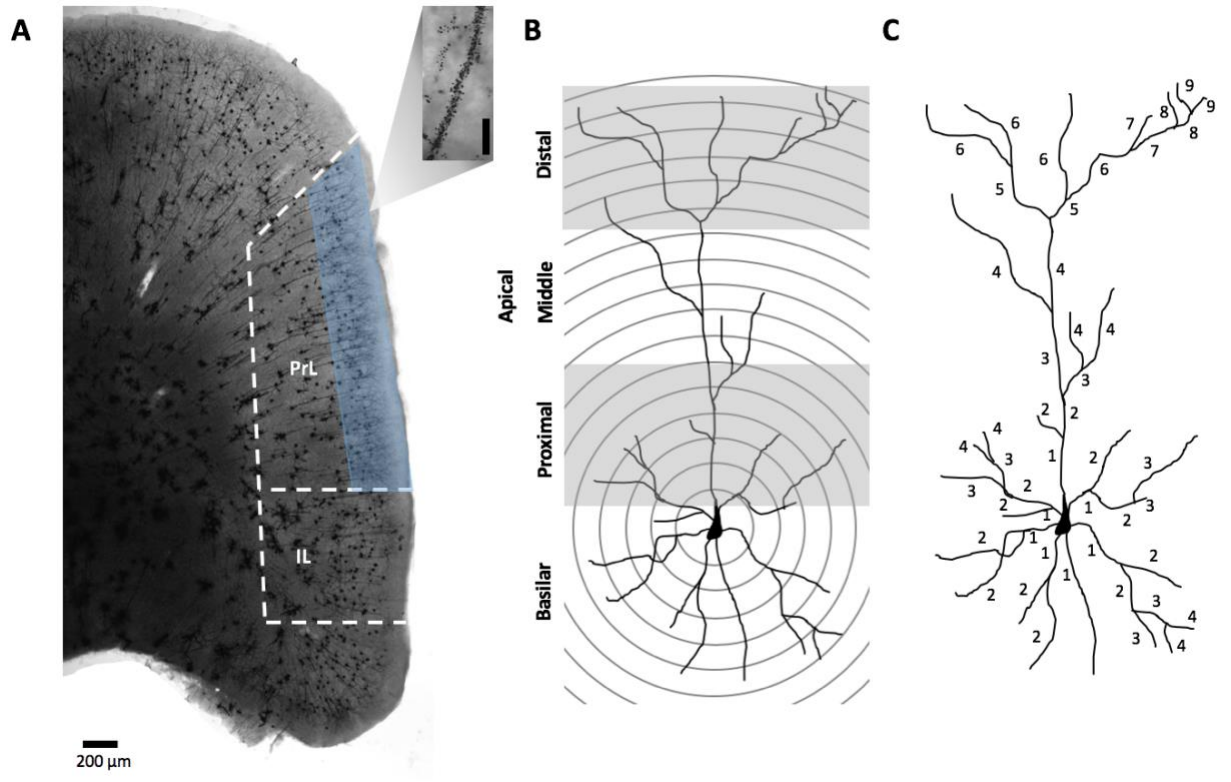

Figure 3. Summary of the methods used to analyse Golgi-Cox stained brain tissue. (A) Golgi-Cox stained brain tissue of a mPFC slice indicating the area of the prelimbic and infralimbic cortices, where pyramidal neurons were selected for analysis in the layer II/III of the prelimbic cortex (blue overlay is the PrL layer II/III; scale bar = 200 µm), random 20 µm-long-segments of dendrites were selected for spine density analysis from the basilar dendrites, and from the proximal, middle, and distal areas of the apical dendrites (example shown at upper right; scale bar = 20 µm). (B) Drawing of a pyramidal neuron with the basilar and proximal, middle, and distal areas of the apical dendrites shown, demonstrating Sholl analysis with concentric circles. (C) Drawing of a pyramidal neuron with branching orders for basilar and apical dendrites.

Chapter 3: Spatial Memory and Functional Association with Dentate Gyrus

Introduction

In the latest quinquennial report by the World Health Organization (WHO, 2016), diabetes mellitus was named as the sixth leading cause of death worldwide, where its impact has doubled since 2000. T2DM accounts for 90-95% of all diabetes cases (Centers for Disease Control and Prevention, 2017), and is characterized by hyperglycaemia, insulin resistance, as well as a slow onset developing later into adulthood (Canadian Diabetes Association, 2019). There is a risk of co-morbidity with T2DM, as the incidence of dementia, including Alzheimer's disease, is higher in patients with T2DM (Biessels et al., 2006; Kopf & Frölich, 2009). Diabetes has been proposed as a form of accelerated aging, whereby its presence accelerates the normal aging process (Kent, 1976). Since spatial memory is already vulnerable to the aging process (Moffat, 2009), it is therefore important to study the mechanisms by which these diseases act, to provide insight into how we can lessen the effects of T2DM.

Studies linking behaviour with the underlying mechanisms of diabetes in a rat model of T2DM are lacking. A model of T2DM called the GK rat is bred to be spontaneously hyperglycaemic (Goto et al., 1975; Goto and Kakizaki, 1981). The onset of hyperglycaemia in GK rats ranges between 3-4 weeks after birth (Movassat et al., 1995), where hyperglycaemia and glucose intolerance remains stable for at least 18 months (Berthelier et al., 1997). GK rats display impaired insulin secretion consistent with an early stage of human T2DM (Kimura et al., 1982).

One area of cognitive dysfunction in GK rats that has not been well studied is spatial memory and the mechanisms associated with possible cognitive deficits. A virtual version of the animal MWM task, has been used in humans to test spatial memory. Patients with unilateral

hippocampal removals to treat intractable epilepsy have been found to experience deficits in this task (Astur et al., 2002). Lesions specifically to the parahippocampal cortex suggest that this area in humans is critical for spatial memory (Ploner et al., 2000). Patients with T2DM have cognitive impairments in association with subcortical ischemic changes in the brain, and increased brain atrophy (Manschot et al., 2006). In humans, there is evidence of cognitive decline associated with diabetes in comparison to controls (Cukierman-Yaffe, 2014), as well as increased general brain atrophy (Araki et al., 1994). Individuals with T2DM have been shown to have mixed results in the literature of impaired and spared spatial memory (Stewart & Liolitsa, 1999). However, most of the studies looking at spatial memory investigate visuospatial abilities, which include tasks where participants construct or organize objects and designs, where most of the differences in performance in these studies are not significant (Awad et al., 2004). It can be argued that spatial memory includes other types of spatial abilities, such as memory for places and navigation. In a self-assessment study, adults with diabetes did not indicate difficulty with memory for places (Tun, Perlmuter, Russo, & Nathan, 1987). More recently, an fMRI study investigating spatial working memory suggested impaired spatial working memory, and mild cognitive dysfunction in middle-age T2DM patients as compared to controls (Huang et al., 2016).

In the ‘Can test’ task, a novel spatial/object learning and memory task where rats were trained to choose a can with a certain print on the front of the can to obtain a reward of water, hyperglycaemic streptozotocin (STZ) rats experienced increased deficits as the task difficulty increased (Popoviç et al., 2001). Ten weeks of untreated hyperglycaemia in STZ rats produces a spatial learning impairment in a water maze task (Biessels et al., 1996). Although, it has been previously illustrated that GK rats have a deficit in the MWM, where GK rats spend an equal

amount of time swimming in each quadrant versus controls which spend more time in the target quadrant (Li et al., 2013; Xiang et al., 2015), these studies used escape latencies instead of path length. Escape latencies are known to increase with motor deficits (Anisman, DeCatanzaro, & Remington, 1978; Conquet et al., 1994), and GK rats are known to have peripheral neuropathy, and motor impairments (Murakawa et al., 2002; Suzuki, Saito, Sakata, Toyota, & Goto, 1990; Suzuki et al., 1990), so path length is the measure that is reported in the current study.

It is important to look at the individual performance in each trial because rats are known to employ search strategies (Graziano, Petrosini, & Bartoletti, 2003). Although rats with impaired hippocampal function use more spatially imprecise strategies (Gil-Mohapel et al., 2013), and never learn the location of the platform, these strategies can alter escape latencies in that some strategies take less time as they are much more efficient than random search (Gallagher, Burwell, & Burchinal, 2015), making escape latencies an inaccurate measure of the animal's cognitive function.

The dentate gyrus (DG) is suggested to reduce interference during acquisition of new spatial memories (Goodrich-Hunsaker et al., 2008; Nakazawa et al., 2004; Scoville & Milner, 1957; Squire et al., 2004). The DG can be divided along the transverse axis into two distinct areas, the DG_{sp} and DG_{ip} blades. Granule cells from the DG_{sp} have greater dendritic length and dendritic spine density than cells from the DG_{ip} (Desmond & Levy, 1982; Green & Juraska, 1985; Seress & Pokorny, 1981). The arbour of granule cells can be divided into three sections from closest to farthest from the soma, the IML, the MML, and the OML (Amaral et al., 2007). The MML conveys more spatial information than the OML (Knierim et al., 2014), where the MML has more dendritic arbour in rats than the OML (Gallitano et al., 2016). As a part of the perforant path, the dentate gyrus carries spatial information, where there is an increased input of

to the DG_{sp} in particular (Gallitano et al., 2016). Rats with blocked neurogenesis specifically in the dentate gyrus are impaired on spatial memory in long-term retention using the MWM (Jessberger et al., 2009).

The present study was designed to validate the GK rat as a model of T2DM by characterizing the spatial memory deficit seen in GK rats using path length, and to explore some of the mechanisms that underlie this cognitive dysfunction to shed light on the processes in individuals living with diabetes. DG granule cells are particularly sensitive to aging (Shetty & Turner, 1999), so if T2DM is a form of accelerated aging (Kent, 1976), then we propose that granule cells in the DG, an area associated with neurogenesis, are vulnerable to the presence of T2DM. In the present study, staining of brain tissue following the Golgi-Cox method was conducted, and granule cell morphology in the DG_{sp} was compared between GK and Wistar rats to understand the level of impact hyperglycaemia has on morphology in this region.

Materials and Methods

Morris water maze.

The apparatus was similar to that described elsewhere (Morris, 1981, 1984), consisting of a circular pool made out of sheet metal, filled with tap water and coloured with blue children's finger paint until opaque. The pool was 183 cm in diameter, and 63.5 cm high. A metal platform was 13 cm in diameter, and 41 cm high hidden under the surface of the water. The pool was filled to around 43 cm high with water. The walls in the room were labelled the directions North (N), South (S), East (E), and West (W). The platform was located in NW quadrant for the entirety of the spatial training trials. Distal cues were placed around the room, Overhead lights were turned off to minimize rat stress, and the door to the water maze room was kept open with outside lights on, as well as a light affixed to the West wall. Data was collected using ANY-maze

Video Tracking System version 4.72 (Stoelting Co., Wood Dale, IL, USA), and recorded with a camera affixed to the ceiling above the pool.

Rats were placed at the start of each trial in the pool facing the wall of the pool according to the corresponding pseudo random direction (N, S, E, W). Habituation trials only occurred on the first day of the task, where rats were placed on the platform for 60 s. In the training trials, there were two sets of three trials for each of the 4 days, where rats were given 60 s to find the platform. Rats that were unsuccessful were gently guided to the platform. After each training trial, regardless of whether the rat found the platform, the rat remained on the platform for 30 s. On the probe trial, which occurred on day 4 after the end of the training trials, the platform was removed. Rats were given 60 s to swim before being removed from the water maze. The path length in each quadrant was recorded. Visual trials were conducted for two days, water maze days 4 and 5, consisting of two sets of three trials per day. The platform was made visible by lowering the water level until the top of the platform was visible.

Search strategies.

Search strategies were classified manually into nine mutually exclusive categories, by a researcher unaware of the experimental groups, by visually identifying the pattern of movement in each trackplot during the spatial training days of the water maze. There is much inconsistency in the literature about what to call each strategy, and what type of movement is considered a strategy, so for the purpose of this study exemplars in prior research (Brody & Holtzman, 2006; Garthe, Behr, & Kempermann, 2009; Gil-Mohapel et al., 2013; Graziano et al., 2003; Janus, 2004), were compared to form a classification guide. Strategies used were as described below (see Figure 4): direct finding (DF; Figure 4A), swimming directly to the platform without re-orienting position; focal search (FS; Figure 4B), searching in a focal region in the target

quadrant; approaching target (AT; Figure 4C), swimming straight then looping once or twice to re-orient position via extramaze distal cues and swimming directing to the platform; chaining (Ch; Figure 4D), circling the pool in the inner third passing through the location of the platform; scanning (S; Figure 4E), swimming back and forth in the inner third of the pool; random search (RS; Figure 4F), there is no visible pattern in the movements of the animal; thigmotaxis (Th; Figure 4G), circling the pool on the outer edge of the wall; perseverance (P; Figure 4H), searching in a focal region in a quadrant other than the target quadrant; circling (C; Figure 4I), tight loops across the surface of the water.

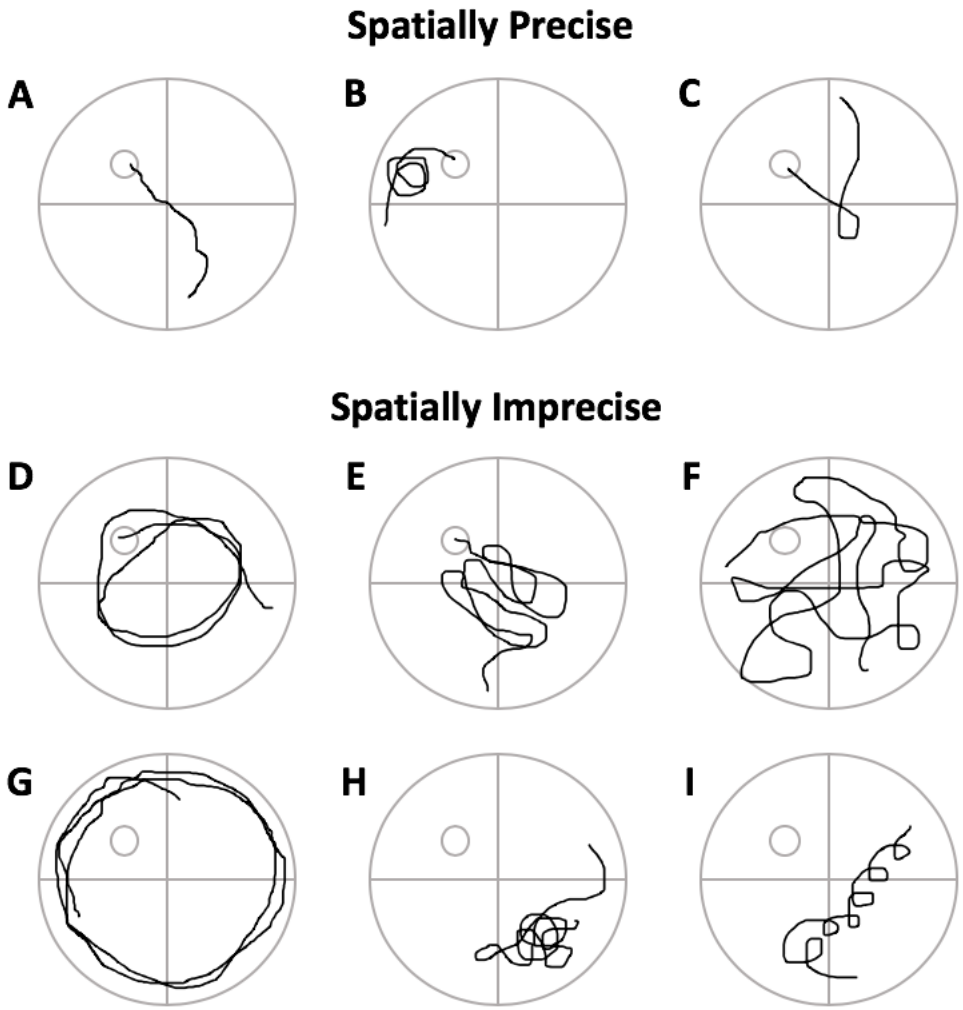

Figure 4. Schematic examples of nine water maze search strategies. (A) Direct finding (DF). (B) Focal search (FS). (C) Approaching target (AT). (D) Chaining (Ch). (E) Scanning (S). (F) Random search (RS). (G) Thigmotaxis (Th). (H) Perseverance (P). (I) Circling (C).

After categorizing each trackplot, the strategies were further classified into whether the search strategy was spatially precise or spatially imprecise based on that described earlier (Gil-Mohapel et al., 2013). Spatially precise strategies included AT, DF, and FS, whereas Th, Ch, RS, C, S, and P were all classified as spatially imprecise strategies. From here precise and imprecise strategies were calculated by coding precise strategies as 1 and imprecise as 0.

Results

Urine glucose.

Statistical analyses were performed using Excel (Microsoft Office 2010, Mississauga, ON, Canada), and SPSS Statistics Version 24 (IBM Corp., Armonk, NY, USA). In each subsequent analysis of variance (ANOVA) the between-subjects factor was strain. All effects are reported as significant at $p < .05$. Urinary glucose was analysed in a 2(Time: before, after) x 2(Strain: GK, Wistar) mixed factorial repeated measures ANOVA, where the dependent variable was urine glucose measured in mmol/L (see Figure 5A for results). This ANOVA revealed a significant main effect of time, $F(1,14) = 64$, $p < .001$, $\eta_{p2} = .821$ (effect size = 2.14; power = 1), and a significant main effect of strain, $F(1,14) = 23.60$, $p < .001$, $\eta_{p2} = .628$ (effect size = 1.3; power = 1), on level of urinary glucose. There was also a significant time by strain interaction, $F(1,14) = 64$, $p < .001$, $\eta_{p2} = .821$ (effect size = 2.14; power = 1). To understand the nature of the interaction, simple effects analyses were conducted. The simple effect of time on urine glucose levels was significant for GK rats, $F(1,14) = 128$, $p < .001$, where GK rats had significantly lower urine glucose after the MWM. Simple contrasts with a Bonferroni adjustment illustrate

that GK rats had significantly greater urine glucose than Wistar rats both before the MWM, $p < .001$, 95% CI [48.152, 102.598], and after, $p = .006$, 95% CI [10.419, 52.331].

Morris water maze.

Spatial training data collected from the 4 training days was analysed using a 2(Strain: GK, Wistar) x 4(Day: day 1, day 2, day 3, day 4) mixed factorial repeated measures ANOVA, with path length as the distance travelled to reach the platform as the dependent variable. Average path length by day was calculated by averaging the distance travelled in each of the six 60 second trials per day (see Table 1). Mauchly's Test of Sphericity was violated, $\chi_2(5) = 14.496$, $p = .013$, therefore, a Greenhouse-Geisser correction was used ($\varepsilon = .729$). There was a significant main effect of day, $F(2.186,30.6) = 11.153$, $p < .001$, $\eta_{p2} = .443$ (effect size = .892, power = 1), on path length travelled, where each strain showed improvement over the 4 training days. There was no significant main effect of strain, $F(1,14) = 1.971$, $p = .182$, $\eta_{p2} = .123$ (effect size = .375, power = .423), and no significant day by strain interaction, $F(2.186,30.6) = .704$, $p = .514$, $\eta_{p2} = .048$ (effect size = .225, power = .424).

Table 1

Means, standard errors, and confidence intervals for MWM spatial learning

Strain	Training Day	M	SE	95% CI	
				Lower	Upper
Wistar	1	9.381	.978	7.284	11.479
	2	7.527	.778	5.859	9.195
	3	4.585	.608	3.281	5.888
	4	5.642	1.028	3.436	7.847

GK	1	10.272	.978	8.174	12.369
	2	7.292	.778	5.624	8.960
	3	6.150	.608	4.846	7.453
	4	7.554	1.028	5.348	9.759

Note: The values represent path length to reach the platform in the target quadrant

Performance in water maze probe trials was analysed by using an independent-samples t-test comparing the distance travelled in the target quadrant between strains (see Figure 5B for results). There was a significant difference between groups, $t(14) = -2.309$, $p = .037$, where GK rats swam less in the target quadrant ($M = 5.057$, $SD = 2.111$), than Wistar rats ($M = 7.208$, $SD = 1.578$). A paired-samples t-test was calculated for both strains comparing the path length in the target and opposite quadrants. The paired-samples t-test revealed that Wistar rats swam more in the target quadrant than the opposite, $t(7) = 5.286$, $p = .001$ (effect size = 3.457, power = 1), whereas GK rats did not, $t(7) = 2.344$, $p = .052$ (effect size = .403, power = .19).

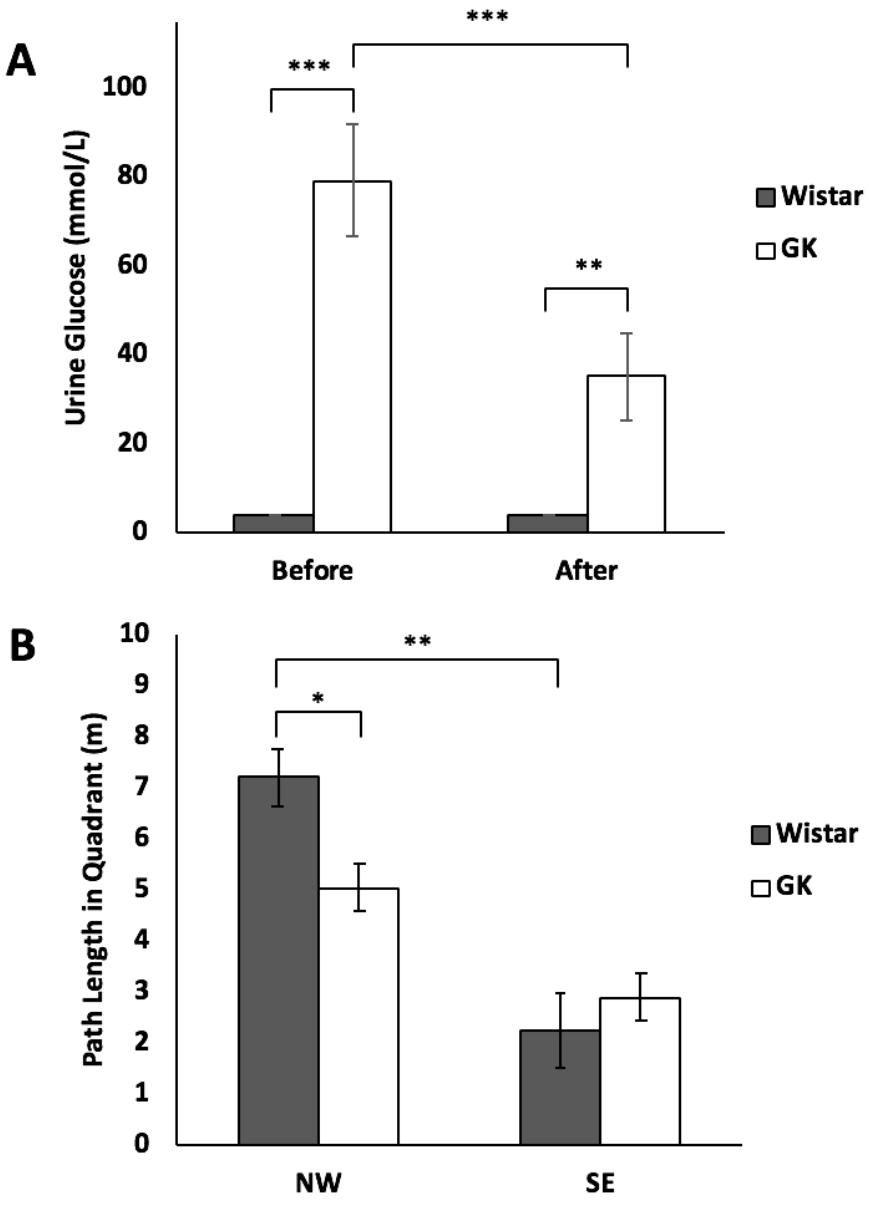

Figure 5. Metabolic and behavioural measurements. (A) Urine glucose measurements in mmol/L taken before and after the MWM for GK and Wistar rats. (B) Average path length in the target (NW) and opposite (SE) quadrants for both strains in the probe trial of the MWM.

Visual training trials were analysed in a 2(Strain: GK, Wistar) x 2(Day: day 1, day 2), repeated measures ANOVA (data not shown). There was no significant main effect of training day, $F(1,14) = 3.621$, $p = .078$, $\eta_{p2} = .206$ (effect size = .509, power = .966), no significant main

effect of strain, $F(1,14) = 1.043$, $p = .325$, $\eta_{p2} = .069$ (effect size = .272, power = .216), and no significant day by strain interaction, $F(1,14) = .428$, $p = .524$, $\eta_{p2} = .030$ (effect size = .176, power =.259).

Search strategies.

The search strategies for the Morris water maze were coded from 1 to 9 (DF, FS, AT, Ch, S, RS, Th, P, C respectively), and swim strategy frequencies were compared across trials within each strain by using Friedman's test (see Figure 6). By the end of the four training days, both GK, $\chi_2(23) = 36.332$, $p = .038$, and Wistar rats, $\chi_2(23) = 54.545$, $p < .001$, replaced spatially imprecise strategies with more spatially precise ones. In addition, search strategies were coded as either spatially precise or imprecise, and the cumulative percentage increase of precise search strategies between days 1 and 4 were calculated for both GK and Wistar rats. Here GK rats increased use of precise strategies by 25.76%, and Wistar rats increased use of precise strategies more by 114.34%. Precise search strategies were coded as 1, and imprecise strategies as 0, where the number of precise strategies was summed for each spatial training day. Number of spatially precise strategies was compared between strains for the 4 days in separate independent-samples t-tests. There was no significant difference in the number of spatially precise strategies used for GK and Wistar rats on day 1, $t(14) = .424$, $p = .678$ (effect size = .212, power = .107), and day 2, $t(14) = -.323$, $p = .751$ (effect size = .168, power = .093). However, GK rats used significantly less spatially precise strategies on day 3, $t(14) = -3.144$, $p = .007$ (effect size = 1.571, power = .91), and on day 4 but this difference was not significant, $t(14) = -2.104$, $p = .054$ (effect size = 1.052, power = .639).

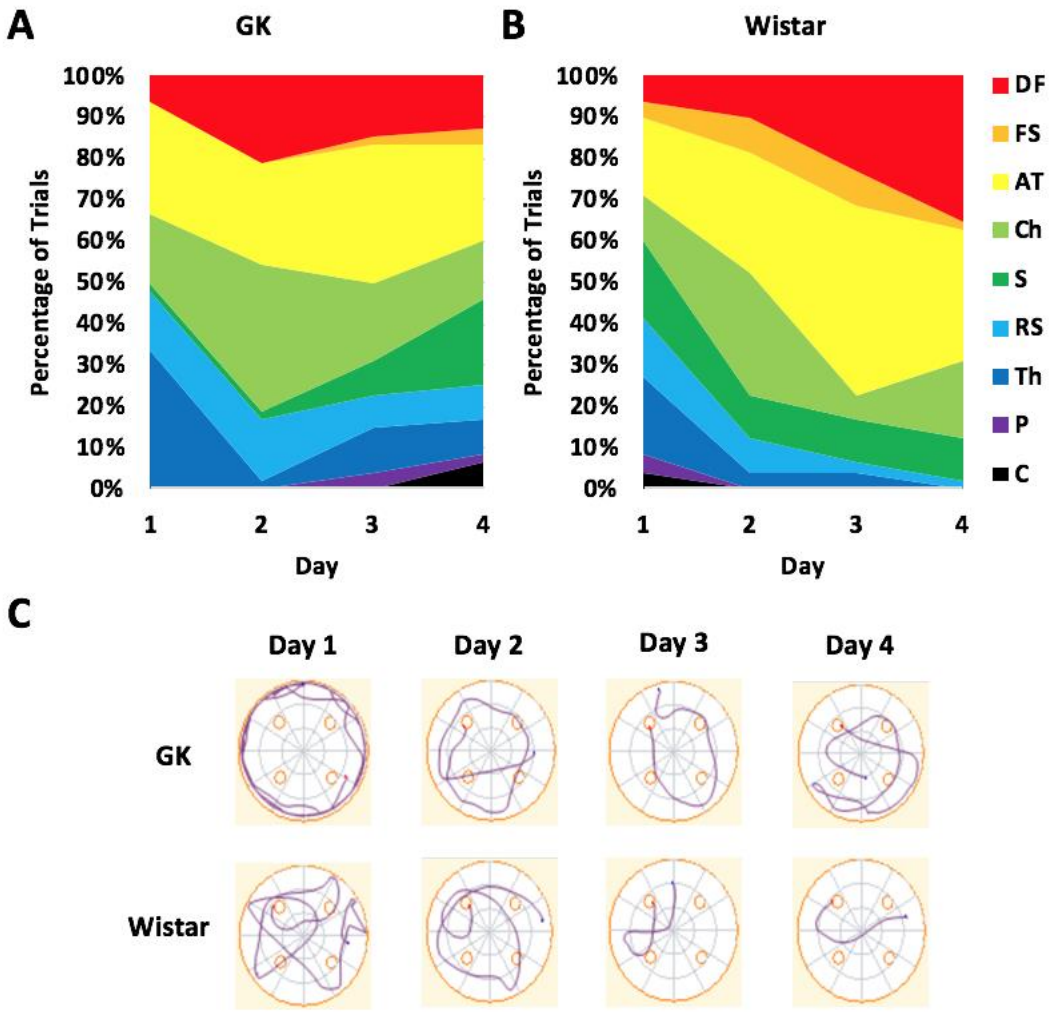

Figure 6. Search strategies used in the MWM. (A) Percentage trials classified in each search strategy across all four days of training for both GK rats, and (B) Wistar rats (see section 4.5 for abbreviations of search strategies). (C) Representative examples of search strategies employed during each day.

Golgi-Cox analyses.

Sholl analysis for granule cells was conducted manually using FIJI for ImageJ (Schindelin et al., 2012), by recording the number of dendritic processes in six randomly imaged granule cells per animal through each 20 µm concentric circle until 380 µm. Sholl analysis for all

rats was randomly split into two and blindly coded by two researchers. A two-way mixed intraclass correlation coefficient for consistency was calculated, where there was a high degree of consistency, Cronbach's $\alpha = .975$. Results were averaged per animal as well as per intersection and were analysed using a 2(Strain: GK, Wistar) x 19(Intersection: 20 μm - 380 μm in 20 μm increments) mixed factorial repeated measures ANOVA, where the dependent variable was number of intersections (see Figure 7A for results). There was a significant main effect of intersection, $F(18,252) = 99.436$, $p < .001$, $\eta_{p2} = .877$ (effect size = .2.67, power = 1), and a significant main effect of strain, $F(1,14) = 14.681$, $p = .002$, $\eta_{p2} = .512$ (effect size = .1.024, power = .999), on the number of dendritic processes through each intersection. There was also a significant strain by intersection interaction, $F(18,252) = 6.078$, $p < .001$, $\eta_{p2} = .303$ (effect size = .659, power = 1). Post hoc simple effects analyses were conducted to understand the interaction. The simple effect of intersection on number of dendritic processes was significant for GK rats, $F(18,252) = 29.8$, $p < .001$, and for Wistar rats, $F(18,252) = 75.71$, $p < .001$. Simple contrasts illustrated that compared to Wistar rats, GK rats had less dendritic processes (see Figure 3A for significance).

Branching complexity up to an order of 7 was collected for each z-stacked image of a granule cell, where the number of branches of each order were recorded, and the same images from the Sholl analysis were used. Branching order was coded blindly by two researchers, where the rats were split up randomly. To assess inter-rater reliability, a two-way mixed intraclass correlation coefficient for consistency was calculated. There was a high degree of consistency between the two coders, Cronbach's $\alpha = .941$. Branching order was calculated by averaging the number of branches of each order across strains and was analysed in a 2(Strain: GK, Wistar) x 7(Branch Order: 1 - 7) mixed factorial repeated measures ANOVA, where the number of

branches was the dependent variable (see Figure 7B). Mauchly's Test of Sphericity indicated the assumption of sphericity was violated, $\chi_2(20) = 61.698$, $p < .001$, therefore the Greenhouse-Geisser correction was used ($\varepsilon = .419$). Levene's Test of Equality of Error Variances was significant for a branch order of 7, $F(1,14) = 14.824$, $p = .002$. There was a significant main effect of branch order, $F(2.512,35.163) = 112.348$, $p < .001$, $\eta_{p2} = .889$, and a significant main effect of strain, $F(1,14) = 23.38$, $p < .001$, $\eta_{p2} = .975$, on number of branches. The ANOVA also revealed a significant branch order by strain interaction, $F(2.512,35.163) = 3.095$, $p = .047$, $\eta_{p2} = .181$. To further understand the interaction simple effects analyses were conducted. The simple effects for branch order on number of branches was significant for both GK rats, $F(6,84) = 45.63$, $p < .001$, and Wistar rats, $F(6,84) = 69.81$, $p < .001$. Simple contrasts revealed that at a GK rats have less branching complexity than Wistar rats at a branch order of 1, $p = .021$, 95% CI [-1.522, -.145], at a branch order of 2, $p = .026$, 95% CI [-2.331, -.169], at a branch order of 3, $p = .003$, 95% CI [-2.899, -.726], at a branch order of 4, $p = .011$, 95% CI [-3.961, -.622], at a branch order of 5, $p = .003$, 95% CI [-4.197, -1.053], at a branch order of 6, $p = .004$, 95% CI [-1.933, -.442], and at a branch order of 7, $p = .037$, 95% CI [-.724, -.026].

Granule cell spine densities were collected by taking six random samples from each of the three molecular layers in the DG_{sp}. These were then averaged across strains in each layer and were analysed in three independent t-tests comparing the average number of spines between both strains in each molecular layer. Comparisons were not made within each strain, as prior research suggests that there is no significant difference between the spine densities of each molecular layer in the DG_{sp} (Gallitano et al., 2016). For results see Figures 7C and D. GK rats had significantly less dendritic spines in the IML ($M = 10.292$, $SD = 2.278$), compared to Wistar rats ($M = 23.708$, $SD = 2.156$); $t(14) = -12.099$, $p < .001$ (effect size = 6.049, power = 1). In the

MML, GK rats had less dendritic spine density (M = 11.604, SD = 2.018), than Wistar rats (M = 22.125, SD = 1.097); $t(14) = -12.956$, $p < .001$ (effect size = 6.478, power = 1). There was significantly less spine density in the GK rats in the OML, (M = 11.5, SD = 1.306), than Wistar rats (M = 23.979, SD = 1.424); $t(14) = -18.267$, $p < .001$ (effect size = 9.134, power = 1).

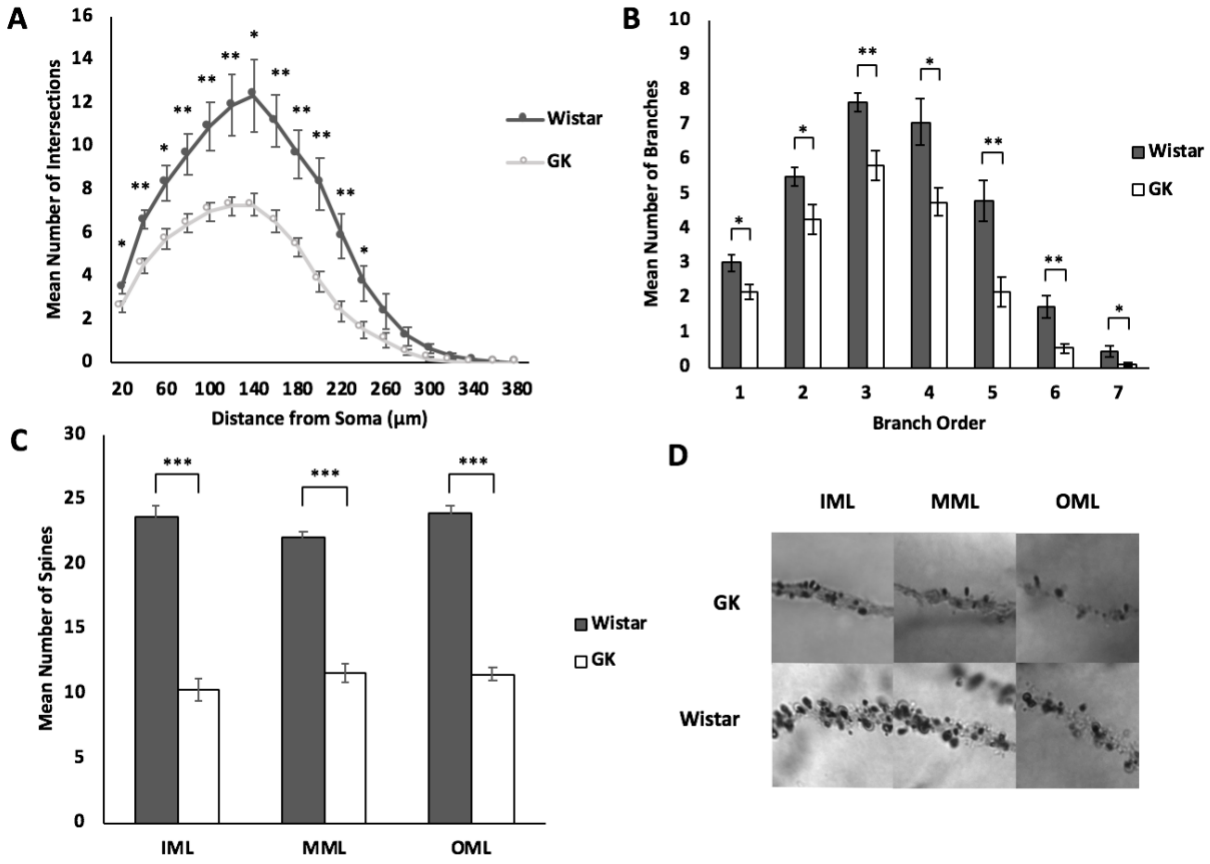

Figure 7. Quantification of Golgi-Cox stained granule cell measurements. (A) Sholl analysis illustrates the deficit of dendritic material in the IML and MML areas. (B) Branching order shows GK rats have fewer branches of each order than Wistar rats. (C) Dendritic spine density is decreased in each area for GK rats. (D) Representative 20-µm-long segments from DG_{sp} granule cell dendrites showing a comparison of dendritic spines from both strains in each molecular layer.

Discussion

In this study, the MWM was utilized to provide a behavioural characterization of the spatial memory deficits in the GK rat model of T2DM. Golgi-Cox staining was conducted to provide insight into some of the mechanisms by which cognitive deficits appear in individuals that have T2DM. The results in this study suggest that spatial learning is spared when looking at the measure of path length, but impaired when looking at individual search strategies in the GK rat model of T2DM. Spatial memory retrieval is impaired in the GK rat model of T2DM. The results of this study also suggest that there are morphological changes in the granule cells in the DG_{sp} of the GK rat, as dendritic arbour, branching complexity, and dendritic spine density are decreased in this model of T2DM.

Urinary glucose was tested a day before and a day after the MWM. As seen in Figure 5A, GK rats had a higher urine glucose level than Wistar rats both before and after the MWM, however, the level of urine glucose was significantly decreased for GK rats after the MWW. Although it was expected that the GK rats have higher urine glucose than Wistar rats, the decrease in urine glucose after water maze exposure supports prior literature that exercise lowers glucose levels in those with diabetes (Sigal et al., 2006). This result was surprising in that some of the GK rats in this study that were hyperglycaemic before the MWM were no longer hyperglycaemic afterwards. Others have suggested that exercise is a preventative measure for T2DM (Tudor-Locke & Schuna, 2012). Whether or not a change in exercise is combined with a change in diet, these regimes have been shown to be equally effective in reducing progression of impaired glucose tolerance to diabetes (Sigal et al., 2006; see also Pan et al., 1997). However, it is suggested that the effect is only temporary (Schneider, Amorosa, Khachadurian, & Ruderman,

1984), and unless the exercise regime is kept-up, glucose tolerance decreases (Rogers et al., 1988).

Learning over the four spatial training days of the MWM was improved by both strains, as path length to reach the platform decreased over the 4 training days (see Table 1). However, the expected decreased performance by GK rats in comparison to Wistar rats was not seen, as they performed equally to Wistar rats. This finding is contrary to those in prior studies, where GK rats experienced a deficit in spatial learning in the MWM (Li et al., 2013; Xiang et al., 2015). It is proposed that this deficit may be more protocol and measure dependent than cognitive dysfunction related. In one study, each of four consecutive trials for a total of 5 training days were separated by 5 min, and trials were allowed to continue to a maximum of 120 s, where the rat would remain on the platform for 15 s; if the rat failed to find the platform it would be gently guided to the platform where it would remain for 15 s (Li et al., 2013). In another study, this exact protocol was repeated with the exception of the 5 minute intertrial interval (Xiang et al., 2015). In the present study, rats were allowed half the time to swim to find the platform. If there was going to be an effect, it would be seen with a shorter amount of time, because if the rat does not know the location of the platform at 60 s, it will not know the location at 120 s. It is therefore a result of chance, and not an actual measurement of learning. In these prior studies, escape latencies were used instead of path length, which may also explain the difference in performance.

Spatial memory, as measured in the probe trial of the MWM, revealed that Wistar rats had an increased path length in the target quadrant than the opposite quadrant, where this difference was not observed in GK rats. GK rats also travelled less in the target quadrant than Wistar rats (see Figure 5B). This finding supports the prior literature mentioned above (Li et al.,

2013; Xiang et al., 2015). We propose there is a spatial memory deficit in the GK rat model of T2DM. The spatial memory deficit may be related at the cellular level as hippocampal extracellular glucose concentrations are associated with the complexity of spatial memory tasks (McNay, Fries, & Gold, 2000). In humans with diabetes, there are mixed results of a spatial memory deficit (Stewart & Liolitsa, 1999), however, it appears that visuospatial memory is spared (Messier, 2005), where spatial working memory involving location may be impaired (Ryan et al., 2006), although more research into this field is needed. Cognitive dysfunction associated with T2DM increases with age unless it is treated before the age of 70 (for a review see Messier, 2005). It appears that the spatial memory deficit is lessened when metabolic control is regained in those with T2DM (Ryan et al., 2006). Since the MWM is highly dependent on the hippocampus, an area thought to be associated with memory, perhaps the spatial memory deficit is suggestive of a wider memory deficit in those with T2DM.

In the visual trials of the MWM, where the water level was lowered to reveal the platform, there was no improvement in path length to reach the platform across the two days, and no difference between GK and Wistar rats. This may suggest that there is no impairment in visual acuity in either strain at the time of testing, but it should be noted that effect size and power for the main effect of strain and the interaction was low. Visual acuity and retinopathy issues are associated with both types of long-term diabetes (Lövestam-Adrian, Agardh, Torffvit, & Agardh, 2001; Voutilainen-Kaunisto, Teräsvirta, Uusitupa, & Niskanen, 2001), where visual acuity was lower in patients with T2DM than controls, and the frequency of retinopathy was considerably higher at a 10-year-follow-up (Voutilainen-Kaunisto et al., 2001), which may explain the low power and effect size.

Search strategies in the MWM across the four training days were classified in nine mutually exclusive categories (see Figure 4), where the percentage of trials classified as precise increased over the four days of the water maze for both strains (see Figure 6). GK rats employed less precise strategies towards the end of the spatial training days of the MWM. A possible explanation for this behaviour is that through the days of the water maze training, Wistar rats possibly became more in tune or paid more attention to their spatial orientation than the GK rats. As spatial learning was analysed by path length, where there was no difference in path length between the GK and Wistar rats, this contrasts with the search strategy results that GK rats use less precise strategies than Wistar rats particularly on days 3 and 4. Perhaps some imprecise strategies took less path length to reach the platform, which would mean that path length was incorrectly reporting no difference in performance when the rats were using different strategies altogether.

There is usually a strong correlation between neuronal dendritic spines or branching atrophy and cognitive dysfunction (Park et al., 2001). Where dendritic atrophy and neuroplasticity can be determined from the analysis of dendritic spines (Fiala, Spacek, & Harris, 2002). In the present study, dendritic arbour of the granule cells in the DG_{sp} was decreased in the IML and MML for GK rats compared to Wistar rats (see Figure 7A). Branching complexity, as measured by the number of branches up to 7 branching orders, showed that GK rats had less branches than the control Wistar rats in each of the 7 branch orders (see Figure 7B). Dendritic spine density in each of the three molecular layers was decreased in GK rats as compared to Wistar rats (see Figure 7C and D). These findings suggest morphological changes in the dentate gyrus are associated with hyperglycaemia, but this deficit is not limited to the dentate gyrus. When exposed to hyperglycaemia at a young age of 4-8 wk, Wistar rats experienced smaller

sized cortical neurons (Malone, Hanna, & Saporta, 2006). Hyperglycaemia in rats produced changes in morphology of the basilar layer II/III pyramidal neurons, and impaired long-term spatial memory (Malone et al., 2008). A review of fMRI studies in humans with T2DM revealed that the most common result was reduced mode network connectivity, and among some of the correlations in studies noted were spatial memory impairments (Macpherson et al., 2017). These findings suggest that there are morphological changes in the dentate gyrus that are not associated with major spatial learning impairments, but with the association of spatial memory retrieval impairments.

A limitation of the current study is the use of urine glucose strips instead of a blood glucose meter. The urine glucose strips were not precise enough to detect changes in the Wistar rat urine glucose, if there was any change at all. It would also be of benefit to precisely see how long the exercise effect lasted for the GK rats, as literature suggests in other models of diabetes this is a temporary effect (Schneider et al., 1984).

As part of the perforant path, the dentate gyrus receives information from the medial perforant path, which contains spatial cells including head direction cells (Taube, 2007), boundary cells (Savelli, Yoganarasimha, & Knierim, 2008), and grid cells (Moser et al., 2014), where the lateral perforant path contains non-spatial cells (Knierim et al., 2014). The medial perforant path responds to spatial tasks (Hunsaker, Mooy, Swift, & Kesner, 2007), where the MML carries more spatial information that the OML (Knierim et al., 2014). Since the dendritic spines and morphology was decreased in the MML, perhaps this pathway is impaired in the GK rat model of T2DM and by extension individuals with T2DM. As few studies have examined the behaviour and hippocampal morphology of the GK rat, more research needs to be conducted examining the cognitive dysfunction associated with this model of T2DM.

Chapter 4: Set-Shifting and Functional Association with Prelimbic Cortex

Introduction

With T2DM becoming ever more present in our society, studies of the effects of this illness on cognitive function are becoming a necessity. The deficits of executive function in individuals with T2DM have been thoroughly investigated (Ryan, 1997; Stewart & Liolitsa, 1999; Strachan et al., 1997; Vincent & Hall, 2015). This wealth of data makes it possible to validate the GK rat as a preclinical model of executive dysfunction from T2DM. Such a valid model may then speed the development of interventions to lessen the effects of the disease.

In a meta-analysis the influence of T2DM on executive functioning, across cognitive flexibility experiments in the literature, performance was worse among humans with T2DM (Vincent & Hall, 2015). Set-shifting, a type of executive function, is where a switch from one task or thought to another is made. A classic set-shifting task in humans is the WCST where participants sort cards by either the number, the colour, or the shapes of the figures appearing on each card (Grant & Berg, 1948). The set-shift in this task comes about by switching the sorting pattern partway through the study. In elderly patients with T2DM, glycaemic control was related to performance on the WCST (Reaven et al., 1990). Further evidence for increased impairments in set-shifting can be seen in a longitudinal study conducted over 12 years of follow-up. A concept-shifting task used in this longitudinal study showed that adults with T2DM performed worse than controls, where the longer the participant was diagnosed with T2DM the worse that participant's performance on the task (Spauwen et al., 2013).

Set-shifting as well as reversal learning in rats has been tested in a number of different types of experiments (Bizon et al., 2012). Dias et al., developed a way to test shifts in primates by using an IDS where the subject is required to solve a problem using the same perceptual

dimension with novel stimuli, and an EDS where the subject needs to solve a problem with a different perceptual dimension and novel stimuli (1996). A task that utilizes these types of set-shifts is the digging set-shift task or attentional set-shift task, where rats were trained to dig in pots for a food reward and distinguish between different stimuli in a particular sensory dimension, such as digging media, texture, or odour. The original baited stimuli exemplars are switched to allow for a reversal. Partway through the task, the pattern that the rats were trained on to dig for food rewards is also reversed to a different sensory dimension than that originally being tested, for example a shift from texture to odour discrimination (Birrell & Brown, 2000; Bizon et al., 2012; Floresco et al., 2008).

As mentioned in Chapter 1, the PrL is part of the ventral medial prefrontal cortex, an area known for its involvement in executive functioning (Kesner & Churchwell, 2011). The breadth of afferent projections to the PrL is extensive, where orbital and limbic associated areas, including hippocampus (CA1/subiculum), and the limbic system contribute to the PrL (Hoover & Vertes, 2007). Efferent projections from the PrL are less extensive, connecting to the ventromedial caudate-putamen, core of the nucleus accumbens, and IL among others (Heidbreder & Groenewegen, 2003; Kesner & Churchwell, 2011). The PrL receives and integrates information which is used to make a comparison of events present and past , and is employed to make a decision (Hoover & Vertes, 2007; Vertes, 2006), as PrL lesions or lesions to PrL circuit produce impairments in delay response tasks and memory (Vertes, 2006).

Effort-based decision-making produces an increase in metabolic activity in the PrL in rats in a PET scan (Endepols et al., 2010). Related to delayed-discounting, lesions to the PrL increase preference for small instant rewards in rats (Mobini et al., 2002), where temporary inactivation of PrL and other mPFC areas increase impulsive choices (Churchwell, Morris, Heurtelou, &

Kesner, 2009). In paired associate learning, rats with lesions to PrL/IL, do not acquire object-place association (Kesner & Ragozzino, 2003), where there are specific deficits to working memory for spatial information (Ragozzino, Adams, & Kesner, 1998; van Haaren et al., 1988), and visual object information (Kesner, Hunt, Williams, & Long, 1996; Ragozzino, Detrick, & Kesner, 1999).

The present study aims to understand the impact that T2DM has on executive functioning by using the GK rat. Performance in the attentional set-shifting task will help us create a behavioural characterization of set-shifting in the GK rat. Since there are set-shifting impairments in the humans with T2DM (Vincent & Hall, 2015), it is expected that GK rats will also display set-shifting impairments through the attentional set-shifting task. Through Golgi-Cox staining, it is expected that there will be less granule cell dendritic spines, as others have noted a deficit in CA1 of the hippocampus of the GK rat (Li et al., 2013; Xiang et al., 2015). Since there is a decreased arbour concentration in the basilar tree layer II/III pyramids of the parietal neocortex in hyperglycaemic rats (Malone et al., 2008), we propose that hyperglycaemia has an impact on dendritic spine density and arbour concentration throughout the brain.

Materials and Methods

Attentional set-shifting task.

The apparatus was similar to that described elsewhere (Birrell & Brown, 2000). See Figure 8 for a rendition of the attentional set-shifting chamber. This task took place in a Plexiglas chamber (45 x 25 x 20 cm), with two Plexiglas panels and a built-in platform. One panel was fully removable, which divided one third of the cage length into two. A built-in platform sat within the one third section of the chamber, which held two ceramic pots and between them a permanent divider is attached to the platform. Eight ceramic pots each had their rims covered in

a different texture. These textures were glued to the pots permanently. On the surface of the built-in platform, before the ceramic pots on either side of the divider, there was a swatch of texture that matched the texture on the corresponding ceramic pot. This swatch of texture was removable via Velcro strips. There was a second removable platform that could be used without the Velcro for dimension changes not requiring the presence of texture. Four extra pots with a plain rim were used for ease of changing stimuli. Odour exemplars were placed inside a tea bag to minimize transfer of scent onto digging media. All trials were manually timed, pots were filled manually, and all trials were recorded with a video camera mounted on the ceiling above the chamber. Ceramic pots and testing area were cleaned after each change of stimuli exemplars to avoid transfer of odours from spices between trials. For simple discriminations trials in the habituation day, and all discrimination trials thereafter, the baited pots were moved, with texture if being tested, according to the pattern left, left, right, right. This pattern began at the start of each stage and continued until the stage was completed. The side which was baited in the attentional set-shifting task was counterbalanced for each shift and each pair of rats. There were six dimension change groups, which were odour to digging medium (OM), digging medium to odour (MO), odour to texture (OT), texture to odour (TO), digging medium to texture (MT), and texture to digging medium (TM).

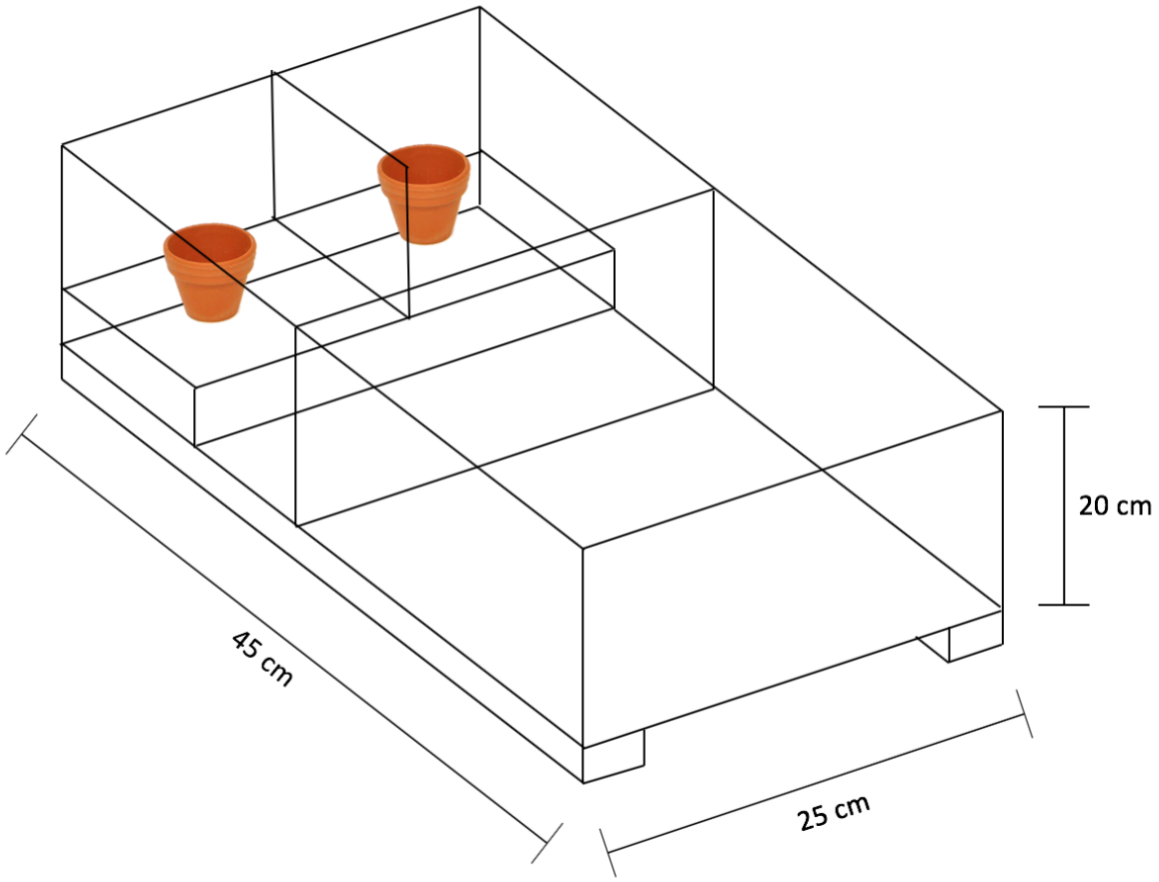

Figure 8. Attentional set-shifting apparatus drawing with measurements not to scale. A platform with two pots was separated with a divider, and the larger removable divider allowed rats to access either side of the platform when the researcher started the trial. The researcher was located on the end by the pots for ease of access to re-bait the pots and change the exemplars.

The task was divided into two days of testing for each rat, where day 1 was a habituation day, and day 2 was the testing day. The protocol for each of these days are described below:

Habituation day.

For habituation trials not involving a texture, a second platform was used that did not have Velcro on each of the sides of the platform. In trials that did not use a texture for discrimination,

plain pots without anything on their rim were used. For trials that did not use a digging medium, plain rat bedding filled the pots.

1. Habituation phase:

This phase occurred on day 1 of the testing for each rat. Rats were placed into the chamber individually with the removable divider down. Pots were filled with bedding. Rats were given access to the chamber for 60 minutes where both pots were baited every 5 minutes with half Froot Loops (Kellogg Canada Inc., Mississauga, ON, Canada). When rebaiting the pots, the removable divider was lowered so that the rat did not take a food reward before the pots were both placed in the chamber. Rats were trained until they reliably dug for the food rewards to three consecutive correct trials of digging for the food reward.

2. Habituation simple discriminations:

Simple discrimination of texture occurred immediately after the habituation phase. The rat was placed in the chamber with the divider down and was given access to the bowls by lifting the divider. Rats were trained to discriminate between two different exemplars from all three dimensions. For texture, exemplars were placed on the platform and around the rim of different pots. The textures were rubber and masking tape, placed from left to right respectively. The simple discrimination of odour always occurred second after texture. The odour exemplars were blackcurrant derived from blackcurrant tea, and vanilla from vanilla sugar which were placed into a tea bag at the bottom of the pots. These were mixed with rat bedding and placed in the pots from left to right respectively. Digging medium simple discrimination always occurred third, after the simple discrimination of odour. Rats discriminated between the two different digging mediums of Styrofoam and shredded paper, which were placed in the pots from left to right respectively, and no rat bedding was used in the pots.

Testing day.

All seven tests during this day were conducted in the same order for each rat (see Table 2 for an example). Since there were six combinations to shift, rats over the sample size of six were used to counterbalance which dimension was the target dimension. The groups were matched, where each combination to shift was used once in each group and matched across the groups (see Table 3 for the summary of combinations that always occurred together). The exemplars for each dimension were only used once. All trials were recorded on the video camera separately. Trial success, trial latency, and number of trials were recorded in addition to the video. These trials lasted to a maximum of 10 minutes or until the rat received the food reward. The trial was terminated if the rat dug in the un-baited bowl or if the rat received the food reward. The criterion to move onto the next shift was five consecutive correct trials. The protocol was similar to the habituation day where rats were placed in the chamber with the removable divider down, and the divider was lifted to allow access to the pots. Rats faced the opposite direction from the pots when they were being baited to avoid rats walking straight to the rewarded pot. A total of seven shifts were tested as described below.

Table 2

Discrimination and exemplar combination order

	Dimensions		First Exemplar Combinations		Second Exemplar Combinations	
Discrimination	Relevant	Irrelevant	Relevant	Irrelevant	Relevant	Irrelevant
Simple discrimination	Texture		**T1**	T2	**T1**	T2

Compound discrimination	Texture	Odour	**T1**/O1	T2/O2	**T1**/O2	T2/O1
Reversal 1	Texture	Odour	**T2**/O1	T1/O2	**T2**/O2	T1/O1
Intradimensional shift	Texture	Odour	**T3**/O3	T4/O4	**T3**/O4	T4/O3
Reversal 2	Texture	Odour	**T4**/O3	T3/O4	**T4**/O4	T3/O3
Extradimensional shift	Odour	Texture	**O5**/T5	O6/T6	**O5**/T6	O6/T5
Reversal 3	Odour	Texture	**O6**/T5	O5/T6	**O6**/T6	O5/T5

Note: Exemplar in bold is followed by rat. Modified from Table 1 in Birrell and Brown (2000).

Table 3

Exemplar combinations for each dimension

Odour	Digging Medium	Texture
Nutmeg/Cloves	Stone Chips/Wooden Beads	Velvet Reverse/Velvet Pile
Paprika/Thyme	Flat Glass Beads/Round Glass Beads	Coarse Sandpaper/Fine Sandpaper
Cumin/Cinnamon	Rat Bedding/Quail Bedding	Wallpaper/Wax Paper

Note: These exemplars were always paired with each other.

1. Simple discrimination:

Similar to the habituation simple discriminations, however, only one of the three dimensions were tested in this stage. Either odour, texture, or digging medium exemplars were used, with only one pot baited.

2. Compound discrimination:

A second dimension was added to the simple discrimination, where this second dimension was to be ignored by the rat. The correct baited exemplar stayed the same from the simple discrimination.

3. Reversal 1:

The exemplars and dimensions were unchanged from the previous two stages, but the baited stimulus from simple and compound discriminations was switched with the unbaited stimulus. The rat needed to learn that the previously incorrect stimulus was now correct.

4. Intradimensional shift:

Shift exemplars were changed out for different exemplars of the same dimensions used in the previous stages, where the previously relevant dimension stayed relevant. This stage was the same as the compound discrimination with the addition of new exemplars.

5. Reversal 2:

As in the first reversal, the previously incorrect exemplar of the same dimension was now the correct exemplar that the rat needed to follow.

6. Extradimensional shift:

As in the IDS, the exemplars were changed out for both pots, where the relevant dimension followed up until this point was now irrelevant. The rat needed to learn to follow the previously incorrect dimension that was being ignored.

7. Reversal 3:

The exemplars and dimensions stayed the same from the EDS, but the correct stimulus was reversed as in the first reversal of the task. The rat needed to follow the previously incorrect stimulus.

Side preference.

Side preference during day 2 was coded from the videos recorded during each of the seven stages in the attentional set-shifting task. The first side of the chamber that was entered after the removable divider was lifted was recorded for each trial as either left or right for each animal. These were summed for left and right across the entire task. Duration of time in seconds spent in each side of the chamber by the pots outside of the holding compartment when the removable divider was lifted was summed for left and right sides across the entire task. The number of entries to each side of the platform by the pots was recorded per trial. The number of entries were summed across the entire task. If there was no side preference, these calculations should be equal. Coding was completed blindly by a researcher.

Immobility.

In the attentional set-shifting task, the amount of time spent immobile in the attentional set-shifting chamber at any location in the chamber was coded from the videos recorded. Immobility was defined as a stance when the rat was not walking, moving its legs, turning around in a circle, reaching to the top of the chamber walls, or digging. Moving the rat's head without any motion from the body was considered immobile. Time spent immobile was recorded in seconds for each trial and summed across the entire task. Coding was completed blindly by a researcher.

Results

Urine glucose.

Statistical analyses were performed using Excel (Microsoft Office 2010, Mississauga, ON, Canada), and SPSS Statistics Version 24 (IBM Corp., Armonk, NY, USA). In each subsequent analysis of variance (ANOVA) the between-subjects factor was strain. All effects are

reported as significant at $p < .05$. Urinary glucose was analysed in a 2 (Time: before, after) x 2 (Strain: GK, Wistar) mixed factorial repeated measures ANOVA, where the dependent variable was urine glucose measured in mmol/L (see Figure 9 for results). There was a significant main effect of time, $F(1,14) = 4.7$, $p = .048$, (effect size = .579, power = .99), a significant main effect of strain, $F(1,14) = 17.724$, $p = .001$, (effect size = 1.126, power = .998), and a significant time x strain interaction, $F(1,14) = 4.7$, $p = .048$, (effect size = .579, power = .99). To understand the nature of the interaction, simple effect analyses were conducted where there was a significant simple effect of time on urine glucose levels for GK rats, $F(1,14) = 9.4$, $p = .008$, where urine glucose in GK rats significantly increased after the attentional set-shifting task. Simple contrasts with a Bonferroni correction were conducted to illuminate the differences between strains and the time urine glucose measurements were taken (see Figure 9 for significance).

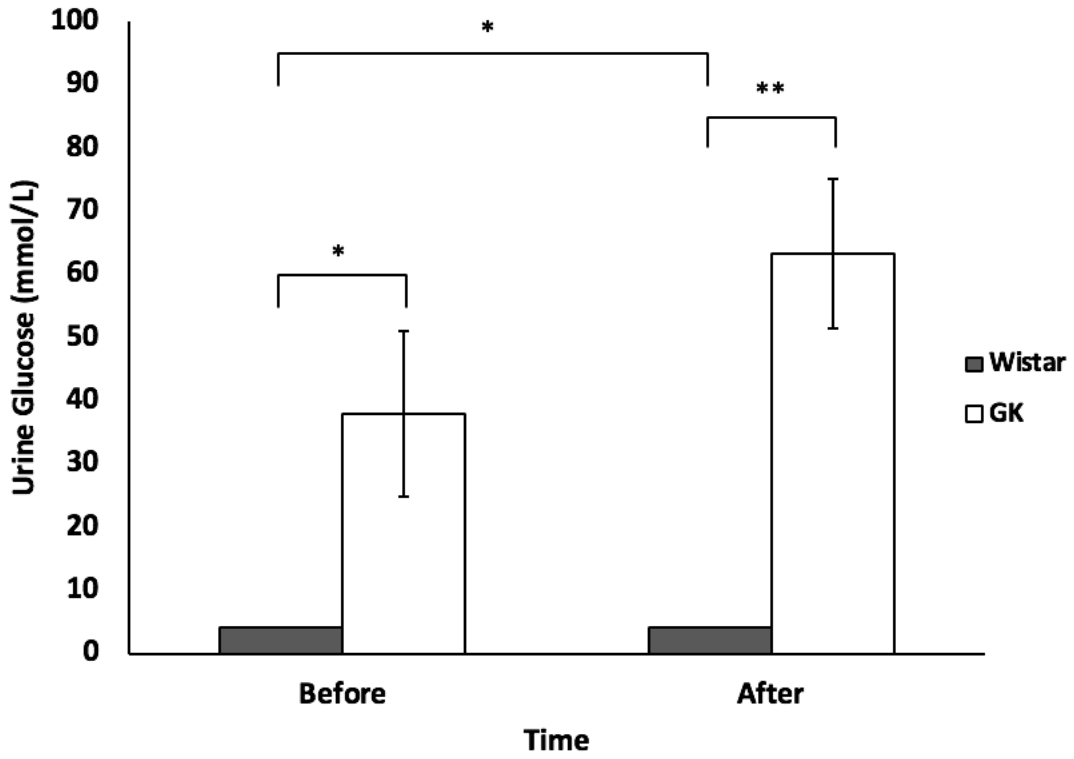

Figure 9. Urine glucose measurements in mmol/L taken before and after the attentional set-shifting task. There was no variability of the data from Wistar rats, as the urine glucose strips could not detect a urine glucose measurement lower than 5 mmol/L.

Habituation (day 1).

Habituation simple discrimination data collected on day 1 of the attentional set-shifting task was calculated by taking the sum of the number of correct consecutive trials to reach a criterion of five correct consecutive trials for each of the three dimensions, texture, digging medium, and odour. The results were analysed in three separate independent-samples t-tests comparing the number of trials to reach criterion in each dimension between strains (see Figure 10A for results). For the simple discrimination habituation of texture, there was no significant difference between groups, $t(14) = 1.79$, $p = .095$ (effect size = .895, power = .523). Levene's test for equality of variances was violated for the habituation simple discrimination of digging medium, $F = 11.008$, $p = .005$, therefore the equal variances not assumed was used. There was also no significant difference between groups for digging medium, $t(8.931) = 1.967$, $p = .081$ (effect size = .983, power = .589). For odour, Levene's test for equality of variances was violated, $F = 9.517$, $p = .008$, so equal variances not assumed correction was used, where there was a significant difference between the groups, $t(8.21) = 2.656$, $p = .028$, (effect size = 1.328, power = .81), where GK rats took a significantly greater number of trials to reach criterion ($M = 10.38$, $SD = 4.596$), than Wistar rats ($M = 5.88$, $SD = 1.356$).

Habituation of simple discriminations was also analysed by taking the duration sum in seconds to reach five correct consecutive trials to criterion for each dimension. Three independent-samples t-tests were conducted to compare the duration of time to reach criterion for each dimension between strains (see Figure 10B for results). For the simple discrimination of

texture, Levene's test for equality of variances was not assumed, $F = 8.44$, $p = .012$, where there was no significant difference between the groups, $t(8.65) = 2.057$, $p = .071$, (effect size = 1.028, power = .622). Levene's test for equality of variances was not assumed for digging medium, $F = 5.862$, $p = .030$, where there was a significant difference between the groups, $t(8.266) = 2.962$, $p = .017$, (effect size = 1.481, power = .879), where GK rats took significantly longer to reach the five correct consecutive trials to criterion ($M = 532.63$, $SD = 360.868$), than Wistar rats ($M = 137.88$, $SD = 108.949$). For the simple discrimination of odour, Levene's test for equality of variances was not assumed, $F = 4.971$, $p = .043$, where there was a significant difference between the duration of time taken to reach criterion between groups, $t(7.969) = 2.868$, $p = .021$, (effect size = 1.434, power = .86), where GK rats took longer to reach criterion ($M = 838.63$, $SD = 650.552$), than Wistar rats ($M = 156.38$, $SD = 171.593$).

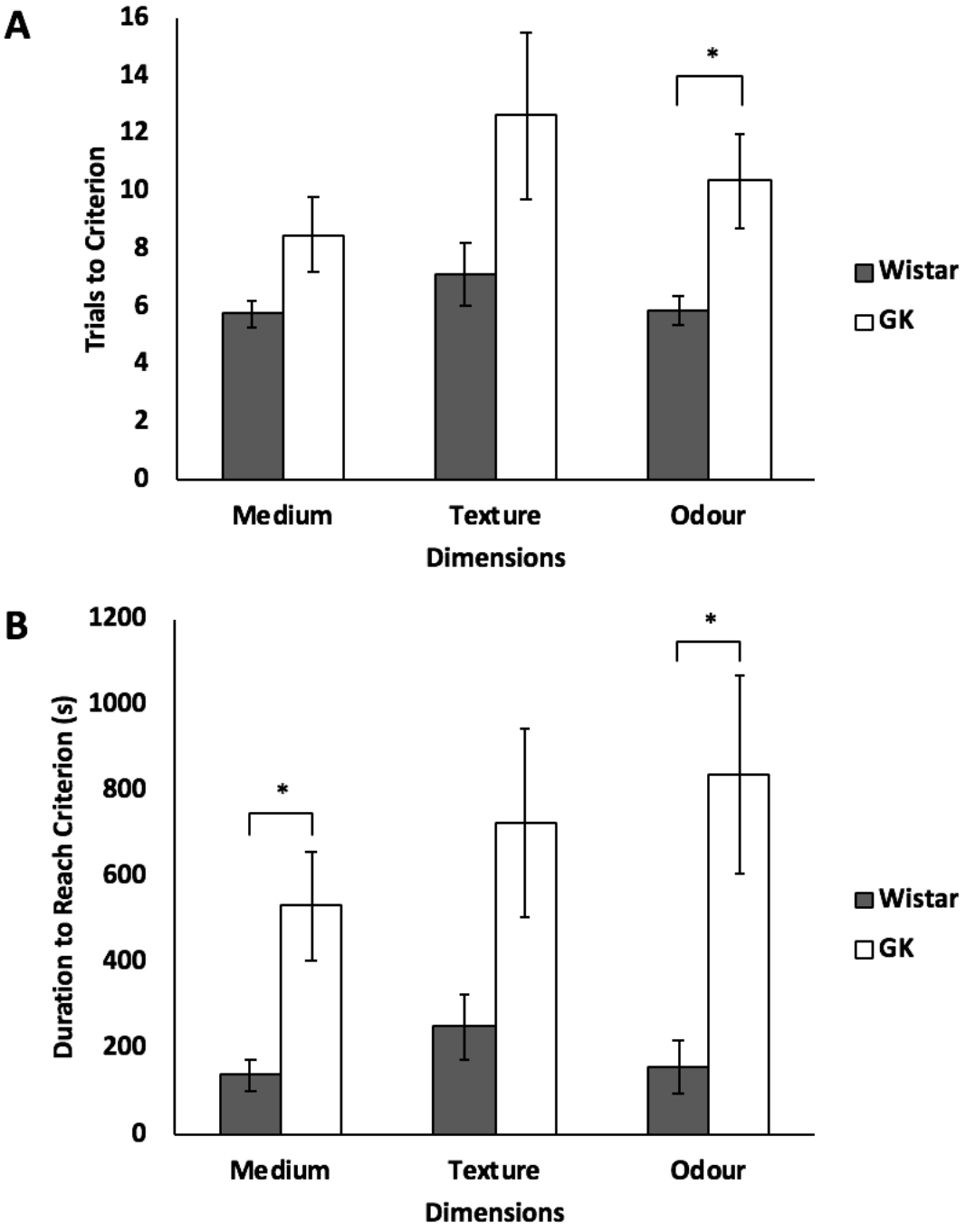

Figure 10. Day 1 of the attentional set-shifting task. (A) Habituation of simple discriminations for all three dimensions in the number of trials to reach a criterion of five consecutive correct trials. (B) Habituation of simple discriminations for all three dimensions in duration of time in seconds to reach criterion.

Series of shifts (day 2).

Performance on day 2 of the attentional set-shifting task, or the testing day, was calculated by summing the number of correct consecutive trials to reach criterion, where the criterion was five correct consecutive trials. Trials to criterion was analysed separately for each type of shift as classified as either a discrimination, reversal, or dimensional shift (see Figure 11A for results). Discriminations were analysed in a 2 (Discrimination: Simple, Compound) x 2 (Strain: GK, Wistar) x 6 (Dimension Change: MO, MT, OM, OT, TM, TO), mixed factorial repeated measures ANOVA, where the dependent variable was number of correct consecutive trials to reach criterion. For number of trials to reach criterion, there was a no main effect of discrimination type, $F(1,4) = 3.122$, $p = .152$, $\eta_{p2} = .438$, (effect size = .883, power = .999), a significant main effect of strain, $F(1,4) = 78.948$, $p = .001$, $\eta_{p2} = .952$, (effect size = 4.453, power = 1), and a significant main effect of dimension change, $F(5,4) = 33.348$, $p = .002$, $\eta_{p2} = .977$, (effect size = 6.518, power = 1), on number of trials to reach criterion. There was no discrimination by strain interaction $F(1,4) = .486$, $p = .524$, $\eta_{p2} = .108$, (effect size = .348, power = .979), no discrimination by dimension change interaction, $F(5,4) = .801$, $p = .602$, $\eta_{p2} = .5$, (effect size = 1, power = .999), and no discrimination by strain by dimension change interaction, $F(5,4) = .931$, $p = .543$, $\eta_{p2} = .538$, (effect size = 1.079, power = .719), on number of trials to reach criterion. However, there was a significant strain by dimension change interaction, $F(5,4) = 18.148$, $p = .007$, $\eta_{p2} = .958$, (effect size = 4.776, power = 1), on trials to reach criterion. To further understand the nature of the strain by dimension change interaction, simple contrasts with a Bonferroni adjustment were conducted. For dimension change, GK rats took a greater number of trials to reach criterion than Wistar rats for the OM order, $p = .031$, 95% CI [.899, 11.101], the

OT order, $p = .015$, 95% CI [2.399, 12.601], and the TM order, $p < .001$, 95% CI [13.143, 20.357].

Performance on the testing day of the attentional set-shifting task was also analysed by using the duration of time, in seconds, it took to reach five correct consecutive trials as criterion. Duration to reach criterion was analysed separately for each type of shift as classified as either a discrimination, reversal, or dimensional shift (see Figure 11B for results). Discriminations were analysed in a 2 (Discrimination: Simple, Compound) x 2 (Strain: GK, Wistar) x 6 (Dimension Change: MO, MT, OM, OT, TM, TO), mixed factorial repeated measures ANOVA, where the dependent variable was duration to reach criterion. For duration of time to reach criterion, there was a no main effect of discrimination type, $F(1,4) = .148$, $p = .720$, $\eta_{p2} = .036$, (effect size = .193, power = .223), a significant main effect of strain, $F(1,4) = 10.315$, $p = .033$, $\eta_{p2} = .721$, (effect size = 1.608, power = .586), and no main effect of dimension change, $F(5,4) = 3.501$, $p = .124$, $\eta_{p2} = .814$, (effect size = 2.092, power = .812), on duration of time to reach criterion. There was no discrimination by strain interaction $F(1,4) = .05$, $p = .833$, $\eta_{p2} = .012$, (effect size = .110, power = .95), no discrimination by dimension change interaction, $F(5,4) = .337$, $p = .868$, $\eta_{p2} = .297$, (effect size = .65, power = .998), no strain by dimension change interaction, $F(5,4) = 2.954$, $p = .158$, $\eta_{p2} = .787$, (effect size = 1.922, power = .743), and no discrimination by strain by dimension change interaction, $F(5,4) = .306$, $p = ..887$, $\eta_{p2} = .276$, (effect size = .617, power = .294), on duration of time to reach criterion.

Performance on the reversals in the attentional set-shifting task for number of trials to reach criterion was analysed in a 3 (Reversal: Reversal 1, Reversal 2, Reversal 3) x 2 (Strain: GK, Wistar) x 6 (Dimension Change: MO, MT, OM, OT, TM, TO), mixed factorial repeated measures ANOVA, where the dependent variable was number of correct consecutive trials to

reach criterion. There was a significant main effect of reversal, $F(2,8) = 10.939$, $p = .005$, $\eta_{p2} = .732$, (effect size = 1.653, power = 1); no main effect of strain, $F(1,4) = 1.851$, $p = .245$, $\eta_{p2} = .316$, (effect size = .68, power = .152); and no main effect of dimension change, $F(5,4) = 2.384$, $p = .21$, $\eta_{p2} = .749$, (effect size = 1.727, power = .702), on the number of trials to reach criterion. There was no reversal by strain interaction, $F(2,8) = .729$, $p = .512$, $\eta_{p2} = .154$, (effect size = .427, power = .209); no reversal by dimension change interaction, $F(10,8) = 2.21$, $p = .137$, $\eta_{p2} = .734$, (effect size = 1.661, power = 1); no strain by dimension change interaction, $F(5,4) = 2.858$, $p = .165$, $\eta_{p2} = .781$, (effect size = 1.888, power = .778); and no reversal by strain by dimension change interaction, $F(10,8) = 1.602$, $p = .258$, $\eta_{p2} = .667$, (effect size = 1.415, power = .997), on the number of trials to reach criterion.

Performance in the reversals in the attentional set-shifting task for duration of time to reach criterion was analysed in a 3 (Reversal: Reversal 1, Reversal 2, Reversal 3) x 2 (Strain: GK, Wistar) x 6 (Dimension Change: MO, MT, OM, OT, TM, TO), mixed factorial repeated measures ANOVA, where the dependent variable was duration of time in seconds to reach criterion. There was a significant main effect of reversal, $F(2,8) = 12.813$, $p = .003$, $\eta_{p2} = .762$, (effect size = 1.789, power = 1); no main effect of strain, $F(1,4) = 2.697$, $p = .176$, $\eta_{p2} = .403$, (effect size = .822, power = .206); and no main effect of dimension change, $F(5,4) = .443$, $p = .802$, $\eta_{p2} = .357$, (effect size = .745, power = .175), on duration of time to reach criterion. There was a significant reversal by strain interaction, $F(2,8) = 5.856$, $p = .027$, $\eta_{p2} = .594$, (effect size = 1.21, power = .976); a significant reversal by dimension change interaction, $F(10,8) = 4.377$, $p = .024$, $\eta_{p2} = .845$, (effect size = 2.904, power = 1); no strain by dimension change interaction, $F(5,4) = 1.595$, $p = .336$, $\eta_{p2} = .666$, (effect size = 1.412, power = .525); and a significant reversal by strain by dimension change interaction, $F(10,8) = 3.792$, $p = .036$, η_{p2}

= .826, (effect size = 2.179, power = 1), on duration of time to reach the criterion. To further understand the nature of the three-way interaction, simple contrasts with a Bonferroni correction were conducted. For the OT order, in reversal 1 GK rats took significantly longer to reach criterion than Wistar rats, p = .032, 95% CI [671.441, 8800.559], and in the TM order, GK rats took significantly longer to reach criterion in reversal 1 than Wistar rats, p = .024, 95% CI [802.923, 6551.077].

The shifts in the attentional set-shifting task for number of trials to reach criterion were analysed in a 2 (Shift: Intradimensional, Extradimensional) x 2 (Strain: GK, Wistar) x 6 (Dimension Change: MO, MT, OM, OT, TM, TO), mixed factorial repeated measures ANOVA, where the dependent variable was number of correct consecutive trials to reach criterion. There was no main effect of shift, $F(1,4) = 6.853$, p = .059, η_{p2} = .631, (effect size = 1.308, power = 1); no main effect of strain, $F(1,4) = .024$, p = .884, η_{p2} = .006, (effect size = .078, power = .051); and no main effect of dimension change, $F(5,4) = 2.077$, p = .249, η_{p2} = .722, (effect size = 1.612, power = .588), on the number of trials taken to reach criterion. There was no shift by strain interaction, $F(1,4) = .014$, p = .912, η_{p2} = .003, (effect size = .055, power = .052); no shift by dimension change interaction, $F(5,4) = 3.239$, p = .139, η_{p2} = .802, (effect size = 2.013, power = .997); no strain by dimension change interaction, $F(5,4) = 1.18$, p = .449, η_{p2} = .596, (effect size = 1.215, power = .368); and no shift by strain by dimension change interaction, $F(5,4)$ = 1.248, p = .427, η_{p2} = .609, (effect size = 1.248, power = .836), on the number of trials it took to reach criterion.

For duration of time to reach criterion, performance in the shifts was analysed in a 2 (Shift: Intradimensional, Extradimensional) x 2 (Strain: GK, Wistar) x 6 (Dimension Change: MO, MT, OM, OT, TM, TO), mixed factorial repeated measures ANOVA, where the dependent

variable was duration of time in seconds to reach criterion. There was no main effect of shift, $F(1,4) = .02$, $p = .893$, $\eta_{p2} = .005$, (effect size = .071, power = .073); no main effect of strain, $F(1,4) = .663$, $p = .461$, $\eta_{p2} = .142$, (effect size = .407, power = .08); and no main effect of dimension change, $F(5,4) = .206$, $p = .943$, $\eta_{p2} = .205$, (effect size = .508, power = .097), on the duration of time it took to reach criterion. There was no shift by strain interaction, $F(1,4) = .056$, $p = .824$, $\eta_{p2} = .014$, (effect size = .119, power = .057); no shift by dimension change interaction, $F(5,4) = 2.09$, $p = .247$, $\eta_{p2} = .723$, (effect size = 1.616, power = .966); no strain by dimension change interaction, $F(5,4) = .407$, $p = .824$, $\eta_{p2} = .337$, (effect size = .713, power = .15); and no shift by strain by dimension change interaction, $F(5,4) = 5.967$, $p = .054$, $\eta_{p2} = .882$, (effect size = 2.734, power = 1), on the duration of time it took to reach criterion.

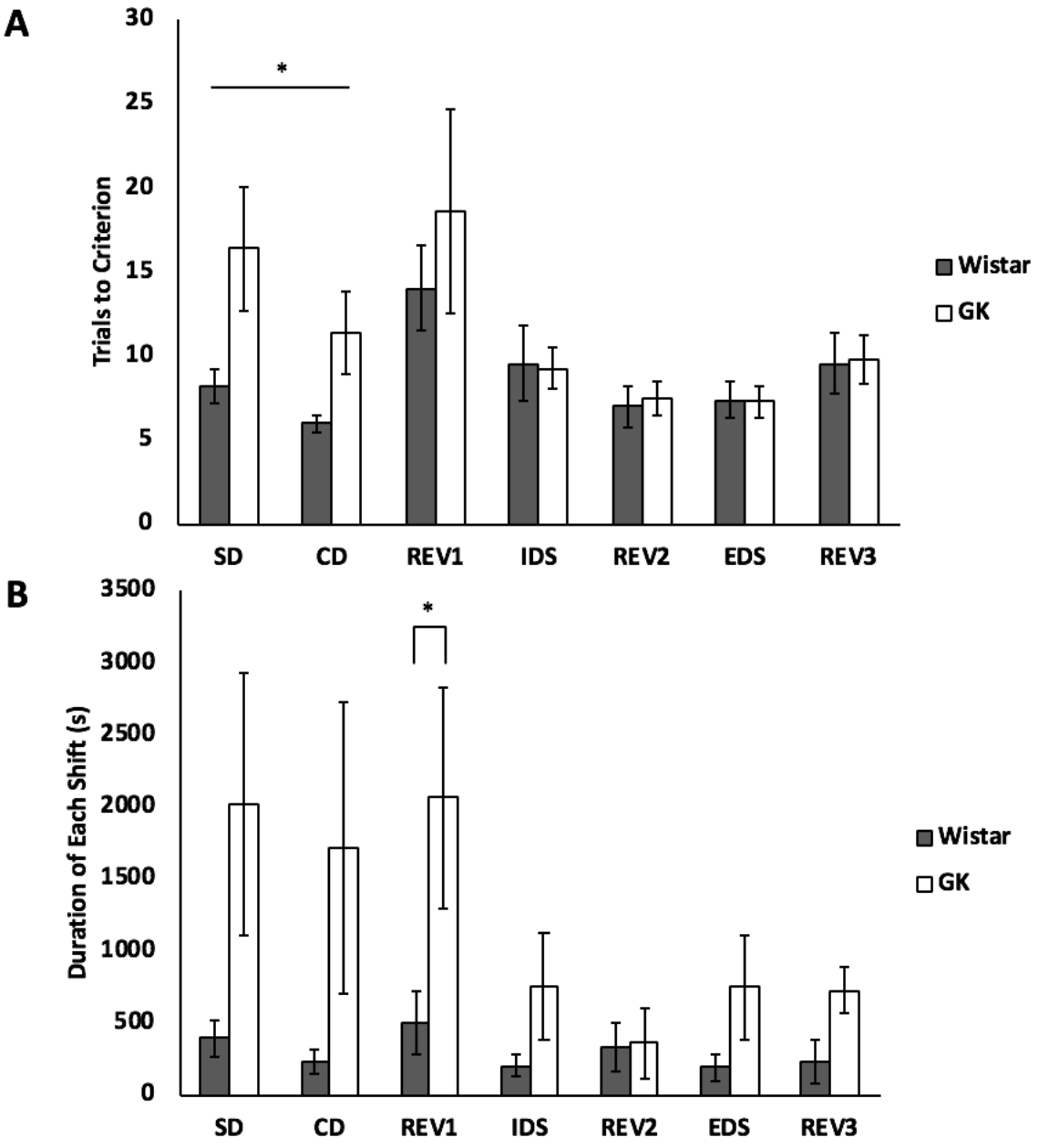

Figure 11. Day 2 of the attentional set-shifting task showing simple discriminations (SD), compound discriminations (CD), reversal 1 (REV1), intradimensional shift (IDS), reversal 2 (REV2), extradimensional shift (EDS), and reversal 3 (REV3). (A) Performance in the task in trials to reach a criterion of five correct consecutive trials for each shift. (B) Performance in the task in duration of time in seconds to reach criterion for each shift.

Side preference.

Side preference in the attentional set-shifting task was calculated by looking at which side the rat went to first on each trial, which was summed across each animal for both left and right sides. The duration of time spent on each side, and the number of entries made to each side was also summed across each animal for the entire task. The data file was split by strain and paired-samples t-tests were run comparing left and right-side preference for each strain (see Table 4). For the side entered first per trial, there was no significant difference between left and right sides for both GK rats, $t(7) = -.929$, $p = .384$, (effect size = .328, power = .348), and Wistar rats, $t(7) = -.272$, $p = .794$, (effect size = .096, power = .101). There was no significant difference for the time spent on each side of the attentional set-shifting platform for both GK rats, $t(7) = -.574$, $p = .584$, (effect size = .203, power = .192), and Wistar rats, $t(7) = -.446$, $p = .669$, (effect size = .158, power = .149). There was also no difference between the number of entries made on each of the platform for both GK rats, $t(7) = -1.548$, $p = .166$, (effect size = .547, power = .671), and Wistar rats, $t(7) = -.472$, $p = .651$, (effect size = .167, power = .157).

Table 4

Side preference averaged across the attentional set-shifting task

	Side Entered First				Duration Spent on Each Side				Number of Entries on Each Side			
Strain	Right		Left		Right		Left		Right		Left	
	M	SD	M	SD	M	SD	M	SD	M	SD	M	SD
GK	34.13	8.079	43.13	27.21	1879.88	762.984	2059.13	1169.525	49.38	10.914	60	25.934
Wistar	29.88	11.47	31.75	16.412	523	259.222	640.63	871.516	49.88	21.781	52.63	16.318

Immobility.

Immobility during the attentional set-shifting task was summed across each rat for the entire task and was measured in seconds. Immobility was analysed in an independent-samples t-test comparing strains (see Figure 12). There was a significant difference between the groups, $t(14) = 3.264$, $p = .006$, (effect size = 1.632, power = .927), where GK rats spent significantly more time immobile ($M = 6518$, $SD = 4148.377$), than Wistar rats ($M = 1339.875$, $SD = 1710.061$).

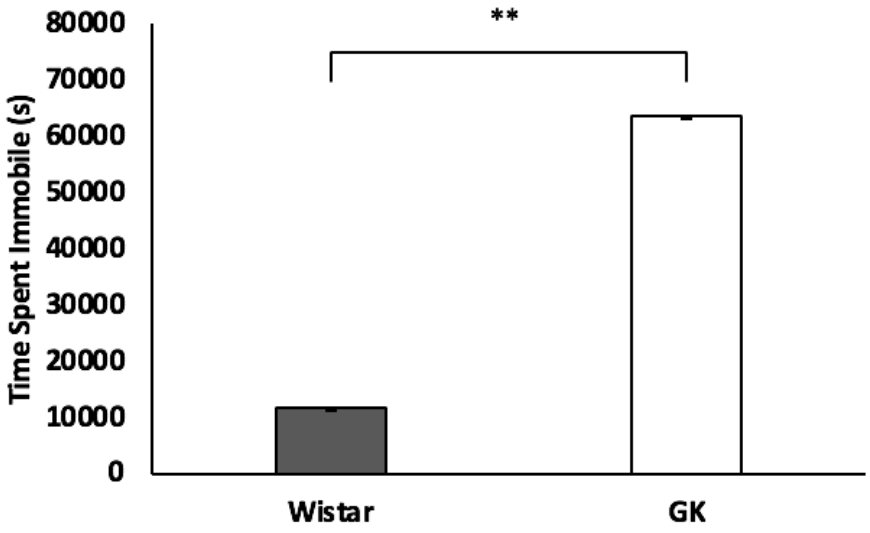

Figure 12. Time spent immobile in seconds summed across the entire task for both strains.

Golgi-Cox analyses.

Sholl analysis for pyramidal neurons was conducted manually using FIJI (Schindelin et al., 2012), by recording the number of dendritic processes in six randomly imaged pyramidal neurons per animal for both basilar and apical dendrites. The number of intersections for basilar dendrites were counted through each 20 μm concentric circle until 280 μm, while dendritic processes for apical dendrites were counted through each concentric circle from 20 μm until 380 μm. Sholl analysis was blindly coded by one researcher, and results were averaged per animal as

well as per intersection. Results for basilar dendrites were analysed in a 2 (Strain: GK, Wistar) x 14 (Intersection: 20 μm - 280 μm in 20 μm increments) mixed factorial repeated measures ANOVA, where the dependent variable was number of intersections (see Figure 13A). There was a significant main effect of intersection, $F(13,182) = 312.849$, $p < .001$, $\eta_{p2} = .957$, (effect size = .957, power = 1), no main effect of strain, $F(1,14) = 2.459$, $p = .139$, $\eta_{p2} = .149$, (effect size = .418, power = .567), and a significant intersection by strain interaction effect, $F(13,182) = 4.69$, $p < .001$, $\eta_{p2} = .251$, (effect size = .579, power = 1), on the number of dendritic processes through each intersection. Post hoc simple effects analyses were conducted to understand the interaction. The simple effect of intersection on the number of dendritic processes was significant for GK rats, $F(13,182) = 127.57$, $p < .001$, and Wistar rats, $F(13,182) = 196.03$, $p < .001$. Simple contrasts with a Bonferroni correction illustrated that compared to Wistar rats, GK rats had less dendritic processes in proximal dendrites (see Figure 13A for significance).

Apical dendrites were analysed in a 2 (Strain: GK, Wistar) x 19 (Intersection: 20 μm - 380 μm in 20 μm increments) mixed factorial repeated measures ANOVA, where the dependent variable was number of intersections (see Figure 13B for results). There was a significant main effect of intersection, $F(18,252) = 58.081$, $p < .001$, $\eta_{p2} = .806$, (effect size = 2.038, power = 1), no main effect of strain, $F(1,14) = 2.639$, $p = .127$, $\eta_{p2} = .159$, (effect size = .435, power = .607), and a significant intersection by strain interaction, $F(18,252) = 1.724$, $p = .036$, $\eta_{p2} = .11$, (effect size = .352, power = 1), on the number of dendritic processes in each intersection. Simple effect analyses were conducted to further understand the interaction. The simple effect of intersection on the number of dendritic processes was significant for both GK rats, $F(18,252) = 25.57$, $p < .001$, and Wistar rats, $F(18,252) = 17.03$, $p < .001$. Simple contrasts with a Bonferroni correction were conducted (see Figure 13B for significance).

Branching complexity up to an order of 7 was collected for each z-stacked image of prelimbic pyramidal neuron layer II/III basilar dendrites, and up to an order of 12 for apical dendrites where the number of branches of each order were recorded, and the same images from the Sholl analysis were used. Branching order was coded blindly by one researcher. Branching complexity for basilar dendrites was averaged across rats and analysed in a 2 (Strain: GK, Wistar) x 7 (Branch Order: 1 - 7) mixed factorial repeated measures ANOVA, where the number of branches was the dependent variable (see Figure 13C). Mauchly's test of sphericity was violated, $\chi_2(20) = 97.835$, $p < .001$, therefore the Greenhouse-Geisser correction was used ($\varepsilon = .446$). There was a significant main effect of branch order, $F(2.674,37.438) = 278.614$, $p < .001$, $\eta_{p2} = .952$, (effect size = 4.453, power = 1), and a significant main effect of strain, $F(1,14) = 10.53$, $p = .006$, $\eta_{p2} = .429$, (effect size = .867, power = .989), on the number of branches. There was also a significant branch order by strain interaction, $F(2.674,37.438) = 4.67$, $p = .009$, $\eta_{p2} = .250$, (effect size = .577, power = .999), on the number of branches. To further understand the interaction, simple effects analyses were conducted. The simple effects analyses for branch order on number of branches was significant for both GK rats, $F(6,84) = 118.44$, $p < .001$, and Wistar rats, $F(6,84) = 176.72$, $p < .001$. Simple contrasts with a Bonferroni correction were conducted (see Figure 13C for significance).

Branching complexity for apical dendrites was averaged across rats and results were analysed in a 2 (Strain: GK, Wistar) x 12 (Branch Order: 1 - 12) mixed factorial repeated measures ANOVA, where the number of branches was the dependent variable (see Figure 13D). There was a significant main effect of branch order, $F(11,154) = 85.438$, $p < .001$, $\eta_{p2} = .859$, (effect size = 2.468, power = 1), a significant main effect of strain, $F(1,14) = 9.96$, $p = .007$, $\eta_{p2} = .416$, (effect size = .844, power = .989), and a significant branch order by strain interaction,

$F(11,154) = 6.395$, $p < .001$, $\eta_{p2} = .314$, (effect size = .677, power = 1), on the number of branches. Simple effect analyses were conducted, where the simple effect of branch order on the number of branches was significant for both GK rats, $F(11,154) = 47.95$, $p < .001$, and Wistar rats, $F(11,154) = 43.88$, $p < .001$. Simple contrasts with a Bonferroni correction revealed GK rats had significantly less branches compared to Wistar rats (see Figure 13D for significance).

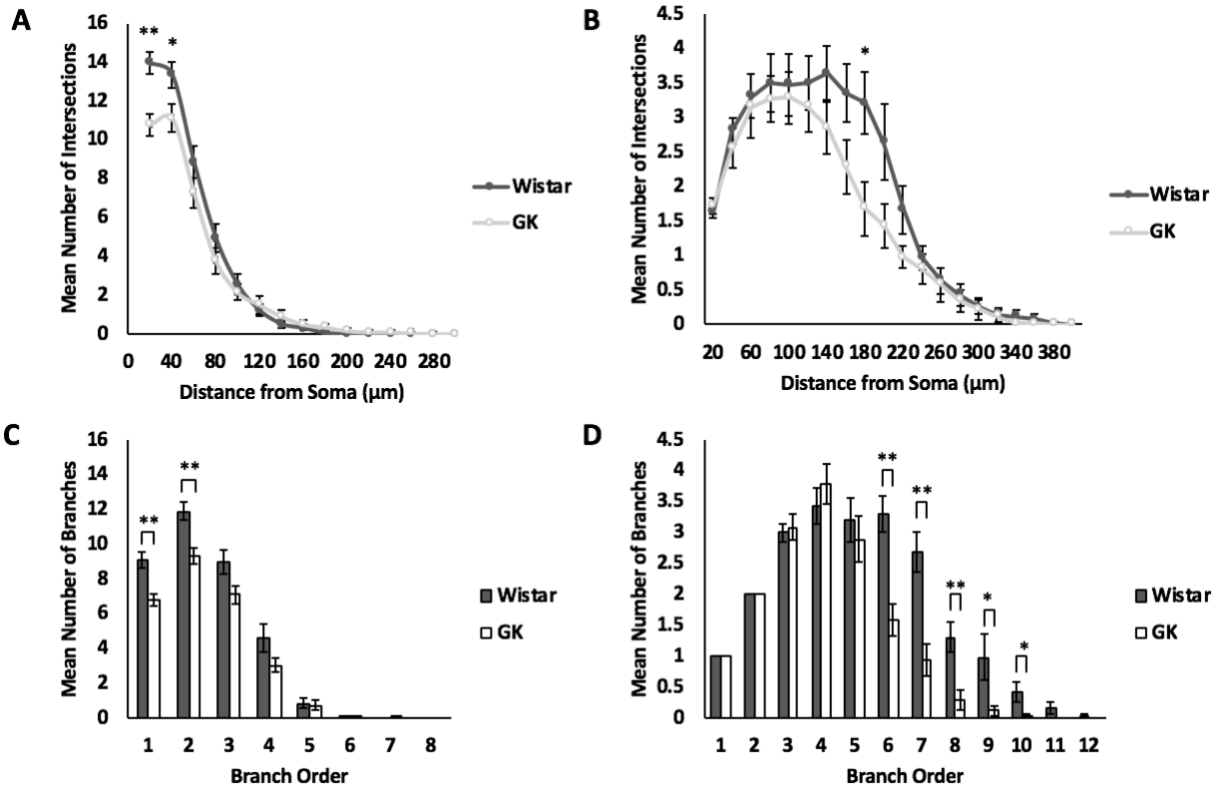

Figure 13. Summary of analysed Golgi-Cox stained tissue in the PrL layer II/III pyramidal neurons. (A) Sholl analysis illustrates the deficit of dendritic material in the proximal area of the basilar dendrites. (B) Sholl analysis of the apical dendrites shows the deficit of dendritic material in the middle area of the apical dendrites. (C) Branching order shows less branches in the proximal area of the basilar dendrites. (D) Branching order illustrates less branching complexity in the middle and distal areas of the apical dendrites.

Pyramidal neuron spine densities were collected by taking six random samples from the basilar dendrites from each rat, and six random samples at three areas along the apical dendrites, the proximal, middle and distal areas for each rat. These were then averaged across strains in each area and were analysed in four independent-samples t-tests comparing the average number of spines between both strains in each area (see Figure 14). Spine densities were counted blindly by one researcher. GK rats had significantly less dendritic spines in the basilar dendrites of the layer II/III pyramidal neurons (M = 11.25, SD = 3.618), as compared to Wistar rats (M = 20.354, SD = 4.735); $t(14) = -4.322$, $p = .001$, (effect size = 2.161, power = .993). In the apical dendrites, at the proximal area GK rats had significantly less dendritic spines (M = 16.625, SD = 4.372), than Wistar rats (M = 27.042, SD = 7.118); $t(14) = -.3.527$, $p = .003$, (effect size = 1.764, power = .956). In the middle area of the apical dendrites, GK rats had significantly less dendritic spines (M = 20.354, SD = 4.141), than Wistar rats (M = 31.396, SD = 7.101); $t(14) = -3.799$, $p = .002$, (effect size = 1.9, power = .975). There were significantly less dendritic spines in the distal area of the apical dendrites for GK rats (M = 17.625, SD = 4.694), than Wistar rats (M = 28.854, SD = 7.59); $t(14) = -3.559$, $p = .003$, (effect size = 1.779, power = .959).

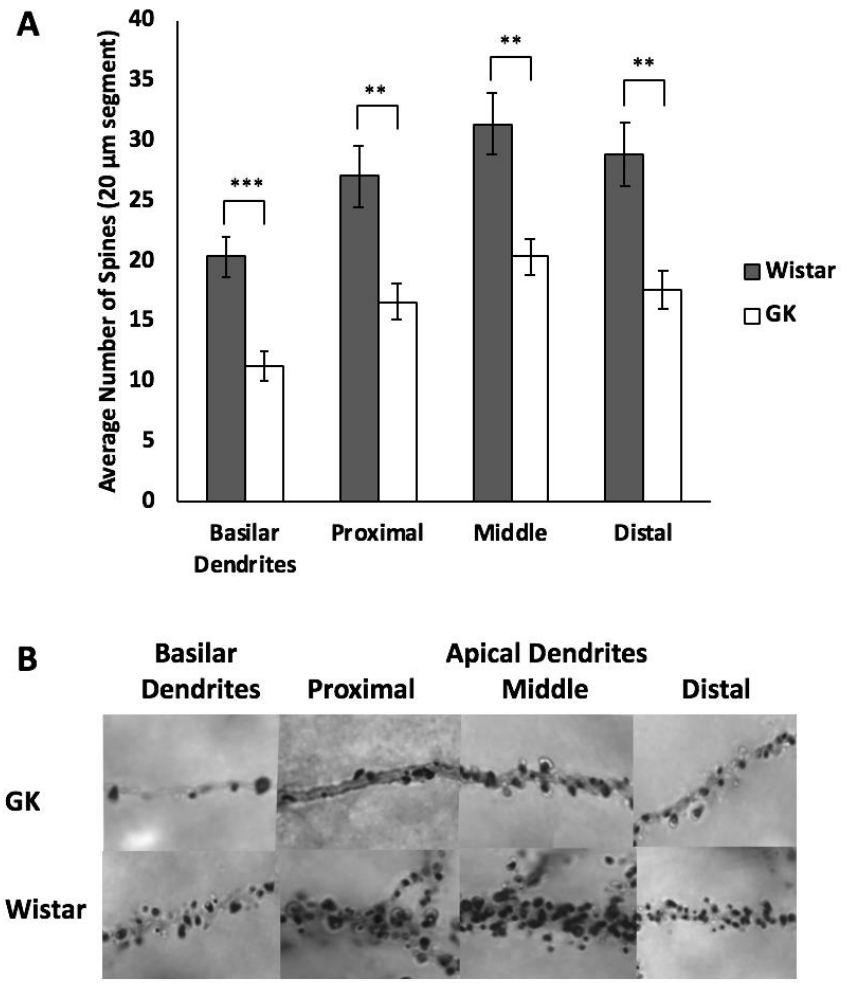

Figure 14. Dendritic spine density analysis of the PrL layer II/III pyramidal neurons. (A) Spine density reveals decreased number of dendritic spines at each of the areas examined. (B) Representative examples of spine densities for both strain in the basilar dendrites, and proximal, middle, and distal areas of the apical dendrites.

Discussion

In the present study, a behavioural characterization of set-shifting ability in GK rats was determined and related to morphology in PrL. Results of the present study suggest that there were impaired discriminations between different sensory dimensions, and impaired reversal learning for the first reversal, but other types of shifts were spared. The results of the Golgi-Cox

staining suggest the morphology of layer II/III pyramidal neurons in the PrL is altered, as spine densities, branching complexity, and dendritic arbour is decreased in the GK rat model of T2DM.

Urinary glucose was tested before all rats were run in the attentional set-shifting task, and a day after each rat completed day 2 of the task. Although the GK rats had higher urine glucose levels before and after the task as compared to the normal Wistar rat, urine glucose increased significantly after the attentional set-shifting task for GK rats (see Figure 9). Since the reward in the attentional set-shifting task was a half Froot Loop (Kellogg Canada Inc., Mississauga, ON, Canada), which contains sugar and the minimum number of rewards over the course of the task was 17.5 Froot Loops (Kellogg Canada Inc., Mississauga, ON, Canada), it could be suggested that this finding supports the results of research investigating high-sugar diets and the incidence of T2DM (Yudkin, 1987), where glucose levels are increased after sugar consumption.

Day 1 of the attentional set-shifting task involved habituation to the chamber, shaping digging for rewards, and simple discriminations of digging media, texture, and odour, which were standard across all animals. As shown in Figure 10A, for the number of trials taken to reach a criterion of five correct consecutive trials, GK rats took more trials to reach criterion in the simple discrimination of odour only, in comparison to Wistar rats. GK rats also took more time to reach criterion than Wistar rats for the simple discriminations of texture and odour (see Figure 10B). Attentional set-shifting day 2, or the testing day, had three kinds of shifts in the task. The first were the simple and compound discriminations. Similar to the results of the habituation day, GK rats of the dimension change orders of OM, OT, and TM in the discriminations took more trials to reach criterion (see Figure 11A). For the duration of time to reach criterion, GK rats took an increased amount of time to reach criterion than Wistar rats (see Figure 11B). The three

reversals were analysed together, where all rats took more trials to reach criterion for the first reversal (see Figure 11A). As illustrated in Figure 11B, GK rats took longer to reach criterion in the first reversal for the dimension change orders of OT and TM than Wistar rats. As seen in Figures 11A and B, there was no significant difference in the performance of either the EDS or the IDS between strains.

The presence of discrimination impairments without the expected set-shifting impairments is surprising. It could be suggested that the deficit observed in reversal 1 is a discrimination impairment and not a set-shifting impairment as only specific orders in reversal 1 were significantly different. If diabetes acted like a lesion to the mPFC, where this area did function normally, then we would have expected to see deficits in the EDS, where dimension being followed was switched, as in a prior study rats with a mPFC lesion took more trials to criterion on that shift (Birrell & Brown, 2000). Humans with T2DM experience widespread executive functioning impairments that include set-shifting (Vincent & Hall, 2015), which may point to the GK model itself as the reason for the difference in deficits observed, as GK rats are bred to be non-obese and spontaneously hyperglycaemic (Goto et al., 1975), and are co-morbid with other complications of T2DM like peripheral neuropathy and retinopathy, but not with hypertension, heart disease, or stress. There is a vulnerability to some executive functions in humans with hypertension (Raz, Rodrigue, & Acker, 2003), and hypertension-induced primates demonstrate impairments in executive functioning (Moore et al., 2002). Research involving humans with T2DM usually does not correct for the presence of hypertension, and thus this may be a factor in why the set-shifting deficits were not seen in this study as the GK rat does not model hypertension. The dimension discrimination impairments seen in attentional set-shifting task may be a factor of peripheral neuropathy, a complication in both types of diabetes that

results in pain, loss of sensation in extremities, and can lead to amputation (Poncelet, 2003). GK rats show peripheral neuropathy from a combination of impaired glucose tolerance, and insulin deficiency (Murakawa et al., 2002). GK rats also show an impairment in odour detection (Lietzau et al., 2018), which may explain the odour discrimination deficit observed in the simple and compound discriminations. However, it should be mentioned that the food restriction of GK rats may have impacted the behaviour and morphological changes during the attentional set-shifting task, but the effects of this change in diet are unknown.

Side preference was analysed separately for both strains, as any difference would be due to immobility, where a rat would be expected to randomly sit in a spot in the chamber and since GK rats have peripheral neuropathy the longer the duration sitting on each side of the platform would be a measure of immobility, rather than a cognitive difference. There was no side preference for the first side entered in each trial, duration of time spent on each side of the chamber, nor the number of times entered on each side of the chamber (see Table 4). Immobility was analysed across the entire task for each animal, where GK rats spent more time immobile than Wistar rats (see Figure 12). Hyperglycaemia in older women is associated with mobility issues such as difficulty walking and frailty (Kalyani et al., 2012), which acts like a long-time complication of diabetes (Volpato et al., 2003). Diabetes has also been a predictor of changes in physical performance in older adults (Seeman et al., 1994). It is possible that this difference was due to peripheral neuropathy or pain due to this reason. There is also the possibility that the increased immobility seen in GK rats as compared to Wistar rats is a motivational impairment, as in a progressive ratio task GK rats performed poorly when the amount of effort necessary to obtain a reward was increased (Moreira, Malec, Östenson, Efendic, & Liljequist, 2007).

In this study, the dendritic arbour of the layer II/III pyramidal neurons was decreased for GK rats in the proximal areas of the basilar dendrites, and the middle area of the apical dendrites (see Figures 13A and B). Branching complexity was also decreased in the lower branch orders in the proximal area of the basilar dendrites in GK rats (see Figure 13C). In the apical dendrites, branching complexity was decreased for GK rats in the middle branching orders (see Figure 13D). Dendritic spine density was decreased in GK rats as compared to Wistar rats in the basilar dendrites, and proximal, middle, and distal areas of the apical dendrites (see Figure 14). Although in Chapter 2 it was mentioned that there is a strong correlation between neuronal dendritic spines or branching atrophy and cognitive dysfunction (Park et al., 2001), this is not always the case. Lesions to the prelimbic cortex are not linked to spatial discrimination or reversal learning impairments (Boulougouris, Dalley, & Robbins, 2007), which suggest deficits in the prelimbic cortex may be task dependent. There are age-related reductions in spine density in the prefrontal cortex in aged rats (Bloss et al., 2011), and in primates, aging results in selective spine loss of small thin-type spines in the dorsolateral PFC pyramidal neurons which coincide with learning impairments (Dumitriu et al., 2010), suggesting there are multiple factors involved in altered morphology. There are many efferent and afferent projections involving the PrL, so perhaps a combination of regions affected would produce such executive functioning deficits that we see in humans with T2DM, where future investigation of associated brain regions would be necessary.

A limitation of the current study was that the dimension change groups, with the exception of TM and counterbalanced MT, in this study were quite small, where only one rat from each strain was compared. It appeared that discrimination of odour and digging medium were affected by the presence of hyperglycaemia in the GK rat, so it is possible that there are

differences for these individual groups that have not been detected as power varied for each analysis.

As mentioned previously, the behavioural deficits associated with lesions to the prelimbic cortex may be more task dependent. In order to further understand why discriminations are impaired instead of set-shifting, additional Golgi-Cox analyses are required such as comparisons of morphology in the perirhinal, postrhinal, and entorhinal cortices which can be made with existing brain tissue. These comparisons may shed some light on to whether the discrimination deficits are sensory or cognitive in nature. Considering digging medium was one of the discriminations where GK rats took more time to reach criterion, comparisons in perirhinal cortex may illuminate whether this is a factor of peripheral neuropathy. As T2DM is becoming more prominent in our society, understanding these mechanisms are of paramount interest.

Chapter 5: General Discussion

The present study aimed to provide a behavioural characterization of the GK rat model of T2DM, a model that has been used widely for diabetes treatment research and understanding of the mechanism behind such behaviours. In Chapter 3, spatial memory and learning was characterized in this model, and DG neuronal morphology was examined. The findings of this research support the notion of impaired spatial memory in the GK rat model of T2DM (Li et al., 2013; Xiang et al., 2015), however, spatial learning over the four training days of the water maze was not impaired when examined using path length, but was impaired in the second half of the water maze when examined by search strategy used. Morphology of DG_{sp} granule cells was altered in the GK rat, shown by reduced arbour and branching complexity as well as decreased dendritic spine density. In Chapter 4, set-shifting abilities and PrL morphology were characterized. In the attentional set-shifting task, no impairments in set-shifting abilities in GK rats were observed contrary to our expectations (Birrell & Brown, 2000). Surprisingly, both simple and compound discriminations were impaired in GK rats compared to controls. The morphology of layer II/III pyramidal PrL neurons was decreased in only the proximal area of the basilar dendrites, and middle area of the apical dendrites. Moreover, spine densities were decreased in both basilar and apical dendrites at each of the locations examined.

At first glance, it is perhaps surprising given the human literature on spatial memory and set-shifting in diabetes patients that these findings should be inconsistent in the present study. In Chapter 3, it was mentioned that many of the studies investigating ‘spatial memory’ were in actuality investigating ‘visuospatial memory’, an ability that is not impaired in humans with T2DM (Awad et al., 2004). Spatial working memory in T2DM was recently investigated in an fMRI study, where T2DM patients were impaired on this measure (Huang et al., 2016), thus it is

possible that the results observed in Chapter 3 are specific to spatial memory, but not other types of memory. With regard to the set-shifting literature, there is a vast amount of evidence suggesting that set-shifting is impaired in humans with T2DM (Stewart & Liolitsa, 1999; Vincent & Hall, 2015), but as mentioned in Chapter 4, many of these studies did not take into account hypertension. As the GK rat model of T2DM is not comorbid with other diseases, and hypertension has demonstrated set-shifting impairments in both humans and animals (Moore et al., 2002; Raz et al., 2003), the addition of hypertension to T2DM may explain why the deficits were not seen in this study.

The behavioural deficits observed in this thesis are part of a larger breadth of impairments in T2DM cognitive functioning. This cognitive dysfunction extends to decreased performance in verbal learning and memory (Ryan & Geckle, 2000), attention (Xia et al., 2015), executive function (Vincent & Hall, 2015), working memory (Ryan et al., 2006), and psychomotor efficiency (Ryan, Williams, Orchard, & Finegold, 1992). However, some areas that are not impacted by the presence of T2DM include constructional ability, visuospatial memory, and general intelligence (Awad et al., 2004; Stewart & Liolitsa, 1999). We may come to the opinion that there is an underlying mechanism explaining why some of these areas are impacted and not others, but why this occurs is not well understood. It is believed that poor glycaemic control is responsible for the cognitive dysfunction (Kloppenborg et al., 2008), and longevity of the diabetes condition contributes to the deficits observed (Spauwen et al., 2013), but if this was a straightforward case it would be sensible to suggest that all areas of cognition would be impacted to some degree in the progression of the disease, where this is clearly not the case. There is a lack of permanency of the deficits, as metabolic and glycaemic control improves the cognitive dysfunction (Gradman et al., 1993; Ryan et al., 2006).

It is interesting to observe that although in Chapter 4 there were no set-shifting differences other than in reversal 1 of the attentional set-shifting task, where some of the dimension orders differed by strain, and there were only decreased morphology in parts of the pyramidal neurons, where spine densities were decreased in the basilar dendrites, and proximal, middle, and distal apical dendrites. This contrasts with Chapter 3, where spatial memory was impaired and there was decreased morphology in the arbour concentration, branching complexity, and spine densities in each of the IML, MML, and OML layers. Perhaps, the morphological changes as seen in Chapter 4 with the absence of set-shifting impairments indicates plasticity. Smaller, weaker spines are thought to be prone to plasticity, where they undergo long-term potentiation to change their morphology (Matsuzaki et al., 2004), which might indicate a possibility that the shape or size of the spines compensates for the reduction in number. However, counts of the specific types of spines in the PrL and DG would need to be done to support this hypothesis.

A limitation of the present study is the number of brain regions investigated in both Chapters 3 and 4. As mentioned in Chapter 1, there is decreased morphology in a number of other brain regions in diabetic rat models. In STZ rats, the spines and branching of basilar dendrites of layer II/III in the parietal neocortex were decreased (Malone et al., 2008), and the spines as well as length of pyramidal neurons were decreased in layer III of the prefrontal cortex, and layer IV of the occipital cortex (Martínez-Tellez et al., 2005). In GK rats, spines were decreased on CA1 pyramidal neurons (Li et al., 2013; Xiang et al., 2015). In Chapter 3, only the DG_{sp} was examined. The DG is part of the perforant path, where the entorhinal cortex interacts with the DG, CA3 and CA1 regions of the hippocampus (Hjorth-Simonsen & Jeune, 1972). Since the medial perforant path responds to spatial tasks (Hunsaker et al., 2007), it would be of

interest to determine whether the deficits seen the DG_{sp} extend to other brain regions in this path. The entorhinal cortex and CA3, could be investigated to see where in the perforant path diabetes has impacted morphology. In Chapter 4, only layers II/III of the PrL, a part of the mPFC, were analysed. The IL is also a part of the mPFC, and although set-shifting was not impaired it would be of interest to see if the decreased morphology continued on to the IL. The prelimbic cortex, as mentioned in Chapter 4, has many afferent projections, and fewer efferent projections (Hoover & Vertes, 2007; Kesner & Churchwell, 2011). The hippocampus in CA1/subiculum, projects onto the PrL (Hoover & Vertes, 2007), and since parts of the pyramidal neurons in the PrL had decreased morphology in Chapter 4, these may be linked to the afferent projection from the hippocampus.

Although there are many avenues that can be pursued in this line of research, the examination of factors that may mitigate spatial memory deficits is warranted. In the human literature, as mentioned previously, limiting the effects of T2DM is usually suggested through the regulation of hyperglycaemia, but the improvement is minimal for some cognitive functions (Gradman et al., 1993), with variability due to the type of treatment (Awad et al., 2004). It is proposed that a meta-analysis be conducted on the current and past treatments tested to limit the effects of T2DM, in order to understand the effectiveness of current approaches to treating this disease. From here, it can be determined which research avenues in treatments appear most promising, or if a new treatment should be proposed. The treatment can be tested on GK rats and assessed using a task such as the water maze to understand whether there is a difference in spatial memory ability with and without the treatment. Brain tissue can be stained with the Golgi-Cox method to note any changes in the morphology of granule cells in the DG_{sp}.

An extension to the attentional set-shifting task findings, where discrimination ability was impaired, could be to induce hypertension in the GK rats to compare set-shifting performance. Hypertension can be induced in rats by the injection of STZ, which also induces hyperglycaemia (Kawashima et al., 1978), but can also be induced by excessive feeding of salt with rat chow (Dahl, 1961). In primates with induced hypertension, set-shifting abilities are impaired (Moore et al., 2002), and in humans set-shifting is vulnerable to hypertension (Raz et al., 2003). It is proposed that hypertension could be induced in GK rats to understand the effect of the addition of hypertension to T2DM on set-shifting. There could be two groups of GK rats, and the Wistar controls tested on the attentional set-shifting task, where one group of GK rats have induced hypertension. As in Chapter 4, the Golgi-Cox staining method could be applied to understand if there are morphological changes to associated brain regions.

This research helped provide a behavioural characterization of the GK rat model of T2DM to help validate its use as an animal model used in treatment research of T2DM. Furthermore, the implications of this research extend farther than characterizing the GK rat model of T2DM, as never before analysed brain regions in this model, such as the DG and PrL, help to broaden our understanding of how diabetes influences morphology in the brain. As the hippocampus in the rat brain is structurally comparable to the hippocampus in the human brain (Clark & Squire, 2013), and although there are differences in the structure of the mPFC in rodents and humans, there is still some homology (Laubach, Amarante, Swanson, & White, 2018), the GK rat model is able to offer us a window into understanding the effects of heritable untreated T2DM in humans.

References

Abbatecola, A. M., Paolisso, G., Lamponi, M., Bandinelli, S., Lauretani, F., Latmer, L., & Ferruci, L. (2004). Insulin resistance and executive dysfunction in older persons. *Journal of the American Geriatrics Society*, *52*(10), 1713–1718. https://doi.org/10.1111/j.1532-5415.2004.52466.x

Amaral, D. G., Scharfman, H. E., & Lavenex, P. (2007). The dentate gyrus: fundamental neuroanatomical organization (dentate gyrus for dummies). *Progress in Brain Research*, *163*, 3–22. https://doi.org/10.1016/S0079-6123(07)63001-5

Anisman, H., DeCatanzaro, D., & Remington, G. (1978). Escape performance following exposure to inescapable shock: Deficits in motor response maintenance. *Journal of Experimental Psychology: Animal Behavior Processes*, *4*(3), 197–218. https://doi.org/10.1037/0097-7403.4.3.197

Araki, Y., Nomura, M., Tanaka, H., Yamamoto, H., Yamamoto, T., Tsukaguchi, I., & Nakamura, H. (1994). MRI of the brain in diabetes mellitus. *Neuroradiology*, *36*(2), 101–103. https://doi.org/10.1007/BF00588069

Astur, R. S., Taylor, L. B., Mamelak, A. N., Philpott, L., & Sutherland, R. J. (2002). Humans with hippocampus damage display severe spatial memory impairments in a virtual Morris water task. *Behavioural Brain Research*, *132*(1), 77–84. https://doi.org/10.1016/S0166-4328(01)00399-0

Awad, N., Gagnon, M., & Messier, C. (2004, November). The relationship between impaired glucose tolerance, type 2 diabetes, and cognitive function. *Journal of Clinical and Experimental Neuropsychology*, Vol. 26, pp. 1044–1080. https://doi.org/10.1080/13803390490514875

Awh, E., & Jonides, J. (2001). Overlapping mechanisms of attention and spatial working memory. *Trends in Cognitive Sciences, 5*(3), 119–126. https://doi.org/10.1016/S1364-6613(00)01593-X

Berthelier, C., Kergoat, M., & Portha, B. (1997). Lack of deterioration of insulin action with aging in the GK rat: A contrasted adaptation as compared with nondiabetic rats. *Metabolism: Clinical and Experimental, 46*(8), 890–896. https://doi.org/10.1016/S0026-0495(97)90075-5

Biessels, G. J., Kamal, A., Ramakers, G. M., Urban, I. J., Spruijt, B. M., Erkelens, D. W., & Gispen, W. H. (1996). Place learning and hippocampal synaptic plasticity in streptozotocin-induced diabetic rats. *Diabetes, 45*(9), 1259–1266. https://doi.org/10.2337/diab.45.9.1259

Biessels, G. J., Kamal, A., Urban, I. J. A., Spruijt, B. M., Erkelens, D. W., & Gispen, W. H. (1998). Water maze learning and hippocampal synaptic plasticity in streptozotocin-diabetic rats: Effects of insulin treatment. *Brain Research, 800*(1), 125–135. https://doi.org/10.1016/S0006-8993(98)00510-1

Biessels, G. J., Staekenborg, S., Brunner, E., Brayne, C., & Scheltens, P. (2006). Risk of dementia in diabetes mellitus: A systematic review. *Lancet Neurology, 5*(1), 64–74. https://doi.org/10.1016/S1474-4422(05)70284-2

Biessels, G. J., Van der Heide, L. P., Kamal, A., Bleys, R. L. A. W., & Gispen, W. H. (2002). Ageing and diabetes: Implications for brain function. *European Journal of Pharmacology, 441*(1–2), 1–14. https://doi.org/10.1016/S0014-2999(02)01486-3

Birrell, J. M., & Brown, V. J. (2000). Medial frontal cortex mediates perceptual attentional set shifting in the rat. *Journal of Neuroscience, 20*(11), 4320–4324. https://doi.org/10.1523/jneurosci.20-11-04320.2000

Bissonette, G. B., Powell, E. M., & Roesch, M. R. (2013). Neural structures underlying set-shifting: Roles of medial prefrontal cortex and anterior cingulate cortex. *Behavioural Brain Research, 250,* 91–101. https://doi.org/10.1016/j.bbr.2013.04.037

Bizon, J. L., Foster, T. C., Alexander, G. E., & Glisky, E. L. (2012). Characterizing cognitive aging of working memory and executive function in animal models. *Frontiers in Aging Neuroscience, 4,* 19. https://doi.org/10.3389/fnagi.2012.00019

Blackstad, T. W. (1965). Mapping of experimental axon degeneration by electron microscopy of golgi preparations. *Zeitschrift Für Zellforschung Und Mikroskopische Anatomie, 67*(6), 819–834. https://doi.org/10.1007/BF00339303

Bloss, E. B., Janssen, W. G., Ohm, D. T., Yuk, F. J., Wadsworth, S., Saardi, K. M., … Morrison, J. H. (2011). Evidence for reduced experience-dependent dendritic spine plasticity in the aging prefrontal cortex. *Journal of Neuroscience*, *31*(21), 7831–7839. https://doi.org/10.1523/JNEUROSCI.0839-11.2011

Boulougouris, V., Dalley, J. W., & Robbins, T. W. (2007). Effects of orbitofrontal, infralimbic and prelimbic cortical lesions on serial spatial reversal learning in the rat. *Behavioural Brain Research, 179*(2), 219–228. https://doi.org/10.1016/j.bbr.2007.02.005

Broadbent, N. J., Squire, L. R., & Clark, R. E. (2004). Spatial memory, recognition memory, and the hippocampus. *Proceedings of the National Academy of Sciences of the United States of America*, *101*(40), 14515–14520. https://doi.org/10.1073/pnas.0406344101

Brody, D. L., & Holtzman, D. M. (2006). Morris water maze search strategy analysis in PDAPP mice before and after experimental traumatic brain injury. *Experimental Neurology, 197*(2), 330–340. https://doi.org/10.1016/j.expneurol.2005.10.020

Buell, S. J. (1982). Golgi-cox and rapid golgi methods as applied to autopsied human brain

tissue: Widely disparate results. *Journal of Neuropathology and Experimental Neurology*, *41*(5), 500–507. https://doi.org/10.1097/00005072-198209000-00003

Cameron, H. A., & Mckay, R. D. G. (2001). Adult neurogenesis produces a large pool of new granule cells in the dentate gyrus. *Journal of Comparative Neurology*, *435*(4), 406–417. https://doi.org/10.1002/cne.1040

Canadian Diabetes Association. (2019). What is diabetes? Retrieved from Diabetes Canada website: https://www.diabetes.ca/diabetes-basics/what-is-diabetes

Centers for Disease Control and Prevention. (2017). National Diabetes Statistics Report: Estimates of Diabetes and its Burden in the US, 2017. In *US Department of Health and Human Services*. Retrieved from https://www.cdc.gov/diabetes/data/statistics/statistics-report.html

Chun, M. M., & Jiang, Y. (1998). Contextual Cueing: Implicit Learning and Memory of Visual Context Guides Spatial Attention. *Cognitive Psychology*, *36*(1), 28–71. https://doi.org/10.1006/cogp.1998.0681

Churchwell, J. C., Morris, A. M., Heurtelou, N. M., & Kesner, R. P. (2009). Interactions Between the Prefrontal Cortex and Amygdala During Delay Discounting and Reversal. *Behavioral Neuroscience*, *123*(6), 1185–1196. https://doi.org/10.1037/a0017734

Clark, R. E., & Squire, L. R. (2013). Similarity in form and function of the hippocampus in rodents, monkeys, and humans. *Proceedings of the National Academy of Sciences of the United States of America*, *110*(Supplement 2), 10365–10370. https://doi.org/10.1073/pnas.1301225110

Conquet, F., Bashir, Z. I., Davies, C. H., Daniel, H., Ferraguti, F., Bordi, F., … Crépel, F. (1994). Motor deficit and impairment of synaptic plasticity in mice lacking mGluR1. *Nature*,

372(6503), 237–243. https://doi.org/10.1038/372237a0

Cox, W. H. (1891). Imprägnation des centralen Nervensystems mit Quecksilbersalzen. *Archiv Für Mikroskopische Anatomie*, *37*(1), 16–21. https://doi.org/10.1007/BF02954290

Cukierman-Yaffe, T. (2014). Diabetes, dysglycemia and cognitive dysfunction. *Diabetes/Metabolism Research and Reviews*, *30*(5), 341–345. https://doi.org/10.1002/dmrr.2507

Dahl, L. K. (1961). Effects of chronic excess salt feeding: Induction of self-sustaining hypertension in rats. *The Journal of Experimental Medicine*, *114*(2), 231–236. https://doi.org/10.1084/jem.114.2.231

De Groot, M., Anderson, R., Freedland, K. E., Clouse, R. E., & Lustman, P. J. (2001). Association of depression and diabetes complications: A meta-analysis. *Psychosomatic Medicine*, *63*(4), 619–630. https://doi.org/10.1097/00006842-200107000-00015

Desmond, N. L., & Levy, W. B. (1982). A quantitative anatomical study of the granule cell dendritic fields of the rat dentate gyrus using a novel probabilistic method. *Journal of Comparative Neurology*, *212*(2), 131–145. https://doi.org/10.1002/cne.902120204

Dias, R., Robbins, T. W., & Roberts, A. C. (1996). Dissociation in prefrontal cortex of affective and attentional shifts. *Nature*, *380*, 69–72. https://doi.org/10.1038/380069a0

Duarte, J. M. N., Skoug, C., Silva, H. B., Carvalho, R. A., Gruetter, R., & Cunha, R. A. (2018). Impact of caffeine consumption on type 2 diabetes-induced spatial memory impairment and neurochemical alterations in the hippocampus. *Frontiers in Neuroscience*, *12*, 1015. https://doi.org/10.3389/fnins.2018.01015

Dumitriu, D., Hao, J., Hara, Y., Kaufmann, J., Janssen, W. G. M., Lou, W., … Morrison, J. H. (2010). Selective changes in thin spine density and morphology in monkey prefrontal cortex

correlate with aging-related cognitive impairment. *Journal of Neuroscience*, *30*(22), 7507–7515. https://doi.org/10.1523/JNEUROSCI.6410-09.2010

Ehses, J. A., Lacraz, G., Giroix, M. H., Schmidlin, F., Coulaud, J., Kassis, N., … Donath, M. Y. (2009). IL-1 antagonism reduces hyperglycemia and tissue inflammation in the type 2 diabetic GK rat. *Proceedings of the National Academy of Sciences of the United States of America*, *106*(33), 13998–14003. https://doi.org/10.1073/pnas.0810087106

Endepols, H., Sommer, S., Backes, H., Wiedermann, D., Graf, R., & Hauber, W. (2010). Effort-based decision making in the rat: an [18F] fluorodeoxyglucose micro positron emission tomography study. *Journal of Neuroscience*, *30*(29), 9708–9714.

Euston, D. R., Gruber, A. J., & McNaughton, B. L. (2012). The Role of Medial Prefrontal Cortex in Memory and Decision Making. *Neuron*, *76*(6), 1057–1070. https://doi.org/10.1016/j.neuron.2012.12.002

Fiala, J. C., Spacek, J., & Harris, K. M. (2002). Dendritic spine pathology: Cause or consequence of neurological disorders? *Brain Research Reviews*, *39*(1), 29–54. https://doi.org/10.1016/S0165-0173(02)00158-3

Floresco, S. B., Block, A. E., & Tse, M. T. L. (2008). Inactivation of the medial prefrontal cortex of the rat impairs strategy set-shifting, but not reversal learning, using a novel, automated procedure. *Behavioural Brain Research*, *190*, 85–96. https://doi.org/10.1016/j.bbr.2008.02.008

Furman, B. L. (2015). Streptozotocin-Induced Diabetic Models in Mice and Rats. *Current Protocols in Pharmacology*, *70*(1), 5–47. https://doi.org/10.1002/0471141755.ph0547s70

Gallagher, M., Burwell, R., & Burchinal, M. (2015). Severity of spatial learning impairment in aging: Development of a learning index for performance in the morris water maze.

Behavioral Neuroscience, *129*(4), 540–548. https://doi.org/10.1037/bne0000080

Gallitano, A. L., Satvat, E., Gil, M., & Marrone, D. F. (2016). Distinct dendritic morphology across the blades of the rodent dentate gyrus. *Synapse*, *70*(7), 277–282. https://doi.org/10.1002/syn.21900

Garthe, A., Behr, J., & Kempermann, G. (2009). Adult-generated hippocampal neurons allow the flexible use of spatially precise learning strategies. *PLoS ONE*, *4*(5), e5464. https://doi.org/10.1371/journal.pone.0005464

Ghasemi, A., Khalifi, S., & Jedi, S. (2014). Streptozotocin-nicotinamide-induced rat model of type 2 diabetes (review). *Acta Physiologica Hungarica*, *101*(4), 408–420. https://doi.org/10.1556/APhysiol.101.2014.4.2

Gibb, R., & Kolb, B. (1998). A method for vibratome sectioning of Golgi-Cox stained whole rat brain. *Journal of Neuroscience Methods*, *79*(1), 1–4. https://doi.org/10.1016/S0165-0270(97)00163-5

Gil-Mohapel, J., Brocardo, P. S., Choquette, W., Gothard, R., Simpson, J. M., & Christie, B. R. (2013). Hippocampal Neurogenesis Levels Predict WATERMAZE Search Strategies in the Aging Brain. *PLoS ONE*, *8*(9), e75125. https://doi.org/10.1371/journal.pone.0075125

Golgi, C. (1873). Sulla sostanza grigia del cervello. *Gazetta Medica Italiana*, *33*, 244–246.

Goodrich-Hunsaker, N. J., Hunsaker, M. R., & Kesner, R. P. (2008). The Interactions and Dissociations of the Dorsal Hippocampus Subregions: How the Dentate Gyrus, CA3, and CA1 Process Spatial Information. *Behavioral Neuroscience*, *122*(1), 16–26. https://doi.org/10.1037/0735-7044.122.1.16

Goto, Y., & Kakizaki, M. (1981). 76. The Spontaneous-Diabetes Rat: A Model of Noninsulin Dependent Diabetes Mellitus. *Proceedings of the Japan Academy, Series B*, *57*(10), 381–

384. https://doi.org/10.2183/pjab.57.381

Goto, Y., Kakizaki, M., & Masaki, N. (1975). Spontaneous Diabetes Produced by Selective Breeding of Normal Wistar Rats. *Proceedings of the Japan Academy*, *51*(1), 80–85. https://doi.org/10.2183/pjab1945.51.80

Gradman, T. J., Laws, A., Thompson, L. W., & Reaven, G. M. (1993). Verbal Learning and/or Memory Improves with Glycemic Control in Older Subjects with Non-Insulin-Dependent Diabetes Mellitus. *Journal of the American Geriatrics Society*, *41*(12), 1305–1312. https://doi.org/10.1111/j.1532-5415.1993.tb06480.x

Grant, D. A., & Berg, E. (1948). A behavioral analysis of degree of reinforcement and ease of shifting to new responses in a Weigl-type card-sorting problem. *Journal of Experimental Psychology*, *38*(4), 404–411. https://doi.org/10.1037/h0059831

Graziano, A., Petrosini, L., & Bartoletti, A. (2003). Automatic recognition of explorative strategies in the Morris water maze. *Journal of Neuroscience Methods*, *130*(1), 33–44. https://doi.org/10.1016/S0165-0270(03)00187-0

Green, E. J., & Juraska, J. M. (1985). The dendritic morphology of hippocampal dentate granule cells varies with their position in the granule cell layer: a quantitative Golgi study. *Experimental Brain Research*, *59*(3), 582–586. https://doi.org/10.1007/BF00261350

Heidbreder, C. A., & Groenewegen, H. J. (2003). The medial prefrontal cortex in the rat: Evidence for a dorso-ventral distinction based upon functional and anatomical characteristics. *Neuroscience and Biobehavioral Reviews*, *27*(6), 555–579. https://doi.org/10.1016/j.neubiorev.2003.09.003

Hjorth-Simonsen, A., & Jeune, B. (1972). Origin and termination of the hippocampal perforant path in the rat studied by silver impregnation. *Journal of Comparative Neurology*, *144*(2),

215–231. https://doi.org/10.1002/cne.901440206

Hoover, W. B., & Vertes, R. P. (2007). Anatomical analysis of afferent projections to the medial prefrontal cortex in the rat. *Brain Structure and Function*, *212*(2), 149–179. https://doi.org/10.1007/s00429-007-0150-4

Huang, R. R., Jia, B. H., Xie, L., Ma, S. H., Yin, J. J., Sun, Z. B., … Luo, D. X. (2016). Spatial working memory impairment in primary onset middle-age type 2 diabetes mellitus: An ethology and BOLD-fMRI study. *Journal of Magnetic Resonance Imaging*, *43*(1), 75–87. https://doi.org/10.1002/jmri.24967

Hunsaker, M. R., Mooy, G. G., Swift, J. S., & Kesner, R. P. (2007). Dissociations of the Medial and Lateral Perforant Path Projections Into Dorsal DG, CA3, and CA1 for Spatial and Nonspatial (Visual Object) Information Processing. *Behavioral Neuroscience*, *121*(4), 742–750. https://doi.org/10.1037/0735-7044.121.4.742

Janus, C. (2004). Search strategies used by APP transgenic mice during navigation in the Morris water maze. *Learning and Memory*, *11*(3), 337–346. https://doi.org/10.1101/lm.70104

Jay, T. M., & Witter, M. P. (1991). Distribution of hippocampal CA1 and subicular efferents in the prefrontal cortex of the rat studied by means of anterograde transport of Phaseolus vulgaris-leucoagglutinin. *Journal of Comparative Neurology*, *313*(4), 574–586. https://doi.org/10.1002/cne.903130404

Jeppesen, P. B., Gregersen, S., Alstrup, K. K., & Hermansen, K. (2002). Stevioside induces antihyperglycaemic, insulinotropic and glucagonostatic effects in vivo: Studies in the diabetic Goto-Kakizaki (GK) rats. *Phytomedicine*, *9*(1), 9–14. https://doi.org/10.1078/0944-7113-00081

Jeppesen, P. B., Gregersen, S., Rolfsen, S. E. D., Jepsen, M., Colombo, M., Agger, A., …

Hermansen, K. (2003). Antihyperglycemic and blood pressure-reducing effects of stevioside in the diabetic Goto-Kakizaki rat. *Metabolism: Clinical and Experimental*, *52*(3), 372–378. https://doi.org/10.1053/meta.2003.50058

Jessberger, S., Clark, R. E., Broadbent, N. J., Clemenson, G. D., Consiglio, A., Lie, D. C., … Gage, F. H. (2009). Dentate gyrus-specific knockdown of adult neurogenesis impairs spatial and object recognition memory in adult rats. *Learning and Memory*, *16*(2), 147–154. https://doi.org/10.1101/lm.1172609

Junod, A., Lambert, A. E., Orci, L., Pictet, R., Gonet, A. E., & Renold, A. E. (1967). Studies of the Diabetogenic Action of Streptozotocin. *Proceedings of the Society for Experimental Biology and Medicine*, *126*(1), 201–205. https://doi.org/10.3181/00379727-126-32401

Junod, A., Lambert, A. E., Stauffacher, W., & Renold, A. E. (1969). Diabetogenic action of streptozotocin: relationship of dose to metabolic response. *The Journal of Clinical Investigation*, *48*(11), 2129–2139. https://doi.org/10.1172/JCI106180

Kalyani, R. R., Tian, J., Xue, Q. L., Walston, J., Cappola, A. R., Fried, L. P., … Blaum, C. S. (2012). Hyperglycemia and incidence of frailty and lower extremity mobility limitations in older women. *Journal of the American Geriatrics Society*, *60*(9), 1701–1707. https://doi.org/10.1111/j.1532-5415.2012.04099.x

Kaplan, S. (1976). Adaption, Structure, and Knowledge. In G. T. Moore & R. G. Golledge (Eds.), *Environmental knowing: Theories, research and methods* (pp. 32–45).

Kasai, H., Matsuzaki, M., Noguchi, J., Yasumatsu, N., & Nakahara, H. (2003). Structure-stability-function relationships of dendritic spines. *Trends in Neurosciences*, *26*(7), 360–368. https://doi.org/10.1016/S0166-2236(03)00162-0

Kawashima, H., Igarashi, T., Nakajima, Y., Akiyama, Y., Usuki, K., & Ohtake, S. (1978).

Chronic hypertension induced by streptozotocin in rats. *Naunyn-Schmiedeberg's Archives of Pharmacology*, *305*(2), 123–126.

Kent, S. (1976). Is diabetes a form of accelerated aging? *Geriatrics*, *31*(11), 140–145.

Kesner, R. P., & Churchwell, J. C. (2011). An analysis of rat prefrontal cortex in mediating executive function. *Neurobiology of Learning and Memory*, *96*(3), 417–431. https://doi.org/10.1016/j.nlm.2011.07.002

Kesner, R. P., Hunt, M. E., Williams, J. M., & Long, J. M. (1996). Prefrontal cortex and working memory for spatial response, spatial location, and visual object information in the rat. *Cerebral Cortex*, *6*(2), 311–318. https://doi.org/10.1093/cercor/6.2.311

Kesner, R. P., & Ragozzino, M. E. (2003). The role of the prefrontal cortex in object-place learning: A test of the attribute specificity model. *Behavioural Brain Research*, *146*(1–2), 159–165. https://doi.org/10.1016/j.bbr.2003.09.024

Kessels, R. P. C., Nys, G. M. S., Brands, A. M. A., van den Berg, E., & Van Zandvoort, M. J. E. (2006). The modified Location Learning Test: Norms for the assessment of spatial memory function in neuropsychological patients. *Archives of Clinical Neuropsychology*, *21*(8), 841–846. https://doi.org/10.1016/j.acn.2006.06.015

Kimura, K., Toyota, T., Kakizaki, M., Kudo, M., Takebe, K., & Goto, Y. (1982). Impaired Insulin Secretion in the Spontaneous Diabetes Rats. *The Tohoku Journal of Experimental Medicine*, *137*(4), 453–459. https://doi.org/10.1620/tjem.137.453

Kloppenborg, R. P., van den Berg, E., Kappelle, L. J., & Biessels, G. J. (2008). Diabetes and other vascular risk factors for dementia: Which factor matters most? A systematic review. *European Journal of Pharmacology*, *585*(1), 97–108. https://doi.org/10.1016/j.ejphar.2008.02.049

Knierim, J. J., Neunuebel, J. P., & Deshmukh, S. S. (2014). Functional correlates of the lateral and medial entorhinal cortex: Objects, path integration and local - Global reference frames. *Philosophical Transactions of the Royal Society B: Biological Sciences*, *369*(1635), 20130369. https://doi.org/10.1098/rstb.2013.0369

Kopf, D., & Frölich, L. (2009). Risk of incident Alzheimer's disease in diabetic patients: A systematic review of prospective trials. *Journal of Alzheimer's Disease*, *16*(4), 677–685. https://doi.org/10.3233/JAD-2009-1011

Laubach, M., Amarante, L. M., Swanson, K., & White, S. R. (2018). What, if anything, is rodent prefrontal cortex? *ENeuro*, *5*(5), ENEURO.0315-18.2018. https://doi.org/10.1523/ENEURO.0315-18.2018

Li, X. H., Xin, X., Wang, Y., Wu, J. Z., Jin, Z. D., Ma, L. N., … Jin, M. W. (2013). Pentamethylquercetin protects against diabetes-related cognitive deficits in diabetic goto-kakizaki rats. *Journal of Alzheimer's Disease*, *34*(3), 755–767. https://doi.org/10.3233/JAD-122017

Lietzau, G., Davidsson, W., Östenson, C. G., Chiazza, F., Nathanson, D., Pintana, H., … Patrone, C. (2018). Type 2 diabetes impairs odour detection, olfactory memory and olfactory neuroplasticity; effects partly reversed by the DPP-4 inhibitor Linagliptin. *Acta Neuropathologica Communications*, *6*(1), 14. https://doi.org/10.1186/s40478-018-0517-1

Lövestam-Adrian, M., Agardh, C. D., Torffvit, O., & Agardh, E. (2001). Diabetic retinopathy, visual acuity, and medical risk indicators. A continuous 10-year follow-up study in Type 1 diabetic patients under routine care. *Journal of Diabetes and Its Complications*, *15*(6), 287–294. https://doi.org/10.1016/S1056-8727(01)00167-2

Luine, V., Villegas, M., Martinez, C., & McEwen, B. S. (1994). Repeated stress causes

reversible impairments of spatial memory performance. *Brain Research*, *639*(1), 167–170. https://doi.org/10.1016/0006-8993(94)91778-7

Macpherson, H., Formica, M., Harris, E., & Daly, R. M. (2017). Brain functional alterations in Type 2 Diabetes – A systematic review of fMRI studies. *Frontiers in Neuroendocrinology*, *47*(2017), 34–46. https://doi.org/10.1016/j.yfrne.2017.07.001

Malone, J. I., Hanna, S. K., & Saporta, S. (2006). Hyperglycemic brain injury in the rat. *Brain Research*, *1076*(1), 9–15. https://doi.org/10.1016/j.brainres.2005.12.072

Malone, J. I., Hanna, S., Saporta, S., Mervis, R. F., Park, C. R., Chong, L., & Diamond, D. M. (2008). Hyperglycemia not hypoglycemia alters neuronal dendrites and impairs spatial memory. *Pediatric Diabetes*, *9*(6), 531–539. https://doi.org/10.1111/j.1399-5448.2008.00431.x

Manschot, S. M., Brands, A. M. A., Van Der Grond, J., Kessels, R. P. C., Algra, A., Kappelle, L. J., & Biessels, G. J. (2006). Brain magnetic resonance imaging correlates of impaired cognition in patients with type 2 diabetes. *Diabetes*, *55*(4), 1106–1113. https://doi.org/10.2337/diabetes.55.04.06.db05-1323

Martínez-Tellez, R., Gómez-Villalobos, M. D. J., & Flores, G. (2005). Alteration in dendritic morphology of cortical neurons in rats with diabetes mellitus induced by streptozotocin. *Brain Research*, *1048*(1–2), 108–115. https://doi.org/10.1016/j.brainres.2005.04.048

Masiello, P., Broca, C., Gross, R., Roye, M., Manteghetti, M., Hillaire-Buys, D., … Ribes, G. (1998). Experimental NIDDM: Development of a new model in adult rats administered streptozotocin and nicotinamide. *Diabetes*, *47*(2), 224–229. https://doi.org/10.2337/diab.47.2.224

Matsuzaki, M., Honkura, N., Ellis-Davies, G. C. R., & Kasai, H. (2004). Structural basis of long-

term potentiation in single dendritic spines. *Nature*, *429*(6993), 761–766. https://doi.org/10.1038/nature02617

Mayeda, E. R., Whitmer, R. A., & Yaffe, K. (2015). Diabetes and cognition. *Clinics in Geriatric Medicine*, *31*(1), 101–115. https://doi.org/10.1016/j.cger.2014.08.021

McCrimmon, R. J., Ryan, C. M., & Frier, B. M. (2012). Diabetes and cognitive dysfunction. *The Lancet*, *379*(9833), 2291–2299. https://doi.org/10.1016/S0140-6736(12)60360-2

McNay, E. C., Fries, T. M., & Gold, P. E. (2000). Decreases in rat extracellular hippocampal glucose concentration associated with cognitive demand during a spatial task. *Proceedings of the National Academy of Sciences of the United States of America*, *97*(6), 2881–2885. https://doi.org/10.1073/pnas.050583697

Messier, C. (2005). Impact of impaired glucose tolerance and type 2 diabetes on cognitive aging. *Neurobiology of Aging*, *26*(1), 26–30. https://doi.org/10.1016/j.neurobiolaging.2005.09.014

Miyake, A., Friedman, N. P., Emerson, M. J., Witzki, A. H., Howerter, A., & Wager, T. D. (2000). The Unity and Diversity of Executive Functions and Their Contributions to Complex "Frontal Lobe" Tasks: A Latent Variable Analysis. *Cognitive Psychology*, *41*(1), 49–100. https://doi.org/10.1006/cogp.1999.0734

Mobini, S., Body, S., Ho, M. Y., Bradshaw, C., Szabadi, E., Deakin, J., & Anderson, I. (2002). Effects of lesions of the orbitofrontal cortex on sensitivity to delayed and probabilistic reinforcement. *Psychopharmacology*, *160*(3), 290–298. https://doi.org/10.1007/s00213-001-0983-0

Moffat, S. D. (2009). Aging and spatial navigation: What do we know and where do we go? *Neuropsychology Review*, *19*(4), 478–489. https://doi.org/10.1007/s11065-009-9120-3

Moore, T. L., Killiany, R. J., Rosene, D. L., Prusty, S., Hollander, W., & Moss, M. B. (2002).

Impairment of executive function induced by hypertension in the rhesus monkey (Macaca mulatta). *Behavioral Neuroscience, 116*(3), 387–396. https://doi.org/10.1037/0735-7044.116.3.387

Moreira, T., Malec, E., Östenson, C. G., Efendic, S., & Liljequist, S. (2007). Diabetic type II Goto-Kakizaki rats show progressively decreasing exploratory activity and learning impairments in fixed and progressive ratios of a lever-press task. *Behavioural Brain Research, 180*(1), 28–41. https://doi.org/10.1016/j.bbr.2007.02.034

Morris, R. G. M. (1981). Spatial localization does not require the presence of local cues. *Learning and Motivation, 12*(2), 239–260. https://doi.org/10.1016/0023-9690(81)90020-5

Morris, R. G. M. (1984). Developments of a water-maze procedure for studying spatial learning in the rat. *Journal of Neuroscience Methods, 11*(1), 47–60. https://doi.org/10.1016/0165-0270(84)90007-4

Moser, E. I., Roudi, Y., Witter, M. P., Kentros, C., Bonhoeffer, T., & Moser, M. B. (2014). Grid cells and cortical representation. *Nature Reviews Neuroscience, 15*(7), 466–481. https://doi.org/10.1038/nrn3766

Movassat, J., Saulnier, C., & Portha, B. (1995). Beta-cell mass depletion precedes the onset of hyperglycaemia in the GK rat, a genetic model of non-insulin-dependent diabetes mellitus. *Diabete et Metabolisme, 21*(5), 365–370.

Munshi, M., Grande, L., Hayes, M., Ayres, D., Suhl, E., Capelson, R., … Katie Weinger, E. (2006). Cognitive dysfunction is associated with poor diabetes control in older adults. *Diabetes Care, 29*(8), 1794–1799. https://doi.org/10.2337/dc06-0506

Murakawa, Y., Zhang, W., Pierson, C. R., Brismar, T., Östenson, C. G., & Sima, A. A. F. (2002). Impaired glucose tolerance and insulinopenia in the GK-rat causes peripheral

neuropathy. *Diabetes/Metabolism Research and Reviews*, *18*(6), 473–483. https://doi.org/10.1002/dmrr.326

Nakazawa, K., McHugh, T. J., Wilson, M. A., & Tonegawa, S. (2004). NMDA receptors, place cells and hippocampal spatial memory. *Nature Reviews Neuroscience*, *5*(5), 361–372. https://doi.org/10.1038/nrn1385

Nathan, D. M. (1993). Long-Term Complications of Diabetes Mellitus. *New England Journal of Medicine*, *328*(23), 1676–1685. https://doi.org/10.1056/NEJM199306103282306

Newman, E. L., Caplan, J. B., Kirschen, M. P., Korolev, I. O., Sekuler, R., & Kahana, M. J. (2007). Learning your way around town: How virtual taxicab drivers learn to use both layout and landmark information. *Cognition*, *104*(2), 231–253. https://doi.org/10.1016/j.cognition.2006.05.013

O'Keefe, J., & Nadel, L. (1978). *The hippocampus as a cognitive map*. Oxford: Clarendon Press.

Östenson, C. G., & Efendic, S. (2007). Islet gene expression and function in type 2 diabetes; studies in the Goto-Kakizaki rat and humans. *Diabetes, Obesity and Metabolism*, *9*(s2), 180–186. https://doi.org/10.1111/j.1463-1326.2007.00787.x

Pan, X. R., Li, G. W., Hu, Y. H., Wang, J. X., Yang, W. Y., An, Z. X., … Howard, B. V. (1997). Effects of diet and exercise in preventing NIDDM in people with impaired glucose tolerance: The Da Qing IGT and diabetes study. *Diabetes Care*, *20*(4), 537–544. https://doi.org/10.2337/diacare.20.4.537

Park, C. R., Campbell, A. M., & Diamond, D. M. (2001). Chronic psychosocial stress impairs learning and memory and increases sensitivity to yohimbine in adult rats. *Biological Psychiatry*, *50*(12), 994–1004. https://doi.org/10.1016/S0006-3223(01)01255-0

Paxinos, G., & Watson, C. (2007). The Rat Brain in Stereotaxic Coordinates Sixth Edition. In

Elsevier Academic Press. New York: Elsevier Academic Press.

Penzes, P., Cahill, M. E., Jones, K. A., Vanleeuwen, J. E., & Woolfrey, K. M. (2011). Dendritic spine pathology in neuropsychiatric disorders. *Nature Neuroscience*, *14*(3), 285–293. https://doi.org/10.1038/nn.2741

Perez-Cruz, C., Müller-Keuker, J. I. H., Heilbronner, U., Fuchs, E., & Flügge, G. (2007). Morphology of pyramidal neurons in the rat prefrontal cortex: Lateralized dendritic remodeling by chronic stress. *Neural Plasticity*, *2007*, Article ID 46276. https://doi.org/10.1155/2007/46276

Ploner, C. J., Gaymard, B. M., Rivaud-Péchoux, S., Baulac, M., Clémenceau, S., Samson, S., & Pierrot-Deseilligny, C. (2000). Lesions Affecting the Parahippocampal Cortex Yield Spatial Memory Deficits in Humans. *Cerebral Cortex*, *10*(12), 1211–1216. https://doi.org/10.1093/cercor/10.12.1211

Poncelet, A. N. (2003). Diabetic polyneuropathy: Risk factors, patterns of presentation, diagnosis, and treatment. *Geriatrics*, *58*(6), 16–18, 24–25, 30.

Popoviç, M., Biessels, G. J., Isaacson, R. L., & Gispen, W. H. (2001). Learning and memory in streptozotocin-induced diabetic rats in a novel spatial/object discrimination task. *Behavioural Brain Research*, *122*(2), 201–207. https://doi.org/10.1016/S0166-4328(01)00186-3

Ragozzino, M. E., Adams, S., & Kesner, R. P. (1998). Differential involvement of the dorsal anterior cingulate and prelimbic- infralimbic areas of the rodent prefrontal cortex in spatial working memory. *Behavioral Neuroscience*, *112*(2), 293–303. https://doi.org/10.1037/0735-7044.112.2.293

Ragozzino, M. E., Detrick, S., & Kesner, R. P. (1999). Involvement of the prelimbic-infralimbic

areas of the rodent prefrontal cortex in behavioral flexibility for place and response learning. *Journal of Neuroscience, 19*(11), 4585–4594. https://doi.org/10.1523/jneurosci.19-11-04585.1999

Ramón y Cajal, S. (1888). Estructura de los centros nerviosos de las aves. *Rev. Trim. Histol. Norm. Pat., 1*, 1–10.

Ramón y Cajal, S. (1891). Sur la structure de l'ecorce cerebrale de quelques mamiferes. *La Cellule, 7*, 124–176.

Ramón y Cajal, S. (1896a). Le bleu de methylene dans les centres nerveaux. *Rev. Trim. Microgr., 1*, 21–82.

Ramón y Cajal, S. (1896b). Les epines collaterales des cellules du cerveau colorees au bleu de methylene. *Rev. Trim. Microgr., 1*, 5–19.

Ramón y Cajal, S. (1909). *Histologie du système nerveux de l'homme & des vertébrés*. Paris: Maloine.

Raz, N., Rodrigue, K. M., & Acker, J. D. (2003). Hypertension and the Brain: Vulnerability of the Prefrontal Regions and Executive Functions. *Behavioral Neuroscience, 117*(6), 1169–1180. https://doi.org/10.1037/0735-7044.117.6.1169

Reaven, G. M., Thompson, L. W., Nahum, D., & Haskins, E. (1990). Relationship between hyperglycemia and cognitive function in older NIDDM patients. *Diabetes Care, 13*(1), 16–21. https://doi.org/10.2337/diacare.13.1.16

Rogers, M. A., Yamamoto, C., King, D. S., Hagberg, J. M., Ehsani, A. A., & Holloszy, J. O. (1988). Improvement in glucose tolerance after 1 wk of exercise in patients with mild NIDDM. *Diabetes Care, 11*(8), 613–618. https://doi.org/10.2337/diacare.11.8.613

Ryan. (1997). Effects of Diabetes Mellitus on Neuropsychological Functioning: A Lifespan

Perspective. *Seminars in Clinical Neuropsychiatry*, *2*(1), 4–14. https://doi.org/10.1053/SCNP00200004

Ryan, C. M., Williams, T. M., Orchard, T. J., & Finegold, D. N. (1992). Psychomotor slowing is associated with distal symmetrical polyneuropathy in adults with diabetes mellitus. *Diabetes*, *41*(1), 107–113. https://doi.org/10.2337/diab.41.1.107

Ryan, C. M., Freed, M. I., Rood, J. A., Cobitz, A. R., Waterhouse, B. R., & Strachan, M. W. J. (2006). Improving metabolic control leads to better working memory in adults with type 2 diabetes. *Diabetes Care*, *29*(2), 345–351. https://doi.org/10.2337/diacare.29.02.06.dc05-1626

Ryan, C. M., & Geckle, M. (2000). Why is learning and memory dysfunction in Type 2 limited to older adults? *Diabetes/Metabolism Research and Reviews*, *16*(5), 308–315. https://doi.org/10.1002/1520-7560(2000)9999:9999<::AID-DMRR141>3.0.CO;2-X

Savelli, F., Yoganarasimha, D., & Knierim, J. J. (2008). Influence of boundary removal on the spatial representations of the medial entorhinal cortex. *Hippocampus*, *18*(12), 1270–1282. https://doi.org/10.1002/hipo.20511

Schindelin, J., Arganda-Carreras, I., Frise, E., Kaynig, V., Longair, M., Pietzsch, T., … Cardona, A. (2012). Fiji: An open-source platform for biological-image analysis. *Nature Methods*, *9*(7), 676–682. https://doi.org/10.1038/nmeth.2019

Schneider, S. H., Amorosa, L. F., Khachadurian, A. K., & Ruderman, N. B. (1984). Studies on the mechanism of improved glucose control during regular exercise in Type 2 (non-insulin-dependent) diabetes. *Diabetologia*, *26*(5), 355–360. https://doi.org/10.1007/BF00266036

Scoville, W. B., & Milner, B. (1957). Loss of Recent Memory After Bilateral Hippocampal Lesions. *Journal of Neurology, Neurosurgery, and Psychiatry*, *20*(1), 11–21.

https://doi.org/10.1136/jnnp.20.1.11

Seeman, T. E., Charpentier, P. A., Berkman, L. F., Tinetti, M. E., Guralnik, J. M., Albert, M., … Rowe, J. W. (1994). Predicting changes in physical performance in a high-functioning elderly cohort: MacArthur studies of successful aging. *Journals of Gerontology*, *49*(3), 97–108. https://doi.org/10.1093/geronj/49.3.M97

Seress, L., & Pokorny, J. (1981). Structure of the granular layer of the rat dentate gyrus. A light microscopic and Golgi study. *Journal of Anatomy*, *133*(2), 181–195.

Serradas, P., Gangnerau, M. N., Giroix, M. H., Saulnier, C., & Portha, B. (1998). Impaired pancreatic β cell function in the fetal GK rat: Impact of diabetic inheritance. *Journal of Clinical Investigation*, *101*(4), 899–904. https://doi.org/10.1172/JCI368

Shetty, A. K., & Turner, D. A. (1999). Vulnerability of the dentate gyrus to aging and intracerebroventricular administration of kainic acid. *Experimental Neurology*, *158*(2), 491–503. https://doi.org/10.1006/exnr.1999.7107

Sholl, D. A. (1953). Dendritic organization in the neurons of the visual and motor cortices of the cat. *Journal of Anatomy*, *87*(4), 387–406.

Sigal, R. J., Kenny, G. P., Wasserman, D. H., Castaneda-Sceppa, C., & White, R. D. (2006). Physical activity/exercise and type 2 diabetes: a consensus statement from the American Diabetes Association. *Diabetes Care*, *29*(6), 1433–1438. https://doi.org/10.2337/dc06-9910

Slamecka, N. J. (1968). A methodological analysis of paradigms in human discrimination learning. *Psychological Bulletin*, *69*(6), 423–438. https://doi.org/10.1037/h0025762

Smith, M. Lou, & Milner, B. (1981). The role of the right hippocampus in the recall of spatial location. *Neuropsychologia*, *19*(6), 781–793. https://doi.org/10.1016/0028-3932(81)90090-7

Smith, M. Lou, & Milner, B. (1989). Right hippocampal impairment in the recall of spatial

location: Encoding deficit or rapid forgetting? *Neuropsychologia*, *27*(1), 71–81. https://doi.org/10.1016/0028-3932(89)90091-2

Spauwen, P. J. J., Köhler, S., Verhey, F. R. J., Stehouwer, C. D. A., & Van Boxtel, M. P. J. (2013). Effects of type 2 diabetes on 12-year cognitive change: Results from the Maastricht Aging Study. *Diabetes Care*, *36*(6), 1554–1561. https://doi.org/10.2337/dc12-0746

Spiro, R., Coulson, R., Feltovich, P., & Anderson, D. (2013). Cognitive Flexibility Theory: Advanced Knowledge Acquisition in Ill-Structured Domains. In *Theoretical Models and Processes of Reading* (p. Tech Report No. 441). https://doi.org/10.1598/0710.22

Spiro, R. J., Vispoel, W. P., Schmitz, J. G., Samarapungavan, A., Boerger, A. E., Britton, B. K., & Glynn, S. M. (1987). Cognitive flexibility and transfer in complex content domains. In B. K. Britton & S. M. Glynn (Eds.), *Executive control processes in reading* (pp. 177–199). Hillsdale, New Jersey: Lawrence Erlbaum Associates, Inc.

Spritz, N., Singh, H., & Marinan, B. (1975). Metabolism of peripheral nerve myelin in experimental diabetes. *Journal of Clinical Investigation*, *55*(5), 1049–1056. https://doi.org/10.1172/JCI108005

Squire, L. R., Stark, C. E. L., & Clark, R. E. (2004). The medial temporal lobe. *Annual Review of Neuroscience*, *27*(1), 279–306. https://doi.org/10.1146/annurev.neuro.27.070203.144130

Stell, W. K. (1965). Correlation of retinal cytoarchitecture and ultrastructure in Golgi preparations. *The Anatomical Record*, *153*(4), 389–397. https://doi.org/10.1002/ar.1091530409

Stewart, R., & Liolitsa, D. (1999). Type 2 diabetes mellitus, cognitive impairment and dementia. *Diabetic Medicine*, *16*(2), 93–112. https://doi.org/10.1046/j.1464-5491.1999.00027.x

Strachan, M. W. J., Deary, I. J., Ewing, F. M. E., & Frier, B. M. (1997). Is type II diabetes

associated with an increased risk of cognitive dysfunction? A critical review of published studies. *Diabetes Care*, *20*(3), 438–445. https://doi.org/10.2337/diacare.20.3.438

Stuss, D. T. (1992). Biological and psychological development of executive functions. *Brain and Cognition*, *20*(1), 8–23. https://doi.org/10.1016/0278-2626(92)90059-U

Suchy, Y. (2009). Executive functioning: Overview, assessment, and research issues for non-neuropsychologists. *Annals of Behavioral Medicine*, *37*(2), 106–116. https://doi.org/10.1007/s12160-009-9097-4

Suzuki, K., Saito, N., Sakata, Y., Toyota, T., & Goto, Y. (1990). A new prostaglandin E1 analogue (TFC-612) improves the reduction in motor nerve conduction velocity in spontaneously diabetic GK (Goto-Kakizaki) rats. *Prostaglandins*, *40*(5), 463–471. https://doi.org/10.1016/0090-6980(90)90109-9

Suzuki, K., Yen-Chung, H., Toyota, T., Goto, Y., Hirata, Y., & Okada, K. (1990). The significance of nerve sugar levels for the peripheral nerve impairment of spontaneously diabetic GK (Goto-Kakizaki) rats. *Diabetes Research (Edinburgh, Lothian)*, *14*(1), 21–25.

Taube, J. S. (2007). The Head Direction Signal: Origins and Sensory-Motor Integration. *Annual Review of Neuroscience*, *30*, 181–207. https://doi.org/10.1146/annurev.neuro.29.051605.112854

Tourrel, C., Bailbe, D., Lacorne, M., Meile, M. J., Kergoat, M., & Portha, B. (2002). Persistent improvement of type 2 diabetes in the Goto-Kakizaki rat model by expansion of the β-cell mass during the prediabetic period with glucagon-like peptide-1 or exendin-4. *Diabetes*, *51*(5), 1443–1452. https://doi.org/10.2337/diabetes.51.5.1443

Toyota, T., Kakizaki, M., Kimura, K., Yajima, M., Okamoto, T., & Ui, M. (1978). Islet activating protein (IAP) derived from the culture supernatant fluid of Bordetella pertussis:

Effect on spontaneous diabetic rats. *Diabetologia*, *14*(5), 319–323. https://doi.org/10.1007/BF01223023

Tudor-Locke, C., & Schuna, J. M. (2012). Steps to preventing type 2 diabetes: Exercise, walk more, or sit less? *Frontiers in Endocrinology*, *3*, 142. https://doi.org/10.3389/fendo.2012.00142

Tun, P. A., Perlmuter, L. C., Russo, P., & Nathan, D. M. (1987). Memory self-assessment and performance in aged diabetics and non-diabetics. *Experimental Aging Research*, *13*(3), 151–157. https://doi.org/10.1080/03610738708259317

Uylings, H. B. M., Ruiz-Marcos, A., & van Pelt, J. (1986). The metric analysis of three-dimensional dendritic tree patterns: a methodological review. *Journal of Neuroscience Methods*, *18*(1–2), 127–151. https://doi.org/10.1016/0165-0270(86)90116-0

van Haaren, F., van Zijderveld, G., van Hest, A., de Bruin, J. P. C., van Eden, C. G., & van de Poll, N. E. (1988). Acquisition of Conditional Associations and Operant Delayed Spatial Response Alternation: Effects of Lesions in the Medial Prefrontal Cortex. *Behavioral Neuroscience*, *102*(4), 481–488. https://doi.org/10.1037/0735-7044.102.4.481

Vertes, R. P. (2006). Interactions among the medial prefrontal cortex, hippocampus and midline thalamus in emotional and cognitive processing in the rat. *Neuroscience*, *142*(1), 1–20. https://doi.org/10.1016/j.neuroscience.2006.06.027

Vincent, C., & Hall, P. A. (2015). Executive Function in Adults with Type 2 Diabetes: A Meta-Analytic Review. *Psychosomatic Medicine*, *77*(6), 631–642. https://doi.org/10.1097/PSY.0000000000000103

Vinereanu, D. (2006). Risk Factors for Altherosclerotic Disease: Present and Future. In B. Maisch & R. Oelze (Eds.), *Cardiovascular Benefits of Omega-3 Polyunsaturated Fatty*

Acids (pp. 7–45). IOS Press.

Volpato, S., Ferrucci, L., Blaum, C., Ostir, G., Cappola, A., Fried, L. P., … Guralnik, J. M. (2003). Progression of lower-extremity disability in older women with diabetes: The women's health and aging study. *Diabetes Care*, *26*(1), 70–75. https://doi.org/10.2337/diacare.26.1.70

Voutilainen-Kaunisto, R. M., Teräsvirta, M. E., Uusitupa, M. I. J., & Niskanen, L. K. (2001). Occurrence and predictors of retinopathy and visual acuity in Type 2 diabetic patients and control subjects10-year follow-up from the diagnosis. *Journal of Diabetes and Its Complications*, *15*(1), 24–33. https://doi.org/10.1016/S1056-8727(00)00126-4

World Health Organization. (2016). *Global Health Estimates 2015: Deaths by Cause, Age, Sex, by Country and by Region, 2000-2015*. Geneva: World Health Organization.

Xia, W., Wang, S., Spaeth, A. M., Rao, H., Wang, P., Yang, Y., … Sun, H. (2015). Insulin resistance-associated interhemispheric functional connectivity alterations in T2DM: A resting-state fMRI study. *BioMed Research International, 2015,* Article ID 719076. https://doi.org/10.1155/2015/719076

Xiang, Q., Zhang, J., Li, C. Y., Wang, Y., Zeng, M. J., Cai, Z. X., … Li, X. H. (2015). Insulin resistance-induced hyperglycemia decreased the activation of Akt/CREB in hippocampus neurons: Molecular evidence for mechanism of diabetes-induced cognitive dysfunction. *Neuropeptides*, *54*, 9–15. https://doi.org/10.1016/j.npep.2015.08.009

Yudkin, J. (1987). Metabolic changes induced by sugar in relation to coronary heart disease and diabetes. *Nutrition and Health*, *5*(1–2), 5–8. https://doi.org/10.1177/026010608700500202

Yuste, R. (2015). The discovery of dendritic spines by Cajal. *Frontiers in Neuroanatomy*, *9,* 18. https://doi.org/10.3389/fnana.2015.00018

Zaqout, S., & Kaindl, A. M. (2016). Golgi-Cox Staining Step by Step. *Frontiers in Neuroanatomy*, *20*, 38. https://doi.org/10.3389/fnana.2016.00038